AGH
UNIVERSITY OF SCIENCE AND TECHNOLOGY

FACULTY OF ELECTRICAL ENGINEERING, AUTOMATICS, COMPUTER SCIENCE AND ELECTRONICS

THE MULTIPLE-INPUT MULTIPLE-OUTPUT SYSTEMS IN SLOW AND FAST VARYING RADIO CHANNELS

PhD Thesis by
mgr inż. Paweł Kułakowski

Supervisor: dr hab. inż. Wiesław Ludwin

KRAKÓW, POLAND
2006

Abstract

Multiple-input multiple-output (MIMO) systems are well known as a technique which allows increasing the throughput of a radio link and overcoming the effects of multipath fading. However, the integration of MIMO systems into the standards of wireless networks is slow, as there are numerous problems still unsolved.

This PhD thesis deals with MIMO systems in slow and fast varying radio channels. First, the general issues of MIMO systems are considered. Multiplexing gain and diversity concepts, channel knowledge, coding techniques as well as multiuser access and wideband transmission are discussed. Next, the channel aspects of MIMO systems are investigated. The phenomenon of multipath propagation, channel models, variations in the radio channel and channel estimation are addressed. Then, the author's research in the area of slow and fast varying MIMO channels is presented. The following theses are formulated and proved:

1. The throughput in slow varying radio channels of indoor MIMO systems can be significantly increased when the locations and the antennas of the access point are carefully chosen.

2. Iterative Channel Estimation (ICE) algorithm allows decreasing the bit error rate in fast varying radio channels without frequent transmissions of training sequences.

The first thesis is founded on the numerical ray tracing calculations concerning slow varying MIMO channels. It is shown how the locations, the separations and the characteristics of the access point antennas can affect the system throughput.

The second thesis is based on the proposed ICE algorithm for fast varying channels. ICE algorithm enables the channel estimation simultaneously with the data transmission. When ICE is applied, the bit error rate can be reduced – in some cases it is more than 50 times.

Acknowledgement

The help of various people has made this thesis possible or complete. First of all, I would like to thank my supervisor dr hab. Wieslaw Ludwin. He introduced me to the field of wireless communications and provided fantastic working conditions. His understanding, valuable comments and continuous encouragement gave the basis for my research.

I would like to express my sincere gratitude to prof. Andrzej Jajszczyk, who was my tutor during nearly three years of PhD studies. Always when it was needed, he acted as an advisor with great kindness and very helpful guidance.

I also feel obliged to all my colleagues at AGH University of Science and Technology for their help and many fruitful discussions. It was a pleasure for me to work with them, also in the teaching area.

But despite the excellent scientific cooperation, the last years would not have been possible without the patience, empathy and support of my Family. They deserve my deepest appreciation.

Table of Contents

Abstract 1
Acknowledgement 2
Table of Contents 3
Abbreviations 6
List of Symbols 8
Introduction 9
1. Fundamentals of MIMO systems 13
1.1. Capacity of MIMO systems 16
1.2. Diversity versus multiplexing gain 18
1.3. Channel state information 19
1.4. Coding for MIMO systems 21
1.4.1. Space-time block codes 21
1.4.2. Differential space-time block codes 23
1.4.3. Space-time trellis codes 24
1.4.4. Layered space-time architecture 26
1.4.5. Spatial multiplexing with full channel state information 28
1.4.6. Capacity achieving coding schemes 29
1.5. Multiuser MIMO channels 31
1.6. MIMO systems in frequency-selective radio channels 34
1.7. MIMO systems in standards of wireless networks 36
1.8. Conclusions 36

2. Radio channel in MIMO systems 38
2.1. Multipath propagation in MIMO systems 39
2.2. MIMO channel models and propagation prediction 41
2.2.1. Stochastic models 43
2.2.2. Deterministic models 47
2.3. Time-varying radio channels 52
2.4. Channel estimation 55
2.5. Radio channel in WLANs and mobile cellular networks 57
3. Capacity of indoor slow varying radio channels 60
3.1. Description of analysed WLAN network 61
3.2. Isotropic antennas 63
3.3. Large separation between AP antennas 66
3.4. Concept of directional antennas 69
3.5. Capacity of WLAN with directional antennas 71
3.6. MIMO-MRC system 73
3.7. Impact of multipath propagation 78
3.8. Influence of other parameters 78
3.8.1. Antenna separation 79
3.8.2. Signal-to-noise ratio 81
3.8.3. Dielectric constant of the walls 82
3.8.4. Room dimensions 83
3.9. Reliability and accuracy of ray tracing algorithm 84
3.9.1. Number of reflections 84
3.9.2. Location of the access point and the user terminals 85
3.9.3. Mutual coupling 86
3.10. Conclusions 87
4. Estimation of fast varying radio channels 88
4.1. Iterative Channel Estimation algorithm 89
4.2. Data transmission with ICE algorithm 91

4.3. Performance analysis of ICE algorithm 96
4.3.1. Simulation methodology 97
4.3.2. BPSK modulation 99
4.3.3. QPSK modulation 102
4.3.4. Length of training sequence 104
4.3.5. MIMO systems with high number of antennas 104
4.4. Conclusions 106
Summary 108
Appendix The standard errors of mean bit error rates 111
Bibliography 117
Streszczenie 125

Abbreviations

3-D	three-dimensional
3GPP	3rd Generation Partnership Project
AP	access point
BER	bit error rate
BLAST	Bell Labs layered space-time architecture
BPSK	binary phase shift keying
CDMA	code division multiple access
COST	European Cooperation in the Field of Scientific and Technical Research
CSI	channel state information
DoA	direction of arrival
DoD	direction of departure
DS-CDMA	direct-sequence code division multiple access
ETSI	European Telecommunication Standards Institute
FDMA	frequency division multiple access
FFT	fast Fourier transformation
GSM	Global System for Mobile Communications
ICE	Iterative Channel Estimation
IEEE	Institute of Electrical and Electronics Engineers
IFFT	inverse fast Fourier transformation
ISI	inter-symbol interference
LDPC	low-density parity-check

LoS	line-of-sight
LST	layered space-time
MIMO	multiple-input multiple-output
MISO	multiple-input single-output
MRC	maximal ratio combining
NLoS	non-line-of-sight
OFDM	orthogonal frequency division multiplexing
OSI	Open Systems Interconnection
PDA	personal digital assistant
PRN	pseudo-random noise
PRNG	pseudo-random number generator
PSK	phase shift keying
QAM	quadrature amplitude modulation
QPSK	quaternary phase shift keying
Rx	receive
SDMA	space division multiple access
SIC	successive interference cancellation
SISO	single-input single-output
SNR	signal-to-noise ratio
STBC	space-time block code
STTC	space-time trellis code
TDMA	time division multiple access
TLST	threaded layered space-time
Tx	transmit
UMTS	Universal Mobile Telecommunications System
UT	user terminal
UTRA	UMTS Terrestial Radio Access
WLAN	wireless local area network

List of Symbols

$\bullet^{*}$	complex conjugate
$\bullet^{T}$	matrix transpose
$\bullet^{H}$	complex conjugate transpose (Hermitian operator)
$\bullet^{1/2}$	any matrix square root such that $\bullet^{1/2}\cdot\left(\bullet^{1/2}\right)^{H}=\bullet$
$\otimes$	Kronecker product
$\left\|\bullet\right\|$	vector norm
$\mathrm{Re}\{\bullet\}$	real part
$\mathrm{Im}\{\bullet\}$	imaginary part
$E\{\bullet\}$	expectation value
$\boldsymbol{I}_n$	$n\times n$ identity matrix
$J_0(\bullet)$	zero-order Bessel function of the first kind
$\delta(\bullet)$	Dirac delta function

The only limits are, as always, those of vision.

James Broughton

Introduction

People do not accept the limits of the existing world and it is the matter of scientists to break these barriers. More than one century ago, Guglielmo Marconi crossed the Rubicon in telecommunications demonstrating the possibilities of a radio transmission. However, it was not earlier than in the last decade, when the wireless communications became ubiquitous in the everyday life with the cellular networks, mainly.

Cellular and wireless local area networks are the two most rapidly developing systems in the radio communications. In spite of well-established standards, the new solutions are desired. As new services for the radio networks are created, the requirements for the throughput and quality of the wireless transmission are still growing. The radio engineers must find the appropriate means to rise to this challenge.

There are two main problems that affect the wireless systems. First, the radio spectrum used by each system is limited. In the consequence, some radio techniques that expand the system spectral efficiency, i.e. the ratio of the throughput to the frequency band, are required to achieve high data rates during the transmission. Usually, the multilevel modulations are used, so each transmitted symbol contains data about many information bits. Nevertheless, according to the well known Claude Shannon's information theory, the requirements for the signal-to-noise ratio are

increasing with the number of the bits contained by the each transmitted symbol. Hence, the power restrictions of the radio transmitters result in the limitations of the throughput during the transmission in the noisy radio channel.

The second issue concerns the quality of the transmission in the radio channel. The typical bit error rates during the radio transmission are much higher than in the wired systems, because of the lower signal-to-noise ratio. Furthermore, the radio wave radiated from the transmit antenna arrives to the receive antenna by many paths. These components of the signal interfere at the receiver resulting with the multipath fading what additionally increases the bit error rate and degrades the overall system performance. The multipath fading is softened when a diversity scheme is applied, e.g. in the time, frequency or space domain.

Ten years ago, the new concept arose which turned out to be the remedy for both these problems. Multiple antennas at both sides of a radio link were proposed to create a multiple-input multiple-output (MIMO) transmission system. These additional antennas can be exploited to perform the spatial multiplexing and enhance the system throughput by transmitting many parallel data streams in the same frequency band. They can also be used in the space diversity schemes to overcome the multipath fading. The multiple antennas further allow beamforming, i.e. changing the radiation patterns of the transmit and receive antennas, dynamically.

MIMO systems are treated as a key solution in the next generations of cellular and wireless local area networks. The standards of these networks assimilate the MIMO technique, but the progress is slow. Many questions still remain unanswered. In the MIMO systems, the analysis of the radio channel is especially difficult, as this channel has multiple inputs and multiple outputs.

The design of cellular and wireless local area networks differs mainly in the aspect of the radio channel. If MIMO concept is planned to be applied to these networks, the radio channel should be considered with the special care. The local area networks are usually designed for the indoor environment. In this case, the radio propagation can be usually modelled as many waves reflecting or passing through the walls and other objects in the vicinity of the transmitter and the receiver.

Moreover, the time variations in the radio channel are rather slow or the channel transfer function is constant in time. On the other hand, the cellular networks operate in diverse environments. The channel models are more complicated. The scattering of the radio waves on the irregular objects is also more significant. Besides, the radio channel can be fast varying, e.g. when the radio terminal is moving with the high speed.

In this thesis, the performance of the MIMO systems in slow and fast varying radio channels is discussed. As an example of the slow varying channel, the wireless local area network with multiple antennas is considered. The network is analysed to find the configurations which allow increasing the average throughput during the transmission between the access point and the user terminals. In the case of fast varying radio channels, the problem of channel estimation is investigated. The knowledge about the radio channel must be frequently updated, but the time needed for the data transmission should not be wasted. The new efficient algorithm of Iterative Channel Estimation is presented. All the research is focused on the physical layer of OSI model. The single link between the user terminal and the base station or the access point is considered.

The theses of this dissertation are defined as follows:

1. The throughput in slow varying radio channels of indoor MIMO systems can be significantly increased when the locations and the antennas of the access point are carefully chosen.

2. Iterative Channel Estimation algorithm allows decreasing the bit error rate in fast varying radio channels without frequent transmissions of training sequences.

The whole thesis is divided into four chapters. In the chapter 1, the general issues of MIMO systems are considered. The concept of the simultaneous transmission in the same frequency band is presented and the tradeoff between the spatial multiplexing and the diversity is explained. The enhanced definition of the channel capacity, suitable for MIMO systems, is introduced. The importance of the

channel knowledge is discussed. Then, the basic MIMO coding schemes are described. The performance of the MIMO systems in the multi-user radio channels is analysed. The problems of the transmission in frequency-selective channels are also addressed. Finally, the telecommunication standards concerning the MIMO systems are elaborated.

The chapter 2 is devoted to the channel aspects of MIMO systems. The phenomenon of multipath propagation is covered. Then, the most important MIMO channel models are presented. The time variations in the MIMO channel are discussed. The issues of the channel estimation are included. Lastly, the MIMO channel in the cellular and wireless local area networks is analysed. Some general conclusions about the capacity of the indoor slow varying MIMO channels are listed. For the fast varying channels, the problem of the efficient channel estimation algorithm is provided.

In the last two chapters, the research results of the author of this thesis are presented. The broad analysis of the wireless MIMO indoor network is performed in the chapter 3. The factors that can influence the system capacity are investigated. The directivity of the access point antennas and their location are carefully studied. The MIMO system with adaptive antennas is also considered. All the calculations are made on the basis of the deterministic ray tracing model.

In the chapter 4, the Iterative Channel Estimation algorithm is introduced with the details. The coding schemes suitable for this algorithm are specified. The Monte-Carlo simulations are presented to verify the algorithm performance.

The thesis closed with the general conclusions about the author's research and the MIMO systems in time-varying channels.

You see, wire telegraph is a kind of a very, very long cat.
You pull his tail in New York and his head is meowing in Los Angeles.
Do you understand this?
And radio operates exactly the same way: you send signals here, they receive them there.
The only difference is that there is no cat.
Albert Einstein

Chapter 1
Fundamentals of MIMO systems

The explosion of interest in multiple-input multiple-output (MIMO) systems dates from the middle of 90-ties. Then the two papers were written, the first one by I. Telatar [70] and the second by G. Foschini and M. Gans [22]. However, what is not widely known is the fact that eight years before Telatar's work, another paper was written by J. Winters [80]. The system with multiple antennas was presented and it was shown that, with appropriate signal processing in the transmitter and the receiver, the possible transmission rate increased linearly with the number of the antennas.

Generally, a MIMO system consists of n transmit (Tx) and m receive (Rx) antennas (Fig. 1.1). It is called a MIMO (n,m) system. All the Tx antennas can send their signals simultaneously in the same bandwidth of a radio channel. Each Rx antenna receives the superposition of all the transmit signals disturbed by the noise

in the radio channel. If no more than $\min[n,m]$ independent signals are transmitted, they can be correctly decoded at the receiver.

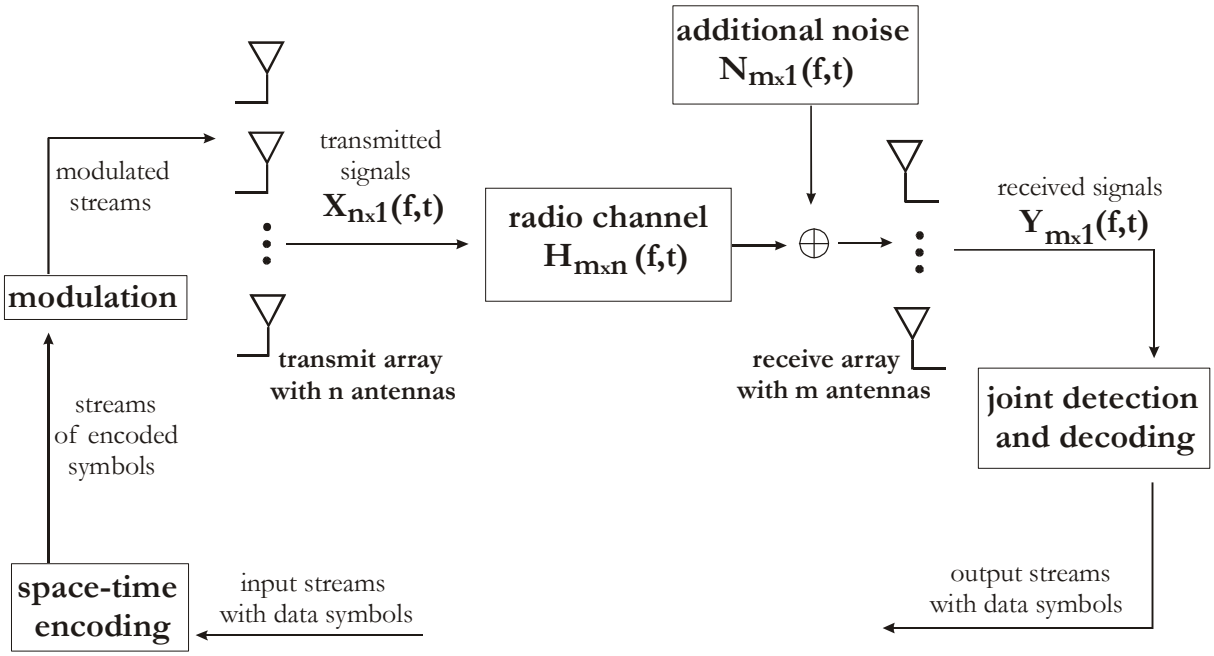

Fig. 1.1. The MIMO (n,m) system.

Before the presentation of the detailed concept of MIMO systems, the basic assumptions should be formulated. According to the paper of Foschini and Gans [22], the following conditions are necessary:

1. The mobility of transmit and receive antennas is limited, so the radio channel can be assumed to be stationary or quasi-stationary.
2. The bandwidth used for the transmission is narrow, so the radio channel is assumed to be flat.
3. There are many scattering objects in the environment and there are many propagation paths between transmit and receive antennas.
4. The separation between the antennas in Tx and Rx arrays is at least 0.5 wavelength (0.5 λ).
5. The characteristics of the radio channel are not known at the transmitter, but the receiver tracks the channel.

The radio channel between n transmit and m receive antennas can be represented as a $m \times n$ channel transfer matrix $\boldsymbol{H}(f,t)$, dependent on frequency f

and time t. The whole transmission system can be characterised by the following equation:

$$\begin{bmatrix} y_1(f,t) \\ y_2(f,t) \\ \vdots \\ y_m(f,t) \end{bmatrix} = \begin{bmatrix} h_{11}(f,t) & h_{12}(f,t) & \cdots & h_{1n}(f,t) \\ h_{21}(f,t) & h_{22}(f,t) & \dots & h_{2n}(f,t) \\ \vdots & \vdots & \ddots & \vdots \\ h_{m1}(f,t) & h_{m2}(f,t) & \cdots & h_{mn}(f,t) \end{bmatrix} \cdot \begin{bmatrix} x_1(f,t) \\ x_2(f,t) \\ \vdots \\ x_n(f,t) \end{bmatrix} + \begin{bmatrix} n_1(f,t) \\ n_2(f,t) \\ \vdots \\ n_m(f,t) \end{bmatrix}, \qquad (1.1)$$

where $x_j(f,t)$ is the signal transmitted from j-th Tx antenna, $y_i(f,t)$ is the signal received at i-th Rx antenna, $h_{ij}(f,t)$ is the transfer function between j-th Tx antenna and i-th Rx antenna and $n_i(f,t)$ is the noise on the i-th Rx antenna. Thus, the MIMO radio channel consists of $n \cdot m$ subchannels. The equation (1.1) can be also written in the vector form:

$$\boldsymbol{Y}(f,t) = \boldsymbol{H}(f,t) \cdot \boldsymbol{X}(f,t) + \boldsymbol{N}(f,t), \qquad (1.2)$$

where $\boldsymbol{X}(f,t)$ and $\boldsymbol{Y}(f,t)$ are the vectors of transmitted and received signals and $\boldsymbol{N}(f,t)$ is the vector of additive noise.

If the aforementioned conditions are satisfied, the elements of channel transfer matrix are complex values constant during a period of time (condition 1) and independent of the signal frequency (condition 2). Hence, the notation can be simplified: the channel matrix can be denoted as $\boldsymbol{H}$ and its entries as h_{ij}.

If the noise was neglected, the whole transmission system would be considered as the set of m equations with n variables. So, if only $n \le m$ and the receiver would know the matrix $\boldsymbol{H}$ (condition 5), these n transmitted signals could be properly detected at the receiver. The accuracy of the detection process is, of course, limited by the noise, but it is possible. To detect n signals, the matrix $\boldsymbol{H}$ should also have the rank equal at least to n, so the elements of the matrix $\boldsymbol{H}$ should not be correlated. This is provided by the proper antenna separation (condition 4) and the environment where multipath propagation is possible (condition 3). As a result, in MIMO (n,m) system, $\min[n,m]$ independent signals can be transmitted simultaneously in the same bandwidth.

The abovementioned conditions limit the applications of MIMO systems. These limitations were broken when the new concepts about MIMO systems appeared. These issues will be discussed in the next sections of this thesis.

1.1. Capacity of MIMO systems

It was shown by C. Shannon in 1948 [64] that the throughput is limited when the reliable transmission in noisy channel is considered. The commonly used measure of the potential of the channel to transmit data is the capacity. It is the maximal transmission rate which is possible in the unit bandwidth with arbitrary low bit error rate. Hence, the capacity is the upper bound of the spectral efficiency achievable in the specific radio channel. For the definition of the capacity, neither the coding scheme nor the modulation is specified. It is the theoretic limit of the transmission rate with coding block assumed to be infinitely long. Shannon showed that the capacity C of the channel with additive white Gaussian noise is limited to:

$$C = \log_2(1 + SNR), \tag{1.3}$$

where SNR is the signal-to-noise ratio at the receive antenna. Capacity unit is bit/s/Hz.

However, in the case of a system with multiple antennas, the Shannon's limit should be extended. It was proven [22, 70] that the capacity of the MIMO channel is equal to:

$$C = \log_2 \det\left(\boldsymbol{I}_m + \frac{\rho}{n} \boldsymbol{H}\boldsymbol{H}^* \right), \tag{1.4}$$

where $\boldsymbol{I}_m$ is $m \times m$ identity matrix, ρ is the ratio of the total transmit power to the noise power, n and m are the numbers of Tx and Rx antennas and $\boldsymbol{H}$ and $\boldsymbol{H}^*$ are the channel transfer matrix and its transpose conjugate version, respectively. The capacity from equation (1.4) is sometimes calculated as [27, 70]:

$$C = \sum_{i=1}^{l} \log_2\left(1 + \frac{\rho}{n} \lambda_i^2 \right), \tag{1.5}$$

where l is equal to the rank of the matrix $\boldsymbol{H}$ and $\lambda_1, \lambda_2, ..., \lambda_l$ are the singular values of $\boldsymbol{H}$ (nonnegative square roots of the eigenvalues of the matrix $\boldsymbol{H}\boldsymbol{H}^*$) [35]. In the case when the transfer functions of the MIMO subchannels are not correlated, e.g. in a richly scattered environment, l is maximal and is equal to $\min[n, m]$. This case will be assumed unless it is stated otherwise. It should be noted that average signal-to-noise ratio at the Rx antennas can be calculated as:

$$SNR = \frac{\rho \cdot \sum_{i=1}^{m} \sum_{j=1}^{n} \left| h_{ij} \right|^2}{n \cdot m}. \tag{1.6}$$

The equations (1.4) and (1.5) present the capacity in most popular instance: when the channel transfer matrix is known only at the receiver side. In this case, the capacity of MIMO channel grows proportionally to l. The capacity is the most important measure of the MIMO channel – it determines the possibility of the radio channel for the data transmission.

In the channels with fading, the notion of capacity is not convenient to describe the radio channel. When a deep fade occurs, no data can be transmitted. According to the definition, capacity of such a channel is equal to zero. Thus, instead of the capacity, two other notions are usually used. They are ε-outage capacity and ergodic capacity. The former is suitable when the changes of the channel characteristics are slow and a deep fade could be very long. In this case, the time can be divided into short periods and the capacity can be calculated for each of these periods. Then, the cumulative distributive function is calculated over these values of capacity. On this basis, the ε-outage capacity is defined as a capacity that cannot be achieved by ε % of time [74]. So, the capacity of the radio channel is lower than a given value with the probability of ε.

In the channels where the fading is rapid, the expectation value of the capacity is usually calculated. Again, the channel can be in a deep fade, but these periods are short and the loss of data can be compensated by the appropriate joint coding and interleaving. This expectation value is called ergodic capacity [27].

1.2. Diversity versus multiplexing gain

There are two main challenges for future wireless communication systems. First, there is a huge gap between the throughput in cable and wireless systems. Radiocommunication networks' users and clients expect high throughput, comparable with cable networks. However, in wireless systems, there is the problem of limited bandwidth. The wireless network cannot use the whole radio frequency bandwidth because of the interference with other radio systems. Therefore, limited bandwidth is assigned to the particular wireless network. In order to extend the throughput, the spectral efficiency should be increased. It could be done, e.g. using multilevel modulations, but it results in the higher requirements for SNR. Thus, the solution is a system with multiple antennas which allows enlarging the throughput and keeping the same bandwidth and SNR. In the MIMO (n,m) system, $l = \min[n,m]$ independent signals can be transmitted, so the spectral efficiency grows l times – there is spatial multiplexing gain equal to l.

The second challenge is the phenomenon of fading: the effect of variations of signal power at the receiver. Large-scale (slow) fading is caused by changes in signal attenuation when the terrain obstacles block some propagation paths between the transmitter and the receiver. On the other hand, small-scale (fast) fading is the effect of the constructive and destructive interference between the replicas of the transmitted signal which arrive to the receiver by different paths. Slow, as well as fast fading can be the result of the movement of the transmitter, receiver or objects in the surroundings of the wireless system. Also, the changes in the atmosphere can cause the large-scale fading effects. Because of fading, the transmission in radio channel cannot be reliable. In some time periods, the outage occurs: the signal attenuation in the radio channel is very strong and there is huge bit error rate (BER) during the data transmission.

To overcome the problem of fading, the diversity is applied to a radio system. The data is transmitted by two or more different, independent ways. The same or correlated signals can be sent in different frequency bands or in different time

periods. At the receiver, these signals can be combined or just the best signal is selected.

The multiple antennas can provide the additional kind of diversity to the system. The encoded signals are simultaneously transmitted from multiple Tx antennas or received by multiple Rx antennas – it is called space diversity. In the MIMO (n,m) system, there are $n \cdot m$ different ways to transmit the data signal. If the characteristics of different subchannels are uncorrelated, the effect of the fading can be overcome. When a subchannel is faded, the others can provide good propagation conditions. The maximal diversity gain in MIMO (n,m) system is equal to $n \cdot m$, because it is the maximal number of independent subchannels.

However, the MIMO system cannot provide the full diversity and multiplexing gain at the same time [74, 85]. It is the matter of coding which aspect of the MIMO system will be exploited. The MIMO system can maximise the transmission rate by sending many independent information streams simultaneously or protect the transmission from the errors caused by fading. Also, the compromise between these two strategies is possible. Switching between the coding schemes achieving the diversity or multiplexing gain can be realised during the transmission [33]. Yet, it is always the tradeoff.

1.3. Channel state information

Generally, the knowledge about the radio channel, also called channel state information (CSI), can be used for two purposes. On its basis, the transmitter can adapt the signal to the radio channel. On the other hand, the receiver uses the channel knowledge to decode the received signal.

The most frequently considered case of a MIMO system is when CSI is known only at the receiver. This knowledge is essential for proper detection of the data symbols. The simplest decoding algorithm can be thought of as a channel transfer matrix inversion and calculation of n variables (n transmitted data signals) – like solving the set of n equations. In practice, the decoding algorithm is more

sophisticated and usually matches the coding scheme. Moreover, because of the noise and channel variations in time, the receiver does not know the radio channel perfectly. It additionally decreases the channel capacity [49]. To cope with fast variations of the radio channel, some special channel estimation algorithms should be applied [47]. It will be discussed in details, further.

The channel knowledge at the receiver is crucial for the whole transmission. However, if the matrix $\boldsymbol{H}$ is known only at the receiver, the transmitter will treat all the transmitted data signals in the same way and will allocate the equal power to all of them. In many cases, such a strategy is very ineffective, as some of these data signals are very strongly attenuated during the transmission. When the matrix $\boldsymbol{H}$ is known also at the transmitter side, the signals can be adapted to the radio channel. The greatest power is allocated to those data signals which are the least attenuated in the radio channel. This algorithm is called waterfilling or waterpouring, because the power is "poured" into the radio subchannels accordingly to their gains. The waterfilling is explained with details in the section 1.4.5 in the context of spatial multiplexing techniques.

The channel state information at the transmitter and the waterfilling algorithm allow increasing the channel capacity in comparison with the case when the channel is known only at the receiver. However, this advantage converges to zero with the SNR increasing [29]. As the waterfilling algorithm needs calculating the singular values of matrix $\boldsymbol{H}$, it is computationally complicated. So, it is rather not worthwhile in the high SNR region.

The MIMO systems with the channel knowledge only at the transmitter are rarely considered. Some information can be found in [49]. In the last case, the channel is known neither at the transmitter not at the receiver. There exists some non-coherent and blind detection techniques. Such techniques can be useful especially for the fast varying radio channels where the training sequences should be transmitted very frequently to track the channel properly. Generally, blind detection is based on the exploiting the information about the statistics of the channel or received signals and the properties of the input signals, i.e. the finite number of symbols in the constellation [73, 75]. Also, the differential codes can be used, particularly when the

transmitted vectors of symbols are orthogonal. The examples are discussed in the section 1.4.2.

1.4. Coding for MIMO systems

The MIMO coding schemes are designed for achieving two purposes: maximal multiplexing or diversity gain. In the former case, it is desired that the signals transmitted from the different Tx antennas carry other information symbols and be uncorrelated. Quite the opposite in the latter: the radio subchannels should also be uncorrelated, but the signals should be kept dependent from each other in order to protect the information symbols from the errors during the transmission. Of course, the diversity achieving codes are more complicated than simple signal repetition. Usually, multiplexing and diversity gains are described as 'spatial' to emphasise that it is done with multiple antennas. The basics coding concepts and systems designs are presented in the next sections.

1.4.1. Space-time block codes

In comparison to the system with single antennas, MIMO systems with space-time block codes (STBCs) do not improve the spectral efficiency, but provide maximal possible diversity of $n \cdot m$ [3, 68, 77]. The symbols transmitted from $2, 3, \cdots, n-$th antennas are the linear combinations and the conjugate versions of the symbols transmitted from the first Tx antenna. So, additional Tx antennas do not transmit additional data symbols. In the most cases, the additional Tx antennas just transmit the same symbols like the first Tx antenna (or their opposite and conjugate versions), but in different order. To apply the STBC scheme, CSI at the transmitter is not required.

The first STBC was the scheme for two Tx antennas and arbitrary Rx antennas proposed by Alamouti [3]. This encoding scheme can be described as follows. In the first time period τ_1, the two symbols x_1 and x_2 are transmitted simultaneously from two Tx antennas. Then, in time period τ_2, the two symbols $-x_1^*$ and x_2^* are

transmitted. The symbols are coded in the domain of space (two Tx antennas) and in the domain of time (two time periods needed for the transmission). The encoding scheme can be expressed as a matrix:

$$\begin{bmatrix} x_1 & -x_2^* \\ x_2 & x_1^* \end{bmatrix}, \tag{1.7}$$

where in each column p there are symbols transmitted in the time period τ_p and in each row n there are symbols transmitted from n-th Tx antenna. So, p is the number of symbols transmitted from each antenna during one block. In this case, four symbols form the block of data, but two of them are repeated. There are two orthogonal transmit vectors: $v_1 = [x_1 \quad x_2]^T$ and $v_2 = [-x_2^* \quad x_1^*]^T$ in this scheme. The transmit vectors in STBC are always orthogonal [68]. The orthogonality of the transmit vectors in STBC allows for iterative channel estimation on the basis of transmitted data symbols [47]. This concept, especially important in fast varying radio channels, will be covered in the chapter 4. The components of transmit vectors can be real (e.g. BPSK constellation) or complex (e.g. QPSK, 16-QAM). The number of Rx antennas is unlimited, the decoding process is simple linear maximum likelihood algorithm with all Rx antennas.

Let k denote number of different data symbols transmitted in one block. For all STBC, the transmission rate is not higher than the rate for uncoded single-input single-output (SISO) transmission, as the additional antennas are used only for diversity purposes. The relative transmission rate can be calculated as:

$$R = \frac{k}{p} \leq 1. \tag{1.8}$$

For Alamouti code, R is equal to 1: during two time periods two symbols are transmitted.

STBC were generalized for n Tx antennas [68]. Unfortunately, it was proven there exists no other STBC with $R = 1$ and simple linear decoding. The STBC with the following encoding matrix was proposed for four Tx antennas [68]:

$$\begin{bmatrix} x_1 & -x_2 & -x_3 & -x_4 \\ x_2 & x_1 & x_4 & -x_3 \\ x_3 & -x_4 & x_1 & x_2 \\ x_4 & x_3 & -x_2 & x_1 \end{bmatrix}. \tag{1.9}$$

However, it is valid only for the constellations with real elements. The similar encoding matrix exists for eight Tx antennas, also only for real constellations. These three codes are the only ones with $R=1$. Except of them, there exist other STBCs for arbitrary number of Tx antennas, but with $R<1$.

Later, the attractive solution was presented for four Tx antennas, $R=1$ and complex constellation, but with nonlinear decoding in the receiver [32]:

$$\frac{1}{\sqrt{2}}\cdot\begin{bmatrix} x_1 & -x_2^* & -z_1^* & -z_2^* \\ x_2 & x_1^* & z_2 & -z_1 \\ x_3 & -x_4^* & x_1^* & x_2^* \\ x_4 & x_3^* & -x_2 & x_1 \end{bmatrix}, \tag{1.10}$$

where x_1, x_2, x_3 and x_4 are the data symbols, $z_1 = \mathrm{Re}\{x_3\} - j\,\mathrm{Im}\{2x_1x_2x_4^*\}$ and $z_2 = x_1^{*2}x_4 + x_2^2x_4^* + x_1^*x_2x_3 - x_1^*x_2x_3^*$.

1.4.2. Differential space-time block codes

The differential STBC scheme for PSK modulation was also proposed [69]. The detection of the differential codes does not need the channel knowledge either at the transmitter or at the receiver. Thus, differential codes are suitable when the training sequences become outdated very quickly, i.e. in the case of fast varying channels. However, in MIMO channels, the differential detection is more complicated than in SISO channels, as many signals are transmitted simultaneously. It is possible for STBCs, because the transmitted vectors are orthogonal.

For a SISO system, the differential PSK modulation can be described as follows. Assuming the PSK constellation with *M* signal points and spectral efficiency of $m=\log_2 M$, the symbols from the constellation are:

$$s_i = \exp\left(j\frac{2\pi c_i}{M}\right) \tag{1.11}$$

where $c_i \in \{0, 1, 2, \cdots, M-1\}$ and i refers to the time period of the transmission. The differential encoder generates the sequence of modulated symbols:

$$x_i = s_i \cdot x_{i-1}. \tag{1.12}$$

So, the data information is coded in the difference between the phases of two subsequent symbols. The first transmitted symbol should be the reference and cannot carry any information.

Differential space-time block codes are designed by the analogy. The transmission scheme for Alamouti code (two Tx antennas) is as follows. What should be sent is the relationship between the data symbols s_{i+1}, s_{i+2} and the previously transmitted symbols x_{i-1}, x_i. Therefore, in each code block, the sum of the phases of new vector $[s_{i+1} \quad s_{i+2}]^T$ and the previously transmitted vectors, $[x_{i-1} \quad x_i]^T$ and $[-x_i^* \quad x_{i-1}^*]^T$, is sent:

$$\begin{bmatrix} x_{i+1} \\ x_{i+2} \end{bmatrix} = \begin{bmatrix} x_{i-1}^* & x_i^* \\ -x_i & x_{i-1} \end{bmatrix} \cdot \begin{bmatrix} s_{i+1} \\ s_{i+2} \end{bmatrix}. \tag{1.13}$$

As the lengths of all vectors are normalised to 1, Eq. (1.13) refers to the dot product of the vectors $[s_{i+1} \quad s_{i+2}]^T$ and $[x_{i-1} \quad x_i]^T$ and the dot product of the vectors $[s_{i+1} \quad s_{i+2}]^T$ and $[-x_i^* \quad x_{i-1}^*]^T$. The vectors $[x_{i-1} \quad x_i]^T$ and $[-x_i^* \quad x_{i-1}^*]^T$ are orthogonal, so the new vector $[s_{i+1} \quad s_{i+2}]^T$ is uniquely represented and can be decoded at the receiver. It was shown [69] that BER performance of differential STBCs in quasi-stationary radio channel is 3 dB worse than the analogous STBC scheme with the channel matrix known at the receiver. So, the Tx power should be increased by 3 dB to achieve the same capacity what is an important drawback of that transmission scheme.

1.4.3. Space-time trellis codes

Similarly to STBCs, space-time trellis codes (STTCs) are also designed for achieving the maximal possible diversity [67, 77]. Yet, there exists STTC for different number of Tx antennas, with relative transmission rate $R = 1$ and complex constellation. Moreover, all STTCs provide additional coding gain.

Despite these advantages, STTCs are not as popular as the simplest STBC – Alamouti scheme. STTCs are generally more difficult to implement, as the decoding algorithm is non-linear. STTCs are the extension of conventional trellis codes for the system with multiple antennas. So, the decoding process is the maximum likelihood algorithm, but based on Viterbi decoder.

There are no blocks in the transmission with STTCs. The transmitted symbols are dependent from the previously transmitted ones, so the encoder needs to keep them in the buffer. The codes for more than two Tx antennas and full transmission rate ($R = 1$) are possible, but the larger number of Tx antennas, the longer memory of the encoder is needed. In the consequence, the encoding and especially decoding processes are more complex. Moreover, the adding Rx antenna to the system gives better results than adding Tx antenna [77] – e.g. the MIMO (2,2) system performs better than MISO (4,1) system. It is the simple consequence of the fact that during STTC transmission the channel knowledge is assumed only at the receiver.

For the explanation of space-time trellis coding, a system with two Tx antennas and QPSK modulation will be considered. The coding scheme is presented in Table 1.1. The whole transmission starts with the encoder in zero state. If the first pair of transmitted bits is e.g. 01, the new state of the encoder is 1 and two symbols: 0 and 1 are transmitted from the first and the second Tx antennas, respectively. If next pair of bits is 11, the state is changed to 3 and the transmitted symbols are 1 and 3. This process is continued till the end of the frame with data.

When STBC or STTC schemes are applied to MIMO systems, only the diversity, no the multiplexing gain is increased. Therefore, these schemes could be found not useful in some cases. Nevertheless, when BER is decreased because of high diversity, the modulation with large constellation can be exploited to increase spectral efficiency. In consequence, the BER is decreasing again, but the transmission rate is higher.

Table 1.1.

The output symbols for space-time trellis code for two Tx antennas and QPSK modulation.

Actual input bits	00	01	10	11
Actual transmitted symbol (state of the encoder)	0	1	2	3
Previous state	Output of both Tx antennas			
0	0 0	0 1	0 2	0 3
1	1 0	1 1	1 2	1 3
2	2 0	2 1	2 2	2 3
3	3 0	3 1	3 2	3 3

1.4.4. Layered space-time architecture

Layered space-time (LST) architecture is the system design intended to achieve high spectral efficiencies, in other words: high multiplexing gain [21, 77]. It is assumed that channel transfer matrix is known only at the receiver. The data stream is demultiplexed onto n substreams with equal transmission rate. All substreams are simultaneously transmitted from n Tx antennas using the same bandwidth, so the transmission rate can be increased even n times. Generally, the data bits are coded with the common codes, e.g. convolutional, LDPC or turbo codes. This coding process can be done before or after the demultiplexing.

At the receiver, the substreams are detected using the m received signals. Usually, m should be greater or at least equal to n. The interference suppression and cancellation are performed by zero-forcing or minimum mean square error algorithms: when the first substream is detected, it is cancelled out from the all m received signals. Thus, the next substreams can be detected correctly with higher probability, as there are less interfering substreams. In other words, the diversity increases when the subsequent substreams are cancelled out. Also, the iterative receiver architecture is possible. When all the substreams are detected, this information is used for the detection performed one more time. Because the detection

of the specific substream is strictly dependent from the detection of other substreams, the repeat detection is more correct. When the substreams are detected, each substream is decoded individually.

There are many versions of LST transmitters (H-BLAST, V-BLAST, D-BLAST), proposed mainly by the researchers from Bell Labs [21, 23, 24, 28]. In the opinion of the author of this thesis, threaded layered space-time (TLST) architecture [26] is the most effective one, as it combines high spectral efficiency with spatial diversity. It can be briefly described as follows. The stream with information bits is divided into n substreams. Now, each substream is treated separately: it is encoded and modulated. Then, the symbols from the substreams are assigned to the specific Tx antennas. So, the symbol from first substream is transmitted from first Tx antenna, etc. However, there is a rotation between the substreams, called spatial interleaving. In each subsequent period of time τ_i, the symbols from the specific substream are transmitted from the other Tx antenna. This operation, called spatial interleaving, is performed to equalise the propagation conditions for all substreams and thus provide the spatial diversity to the substreams. After the assignment of the symbols to the Tx antennas, the symbols in each substream are additionally interleaved in time to prevent from block errors during the transmission in a fading radio channel.

The symbol allocation scheme for four Tx antenna system is presented in Table 1.2. The symbols from each substream are sequentially transmitted from the first, second, third and fourth Tx antenna.

Table 1.2.

The allocation of the substreams to the Tx antennas.

S_i denotes a symbol from the *i*-th substream.

Period of time	τ_1	τ_2	τ_3	τ_4	τ_5	…
Tx antenna 1	$S_1(\tau_1)$	$S_4(\tau_2)$	$S_3(\tau_3)$	$S_2(\tau_4)$	$S_1(\tau_5)$	…
Tx antenna 2	$S_2(\tau_1)$	$S_1(\tau_2)$	$S_4(\tau_3)$	$S_3(\tau_4)$	$S_2(\tau_5)$	…
Tx antenna 3	$S_3(\tau_1)$	$S_2(\tau_2)$	$S_1(\tau_3)$	$S_4(\tau_4)$	$S_3(\tau_5)$	…
Tx antenna 4	$S_4(\tau_1)$	$S_3(\tau_2)$	$S_2(\tau_3)$	$S_1(\tau_4)$	$S_4(\tau_5)$	…

1.4.5. Spatial multiplexing with full channel state information

If high spectral efficiency is desired and the channel transfer matrix is known at both sides of the radio channel, the transmitter can perform better than just demultiplex the data stream into n equal substreams and assign the same power to all the Tx antennas. As it was mentioned in the section 1.3, the waterfilling algorithm can be applied to increase the channel capacity. The main data stream is divided into the group of substreams with different transmission rates. The different powers are allocated to the substreams, according to the potential of the MIMO channel to carry them. Sometimes, despite of multiple Tx antennas, there is only one stream, as it is not worthwhile to transmit the others.

The whole transmission process is as follows. At the transmitter, the operation of singular value decomposition of matrix $\boldsymbol{H}$ is performed:

$$\boldsymbol{H} = \boldsymbol{U} \cdot \boldsymbol{\Lambda} \cdot \boldsymbol{V}^{*}, \tag{1.14}$$

where $\boldsymbol{U}$ and $\boldsymbol{V}$ are $m \times m$ and $n \times n$ unitary matrices and $\boldsymbol{\Lambda}$ is a $m \times n$ matrix with off-diagonal elements equal to zero. The diagonal elements of $\boldsymbol{\Lambda}$ are the singular values of $\boldsymbol{H}$: $\lambda_1, \lambda_2, \cdots, \lambda_l$. If $l < \min[n, m]$, the diagonal of $\boldsymbol{\Lambda}$ is filled with zeros. After that, the power levels for the substreams are calculated as [27, 70, 74]:

$$P_i = \begin{cases} \mu - \dfrac{N}{\lambda_i^2}, & \text{for} \quad \lambda_i^2 \mu > N \\ 0, & \text{for} \quad \lambda_i^2 \mu \le N \end{cases}, \tag{1.15}$$

where N is average noise power and μ is chosen to satisfy the total power constraint:

$$P = \sum_{i=1}^{l} P_i \,. \tag{1.16}$$

In this case, the MIMO channel capacity is given by:

$$C = \sum_{i=1}^{l} \log_2 \left(1 + \frac{P_i \lambda_i^2}{N} \right) \tag{1.17}$$

or:

$$C = \sum_{i=1}^{l} \log_2 \left(\mu \cdot \lambda_i^2 \right), \tag{1.18}$$

what is a simple mathematic consequence of the equations (1.15) and (1.17). Therefore, the MIMO channel is decomposed into l SISO channels with the capacities:

$$C_i = \log_2\left(1+\frac{P_i\lambda_i^2}{N}\right),\ i\in\{1,2,\cdots,l\}. \tag{1.19}$$

Note that l is the maximal number of SISO channels. Some of them could have the capacity equal to zero, as P_i could be zero for them.

Now, the main data stream can be divided into l substreams with the transmission rates appropriate to the capacities of the above SISO channels. The vector of l substreams is filled with zero entries to obtain the n-dimensional one. So, this vector is:

$$\tilde{\boldsymbol{X}} = \begin{bmatrix} x_1 & x_2 & \cdots & x_l & 0 & \cdots & 0 \end{bmatrix}^T. \tag{1.20}$$

The power of P_i is assigned to the symbol x_i. Then, the pre-processing before the transmission is done. The vector of transmitted signals $\boldsymbol{X}$ is:

$$\boldsymbol{X} = \boldsymbol{V}\cdot\tilde{\boldsymbol{X}}. \tag{1.21}$$

The vector of received signals $\boldsymbol{Y}$ is post-processed to obtained the output vector of data substreams:

$$\tilde{\boldsymbol{Y}} = \boldsymbol{U}^*\cdot\boldsymbol{Y}. \tag{1.22}$$

As the $\boldsymbol{V}$ and $\boldsymbol{U}$ are the unitary matrices, $\boldsymbol{V}\cdot\boldsymbol{V}^* = \boldsymbol{U}\cdot\boldsymbol{U}^* = \boldsymbol{I}$ [35]. Thus, the pre-processing and post-processing neutralise the cross-dependence between the different input and output data streams. In the result, the relationship between the output and input streams is very simple. Each output stream in just the input data stream attenuated by the radio channel and disturbed by the noise. The whole process of the transmission is also illustrated in Fig. 1.2.

1.4.6. Capacity achieving coding schemes

When multiple Tx antennas are used to provide multiplexing gain and different data substreams are transmitted, one needs a scheme for source coding. If e.g. LST codes are used, there are rules and principles how the data substreams are treated. However, it is not defined how the information bits in the substreams are

coded. There should be a coding scheme which is spectrally efficient and prevents the data bits from errors during the radio transmission. Two coding techniques are known to achieve the capacity close to Shannon's limit. These are turbo codes and low-density parity-check (LDPC) codes.

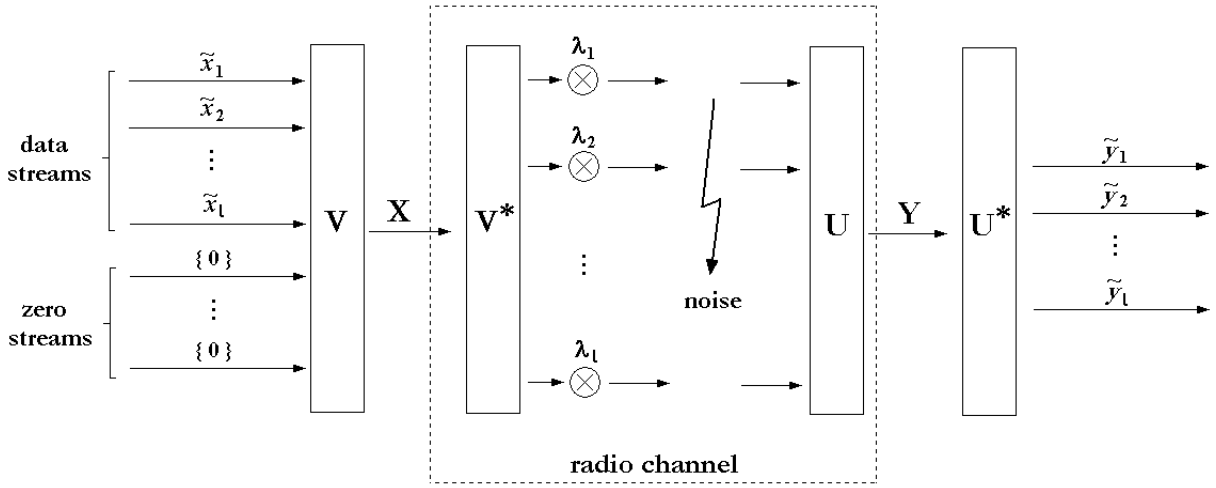

Fig.1.2. The transmission process with singular value decomposition and waterfilling.

Turbo codes with iterative decoding at the receiver were introduced by C. Berrou *et al.* in 1993 [5, 6]. It was shown that turbo codes were only a fraction of dB below Shannon's capacity. It meant that Tx power should be increased only by less than 1 dB in comparison to the Shannon's theory to achieve the same capacity. Other coding techniques, known at that time, were about 3 dB below this limit.

The turbo coding strategy is realised by the concatenation of two encoders. They can work in parallel or serial manner. While the first one just encodes the data bits into a certain form of block code, the second one performs the similar operation, but the input bits are interleaved. The encoders can work in parallel – encoding the same data bits, or in serial form – the output of the first encoder is the input of the second one [31]. On the end, parity bits are added. On the other hand, the decoder also consists of two parts. The decoding process is done iteratively in each part, the results are exchanged and this operation is repeated.

Turbo codes, designed for SISO systems, were successfully applied to multiple antenna transmitters and receivers. The system with space-time bit-interleaved coded modulation can attain the capacity close to the limit for MIMO channels with

reasonable complexity [31]. Also, some methods with iterative detection and decoding were proposed with very good results [34].

After the turbo codes revolution, it appeared that the similar solution had been known from the 1960s, when R. Gallager had invented LDPC codes with the iterative decoding algorithm [25]. The name of these parity-check block codes is derived from the fact that each parity bit checks only small fraction of data bits. When the infinite length of the coding block is considered, the capacity with the 0.0045 dB from the Shannon's limit can be achieved. The decoding of LDPC codes is performed iteratively. The information is exchanged between two parts of the decoder: the first one decodes the data bits, the second one – parity bits [61].

The LDPC codes can also be applied to MIMO systems and high spectral efficiency is achieved. The results are only 1.25 dB below the capacity limit what outperforms the MIMO systems with turbo codes [9]. This coding technique seems to be very promising for multiple antenna systems.

1.5. Multiuser MIMO channels

In cellular or wireless local area networks, there are many users who need an access to the radio channel at the same time. Thus, multiple access techniques, like TDMA, FDMA and CDMA (time, frequency and code division multiple access), are developed. The systems with multiple antennas allow the multiple access also in the space dimension.

In a radio network, there are many mobile terminals communicating with the base station or the access point. It is usually expected that the base station can be equipped with multiple antennas, while the mobile terminals are rather single antenna devices. It is caused by many factors. First, the mobile terminals should be cheap and have low complexity. Second, it is more realistic to exchange or rebuild some base stations to boost the network performance in a chosen region than press users to buy new terminals. Finally, the size of the mobile station can be too small to mount the multiple antennas with the required separation. Thus, in the case of

cellular networks, mobile stations are expected to have one or at most two antennas. In wireless local area networks (WLANs), where user terminals, e.g. laptops, are large and expensive units, it is possible to equip them with more, e.g. four antennas. However, even in the worst case, with only single antennas at the mobile terminals, MIMO techniques can be applied very efficiently. The system with n antennas at the base station and K users with single antennas can be seen as a MIMO (n, K) system.

In the uplink, when n mobile terminals transmit simultaneously, their signals can be detected if there are at least n antennas at the base station. This case is similar to the MIMO-LST architecture: n independent substreams can be transmitted and detected when the radio channel is known at the receiver. There is no need for the cooperation between the mobile terminals and they can be unaware of the radio channel. So, multiple antennas create the possibility for a new multiple access technique – space division multiple access (SDMA) in the area of a single base station. Moreover, alike in BLAST architecture, these n substreams can be decoded in turn. In the result, each decoded substream is cancelled from the received signal to suppress the interference during the decoding of the next substreams. The strongest signals, resulting in the strongest interference to other signals, should be decoded and cancelled first. Then, the weaker ones, e.g. from the remote stations, can also be successfully decoded. This technique, called successive interference cancellation (SIC), can be applied with CDMA, also [74].

In the downlink, the migration from MIMO system is not so obvious, as the mobile terminals (receivers) cannot cooperate. Thus, the signals transmitted from n antennas at the base station must be smartly precoded, so each mobile terminal can detect the appropriate one.

The solution of this problem is orthogonal transmit beamforming (Fig. 1.3). For this purpose, the radio channel must be known at the transmitter (base station). All antennas at the base station make one antenna with dynamically shaped pattern. With n antennas, the pattern with $n-1$ nulls can be created. The signal for the specific mobile terminal is transmitted with the pattern with nulls in the directions of other $n-1$ mobile terminals. The signals for n users can be superposed and transmitted at the same time, but with other antenna patterns. Therefore, each mobile

station receives its own signal and the strongly suppressed other signals, as they are transmitted in the null direction of the antenna pattern. In fact, this technique was well known before the interest in MIMO systems [59].

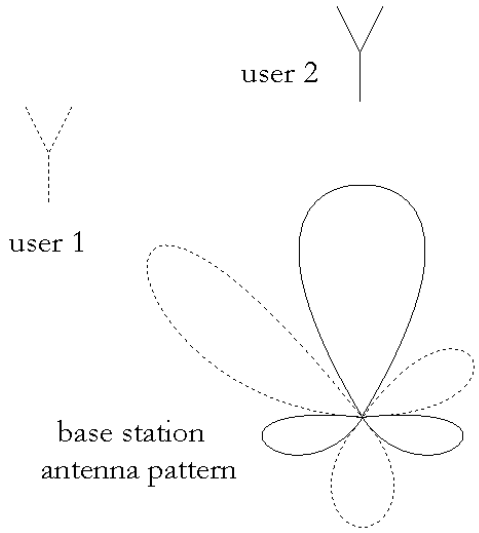

Fig. 1.3. Orthogonal antenna patterns for the communication with different users.

There are also other ideas how to take advantage from additional antennas at the base station. The algorithm, called dirty-paper precoding, was proposed by Costa [13] and later expanded to the multiple antenna case [11]. The transmitted signal is precoded at the base station to avoid the interference at the mobile stations. It exploits the fact that the transmitter (base station) knows how the transmitted signals interfere at the receivers.

If only one mobile terminal is transmitting at the same time, the multiple antennas at the base station can be used to obtain the maximal SNR during the transmission. The antenna pattern is dynamically adapted to achieve maximal possible antenna gain. For that purpose, the maximal ratio combining algorithm can be used. It is described in details in the section 3.6, together with the research results concerning the capacity of WLAN with multiple antennas.

1.6. MIMO systems in frequency-selective radio channels

In a narrowband MIMO system, each radio subchannel can be assumed to be frequency-flat. However, when a system with wide bandwidth is considered, the radio channel is frequency-selective. The problems, existing also for SISO systems, arise. The main challenge is the phenomenon of the multipath propagation resulting in the inter-symbol interference (ISI). If only the channel delay spread is large compared with the duration of the transmitted symbol (in other words: the transmission bandwidth is large in comparison with channel coherence bandwidth), ISI appears. In this case, the delayed replicas of the transmitted signals, which arrive to the receiver, deteriorate the signal detection. In the rich multipath propagation environment the signal detection can be impossible. This issue can be solved by the signal equalisation at the receiver, e.g. like in GSM system. However, the complexity of the equalisation grows exponentially with the number of propagation paths between the transmitter and the receiver. It is even more difficult in MIMO systems where there are $n \cdot m$ radio subchannels.

Two mainly considered techniques to overcome ISI problem in MIMO systems are direct-sequence code division multiple access (DS-CDMA) and orthogonal frequency division multiplexing (OFDM) [49]. In both cases, the whole high data rate stream is divided into many substreams with low symbol rates – each occupying small bandwidth. In DS-CDMA, the data symbols of each substream are summed modulo 2 with a high rate pseudo-random noise (PRN) sequence. In the result, the narrow bandwidth of each substream is spread over the whole wide bandwidth assigned to the transmission of all data substreams. At the receiver, the signal is again summed modulo 2 with the appropriate PRN sequence. As the PRN sequences used for other substreams are different and orthogonal to each other, these substreams can be distinguished and properly decoded. Thus, the transmission of many substreams or access of multiple users to the wireless channel is realised in the code domain. The data substreams have low symbol rate, so ISI can be neglected and the equalisation at the receiver is not required. Moreover, each two versions of one

PRN sequence shifted in time are also orthogonal to each other. Hence, the delayed replicas of the transmitted signal are received as the attenuated noise.

Two main disadvantages of joint MIMO and DS-CDMA concept are usually mentioned, when high-speed broadband networks are discussed. All the signals are spread over the whole bandwidth, so the differences in the fading statistics received by the different users are decreased. Therefore, the efficiency of multiuser diversity technique is limited [49]. Secondly, in CDMA networks, the near-far problem exists [59, 74]. Very careful power control must be implemented in the network. Otherwise, the signals from users located far from the base station are received with unacceptable low SNR.

These problems are not present in OFDM based systems. Here, each data substream is transmitted using a different carrier. A subset of carriers can be chosen for the transmission of the single user to increase his data rate. Despite the fact these carriers overlap in the frequency domain, all the signals can be distinguished at the receiver because of the orthogonality of the carriers. Thus, the whole system is spectrally efficient. From the other side, OFDM is very prone to frequency offset problems [81]. To keep the carriers orthogonal, they must be exactly placed in the frequency domain. The Doppler frequency shifts must be measured and corrected. Of course, as the transmission is maintained at each carrier separately, the radio channel must be estimated for all the carriers. To provide the transmission with the appropriate frequency carriers, digital signal processing with IFFT operation is applied at the transmitter and the complementary FFT is performed at the receiver.

OFDM transforms the frequency selective fading channel into many narrowband flat fading channels. Similarly to DS-CDMA, each substream has low data rate, so ISI does not degrade the transmission performance. Furthermore, in the MIMO-OFDM system, the efficient combination of many techniques can be applied: the orthogonal beamforming at the base station, successive interference cancellation and multiuser as well as frequency diversity with different carriers. In the result, there is strong expectation that joint MIMO-OFDM technique will be the basis for future high-speed data networks [14, 55].

1.7. MIMO systems in standards of wireless networks

Despite the fact that MIMO systems can superbly supplement WLANs and mobile 3G networks, the progress in their integration into telecommunication standards is rather sluggish. In 2003, the IEEE 802.11n Task Group was created to enhance the throughput in 802.11 WLANs by applying MIMO techniques [36]. Some proposals, prepared by different telecom consortia, were submitted, but none of them was accepted. In May 2006, the last proposed draft was rejected, so, in the consequence, the approval of the standard can be expected no sooner than in the middle of 2007. On the other hand, there is strong eagerness for 802.11n standard in the telecommunications market. Some companies, e.g. Dell or Acer, announce their products as being in compliance with draft of the standard.

MIMO systems were also proposed as a part of the future UMTS standard [1]. The MIMO-CDMA radio access (UTRA) link with no more than four antennas at both sides was considered. In the mobile terminal, the smaller number of antennas should be expected. Many transmission techniques were proposed, including spatial multiplexing, Alamouti scheme, transmit beamforming, SDMA, successive interference cancellation and turbo codes. Sometimes, the feedback to the transmitter or its limited version called channel quality indicator is assumed. In the moment of writing this thesis (October of 2006), the abovementioned proposals are still not accepted as an ETSI standard.

1.8. Conclusions

The MIMO concept, presented about ten years ago, was enthusiastically approved by the scientific community. MIMO systems provided the solution for overcoming the well known barriers in wireless communications: the limited spectral efficiency and the low quality of the transmission caused by the fading. While a compromise must be still agreed between these two limitations, the multiple

antennas can boost the system performance in both areas. Nowadays, when the need for mobile broadband multimedia networks is growing continuously [12], MIMO systems fill the important gap in the variety of wireless systems.

The idea of MIMO turned out to be difficult to implement in wireless systems. Great performance is paid with the increased signal processing and power consumption both at the transmitter and the receiver. Moreover, the precise channel knowledge is usually needed for the system to work properly. Despite the years of the research, many issues are still not clear and more efficient solutions are desired. The research in the whole MIMO area is still in progress.

As this thesis is concentrated on time variations in MIMO channels, the problems concerning just these topics will be discussed in the next chapters. The issues of the MIMO channel, like multipath propagation, channel modelling, estimation and time variations will be described in details. Then, the results of the author's research will be presented. The capacity calculations for quasi-stationary indoor MIMO channels will be provided. Finally, the problem of channel estimation in fast time-varying radio channel and the proposed Iterative Channel Estimation algorithm will be explained.

All exact science is dominated by the idea of approximation.

Bertrand Russell

Chapter 2

Radio channel in MIMO systems

The radio propagation channel is the physical basis of each radio system. It is also the element that cannot be changed or designed when the specific system is planned and built. The radio system must be adapted to the radio channel. Hence, the knowledge about the radio channel is crucial for proper system design. It is especially important in the MIMO systems where $n \cdot m$ subchannels exist.

Because of the multipath propagation, the radio channel cannot be modelled as a channel gain and a propagation delay, only. The accurate model must take into consideration the strengths and the delays of the individual components of the transmitted signal that arrive to the receiver by many paths. In MIMO systems, the correlation between the transfer functions of different subchannels is also very important, as it influences the capacity of the whole system.

Finally, time variations of the MIMO channel should be considered. Nowadays, the wireless systems are planned also for the users moving at high speed, e.g. in the fast cars or trains. In fast varying radio channels, a new problem arises: the channel knowledge should be updated very frequently to keep it accurate. Another goals should be set for the radio system design depending on whether the channel is slow or fast varying.

In this chapter, the channel aspect of MIMO systems is analysed. The problems of channel modelling and estimation are covered. The issues of the channel variations are particularly addressed. Some research efforts for slow and fast varying channels are discussed as an introduction to the results reported in the next two chapters.

2.1. Multipath propagation in MIMO systems

The multipath propagation is generally regarded as a malady of wireless communication systems. In the effect of multiple interfering radio waves the signal can be strongly faded. Moreover, as the path lengths of the radio waves are usually very different, the signal is spread in time and inter-symbol interference appears – it was mentioned in the section 1.6.

Though, for MIMO systems, the multipath propagation is an advantage which increases the possibility to achieve high diversity or multiplexing gain. If the signals transmitted from Tx antennas were received only by line-of-sight (LoS) path, they would be strongly correlated. It can be understood with the aid of Fig. 2.1. The propagation paths are very long in comparison with the antenna separations. Thus, these paths are nearly parallel, even if the separations are equal to $10 \div 20$ wavelengths. Both transmitted signals are received on both Rx antennas with nearly the same amplitude. The antenna R_2 receives the signals with the phases shifted in comparison to the antenna R_1, but the phase shift is the same for both transmitted signals, as both propagation paths are lengthened by the same distance d. The signal received by the antenna R_2 is nothing more than signal from the antenna R_1, but with the changed phase. So, the channel matrix has rank 1. In the result, the signals would be difficult to separate at the receiver and the fading of the subchannels would be also correlated.

The situation is different, when the radio signals propagate from the transmitter to the receiver by two paths, e.g. the direct path and the reflected one (Fig. 2.2). Now, the radio waves arrive to the receiver from two different directions.

The reflected waves interfere with the direct waves and, in the result, all the transfer functions have different amplitudes and phases. In this case, the rank of channel matrix is equal to 2 and both transmitted signals can be separated at the receiver. In the MIMO (n,m) system, at least $\min[n,m]$ propagation paths between the transmitter and the receiver should exist to achieve the full rank of the channel matrix which is equal to $\min[n,m]$. Hence, the number of these paths is an additional limitation for the possibility of transmitting multiple independent streams in the MIMO system. Together with the number of Tx antennas and number of Rx antennas, number of the propagation paths is the lower bound for multiplexing gain. These paths should be resolvable as different ones, so their angles of departures and angles of arrivals should also differ significantly. Large angular spread of transmitted and received signals increases the MIMO channel capacity and allows for smaller antenna separations [74].

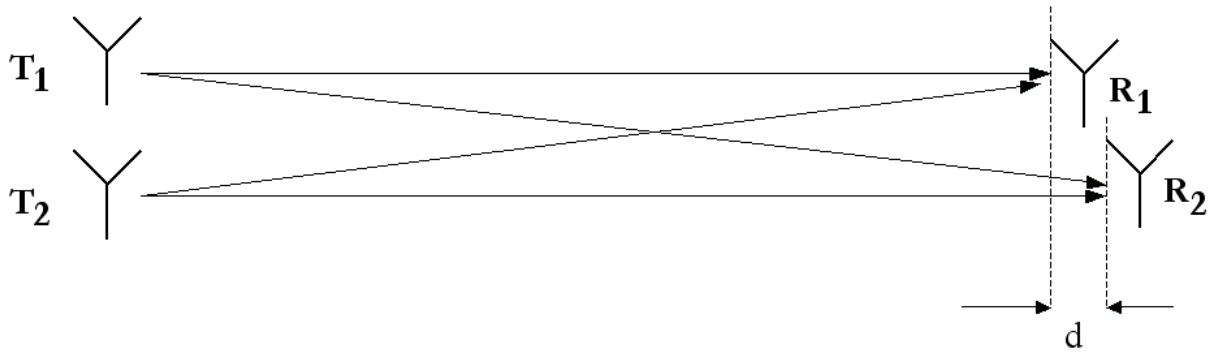

Fig. 2.1. MIMO (2,2) system with LoS propagation only.

The multipath propagation is crucial for MIMO systems. The spatial multiplexing and, in consequence, increased transmission rate is not possible without richly scattered environment where the multipath propagation occurs. This is the reason why MIMO systems perform very well in an indoor and micro-urban environment where there are many walls and other obstacles which reflect radio waves. Some numerical calculations confirming these statements are presented in the section 3.7.

2.2. MIMO channel models and propagation prediction

The design of a wireless system requires the knowledge about the radio propagation in the environment. It can be obtained either through the measurements or by applying the propagation models. The measurements are, in general, very expensive and time-consuming, so it is impossible to perform such experiments before each system planning and configuration changes. It is why the huge amount of propagation channel models were proposed. Despite the fact they cannot illustrate each radio channel so accurately as the measurements, they are extremely useful when a wireless system is planned, rebuilt or tested. Surprisingly, for some applications they are more useful than measurements.

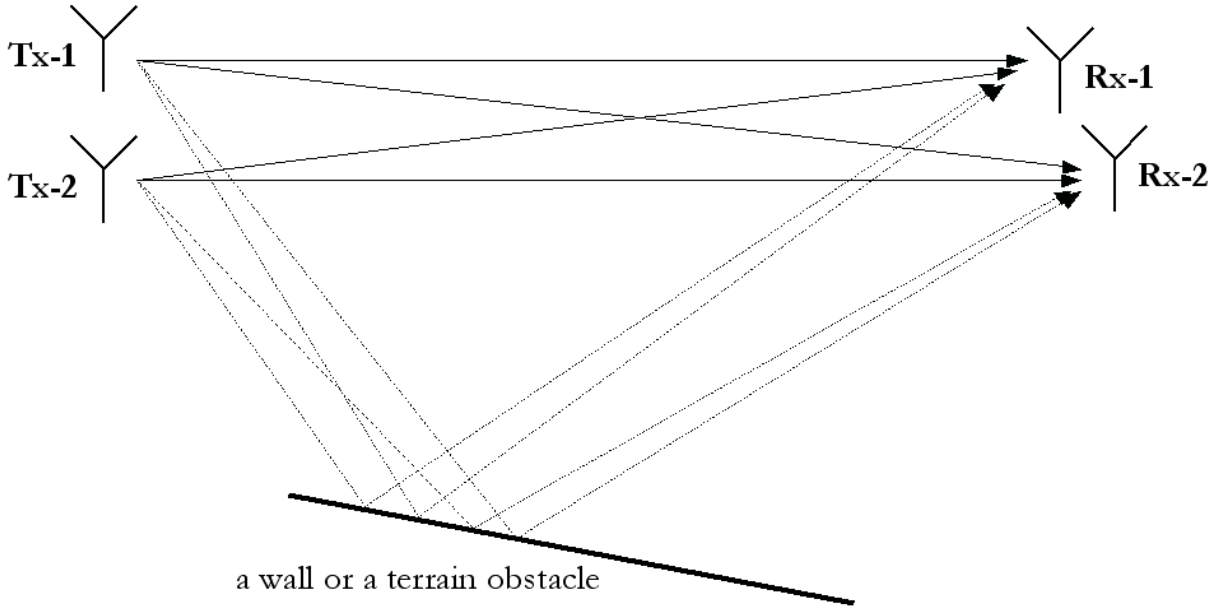

Fig. 2.2. MIMO (2,2) system with propagation by two paths.

As in SISO wireless systems, the channel modelling and radio propagation prediction are fundamental parts of the research in the MIMO area. Both site-specific and site-independent models are required. Site-specific models, where the environment with all objects and terrain obstacles is clearly and exactly defined, play the key role in the accurate network planning for the specific area. By contrast, when a wireless system is designed and some particular techniques are tested, the site-

independent model is usually used, where the environment is only defined in general, but the important characteristics and MIMO channel features are correctly addressed.

Multiple antenna systems are difficult to model not only because of the large number of antennas and, in consequence, large number of transfer functions. The essential issue is the correlation between the different transfer functions. The particular subchannels in a MIMO system cannot be modelled separately on the basis of well known models for SISO channels. This correlation, usually in the relationship with the antenna separation and the richness of scattering and multipath propagation, should be additionally considered.

Generally, there are two main approaches to wireless channels modelling. The first one is stochastic, where the parameters describing the MIMO channels are random variables from some probability distributions chosen on the basis of many measurements and observations. With stochastic methods, a MIMO channel can be modelled very fast – these methods are well suited for site-independent modelling, when a MIMO system or its part is tentatively evaluated and tested.

The second approach is deterministic. The deterministic methods usually need a large database with the information concerning the environment – geometric and electromagnetic data about the objects in the vicinity of the considered radio system. This data is used to calculate the desired channel parameters. These methods have good accuracy and are suitable for site-specific modelling. However, they are rather complex and need long computation time. Moreover, the appropriate and exact database is sometimes impossible to create. Despite these disadvantages, deterministic methods are becoming commonly used due to their ability to analyse very large structures with high precision.

Below, some MIMO channel models and propagation prediction techniques are presented. Both stochastic and deterministic methods are considered. Some difficulties concerning MIMO channel modelling and the proposed solutions are also reported.

2.2.1. Stochastic models

One of the most simple but also the most popular stochastic MIMO channel models is the Rayleigh model [22] based on its SISO version. The MIMO channel is assumed to be narrowband, so the transfer function of each subchannel can be described as a single complex value. The channel transfer matrix consists of i.i.d. (independent identically distributed) entries. Their amplitudes are given by Rayleigh distribution with zero mean and unit variance [37]. Their phase is uniformly distributed within the $\langle 0,2\pi \rangle$ range. In other words, both real and imaginary parts of each transfer function are modelled as independent Gaussian random variables with zero mean and variance equal to $0.5\sqrt{2}$. The entries of the matrix $\boldsymbol{H}$ are also called zero-mean unit-variance circularly symmetric complex joint Gaussian random variables. The channel gain is assumed to be equal for all subchannels and is extracted from the matrix $\boldsymbol{H}$. So, the i.i.d. Rayleigh model is extremely simple to implement. It is widely used for NLoS environments where the transmit and receive antenna separations are large enough to assume the lack of correlation between the subchannels. Obviously, it cannot be applied when the particular propagation conditions are going to be modelled, but it is widely accepted for the simulations when the richly scattering environment is assumed. This model is also used for the simulation described in the chapter 4.

During the European Union IST SATURN and METRA projects, the Kronecker product channel model was presented and verified [41, 82, 84]. As the Rayleigh model, it is the stochastic description of a NLoS environment. However, the correlation between the channel matrix entries is taken into account. The whole channel transfer matrix is modelled as:

$$\boldsymbol{H} = \left(\boldsymbol{R}_{\boldsymbol{H}}^{\boldsymbol{Rx}}\right)^{1/2} \cdot \boldsymbol{G} \cdot \left[\left(\boldsymbol{R}_{\boldsymbol{H}}^{\boldsymbol{Tx}}\right)^{1/2}\right]^{\mathrm{T}}, \tag{2.1}$$

where $\boldsymbol{G}$ is the $m \times n$ matrix with the i.i.d. Rayleigh distributed entries and $\bullet^{1/2}$ denotes any matrix square root such that $\bullet^{1/2} \cdot \left(\bullet^{1/2}\right)^{H} = \bullet$. The matrices $\boldsymbol{R}_{\boldsymbol{H}}^{\boldsymbol{Tx}}$ and $\boldsymbol{R}_{\boldsymbol{H}}^{\boldsymbol{Tx}}$ are covariance matrices for the transmit and receive arrays, respectively. These matrices are defined as:

$$\boldsymbol{R}_{\boldsymbol{H}}^{\boldsymbol{Tx}} = E\left\{\left(\boldsymbol{h}_i^{*} \cdot \boldsymbol{h}_i\right)^{\mathrm{T}}\right\},\ \ i \in \{1, 2, \ldots, n\} \tag{2.2}$$

$$\boldsymbol{R}_{\boldsymbol{H}}^{\boldsymbol{Rx}} = E\left\{\boldsymbol{h}^{j} \cdot \left(\boldsymbol{h}^{j}\right)^{*}\right\},\ \ j \in \{1, 2, \ldots, m\} \tag{2.3}$$

where $E\{\cdot\}$ denotes the expectation value, $\boldsymbol{h}_i$ and $\boldsymbol{h}^j$ are i-th row and j-th column of matrix $\boldsymbol{H}$, respectively. The main assumption of this model is that the correlation between the transfer functions for different Rx antennas is independent from the Tx antennas and vice versa. It allows calculating the Tx covariance matrix for any row of matrix $\boldsymbol{H}$ and the Rx covariance matrix for any column of $\boldsymbol{H}$, as in the equations (2.2) and (2.3). The total channel covariance matrix can be approximated as:

$$\boldsymbol{R}_{\boldsymbol{H}} = \boldsymbol{R}_{\boldsymbol{H}}^{\boldsymbol{Tx}} \otimes \boldsymbol{R}_{\boldsymbol{H}}^{\boldsymbol{Rx}}. \tag{2.4}$$

where $\otimes$ denotes the Kronecker product of the matrices.

If the multipath components of the received signal are uniformly distributed in the angle in the plane of azimuth, the elements of both $\boldsymbol{R}_{\boldsymbol{H}}^{\boldsymbol{Tx}}$ and $\boldsymbol{R}_{\boldsymbol{H}}^{\boldsymbol{Rx}}$ matrices can be computed as [37, 38]:

$$r_{ij} = J_0\left(\frac{2\pi}{\lambda} \cdot \left\|\boldsymbol{x}_i - \boldsymbol{x}_j\right\|\right), \tag{2.5}$$

where $J_0(\cdot)$ is zero-order Bessel function of the first kind, $\boldsymbol{x}_i$ and $\boldsymbol{x}_j$ are the coordinates of the i-th and j-th antenna in the appropriate array and $\|\cdot\|$ is the vector norm.

If the wideband MIMO channel is considered, the transfer function of each subchannel cannot be described by its amplitude and phase, only. By the analogy to SISO channels, one can expect that each transfer function is the sum of many delayed taps resulting from many multipath components of the transmitted signal. In the wideband Kronecker product model [58, 83, 84], the MIMO channel transfer matrix is characterized as a sum of L matrices, each associated with one tap:

$$\boldsymbol{H}(t) = \sum_{l=1}^{L} \boldsymbol{H}_l \cdot \delta(t - \tau_l), \tag{2.6}$$

where $\delta(\cdot)$ denotes Dirac delta function. Each matrix $\boldsymbol{H}_l$ is constructed as in the narrowband model. The power of each tap can be determined from the average power delay profile. This profile is, generally, exponential and it can be obtained

from the measurements performed during the SATURN and METRA projects or other measurements campaigns reported in open literature. So, the transfer function of each subchannel is modelled as a sum of L multipath components. The time delays of these components are the same for each subchannel, but they have different amplitudes. Such model can be reasonable in the situation when the dimensions of the Tx and Rx antenna arrays are small in comparison with the distance between the transmitter and the receiver. In this case, the propagation paths are generally the same for all the subchannels.

Because of its simplicity, the Kronecker product model was very attractive for the initial analysis of the indoor MIMO systems. However, its main weakness lays in its basic assumption: the separation of the correlation properties at both sides of the link leads to the errors increasing with the number of the antennas [38]. Hence, currently, the applications of this model are rather limited. Recently, another stochastic model, the generalisation of the Kronecker one, was proposed and verified by the measurements [79]. It avoids the above mentioned erroneous assumption, but it can be simplified to the Kronecker model in the special case when the correlation properties at the Tx and Rx antennas are really separable.

Modelling of the transfer functions for each subchannel, as well as the correlation between them may not suffice for the proper MIMO channel assessment. When the orthogonal beamforming and other directional techniques are considered, the analysis of the directions of departures (DoDs) of the rays launching from the transmitter and directions of arrivals (DoAs) to the receiver is essential. It is also the main motivation of the double-directional model [65]. The transfer function of each subchannel is represented as a sum of the multipath radio components distinguished by their delay, DoD and DoA. On this basis, the whole channel matrix can be calculated and, moreover, the information required for the beamforming techniques is not wasted.

Some attention in MIMO channel modelling area was also drawn by the stochastic cluster models. In the well known Saleh-Valenzuela model [63] suitable for stationary indoor environments, it is assumed that the multipath components arrive to the receiver in clusters. The taps in a single cluster can be associated with the radio

rays reflected from a single object. The power of the taps within each cluster decays exponentially with the time. The mean power of the clusters also decays exponentially as the clusters are delayed. The Saleh-Valenzuela model was extended to analyse the DoDs and DoAs of radio rays and adapted for MIMO channels [39].

However, treating the channel transfer function as a mere sum of radio rays seems questionable. The impulse responses of the radio channels consist of some strong multipath components but they also contain the energy of the radiation diffused and scattered in the vicinity of the transmitter and the receiver. In many cases – especially outdoor environments, this diffused background energy cannot be neglected. Some solutions to this problem can be found in [62]. It was proposed to model the diffused and scattered energy as a component that decays exponentially in time and is added to the power delay profile of the received signal. The example of power delay profile illustrating the above mentioned phenomena is presented in Fig. 2.3 [7].

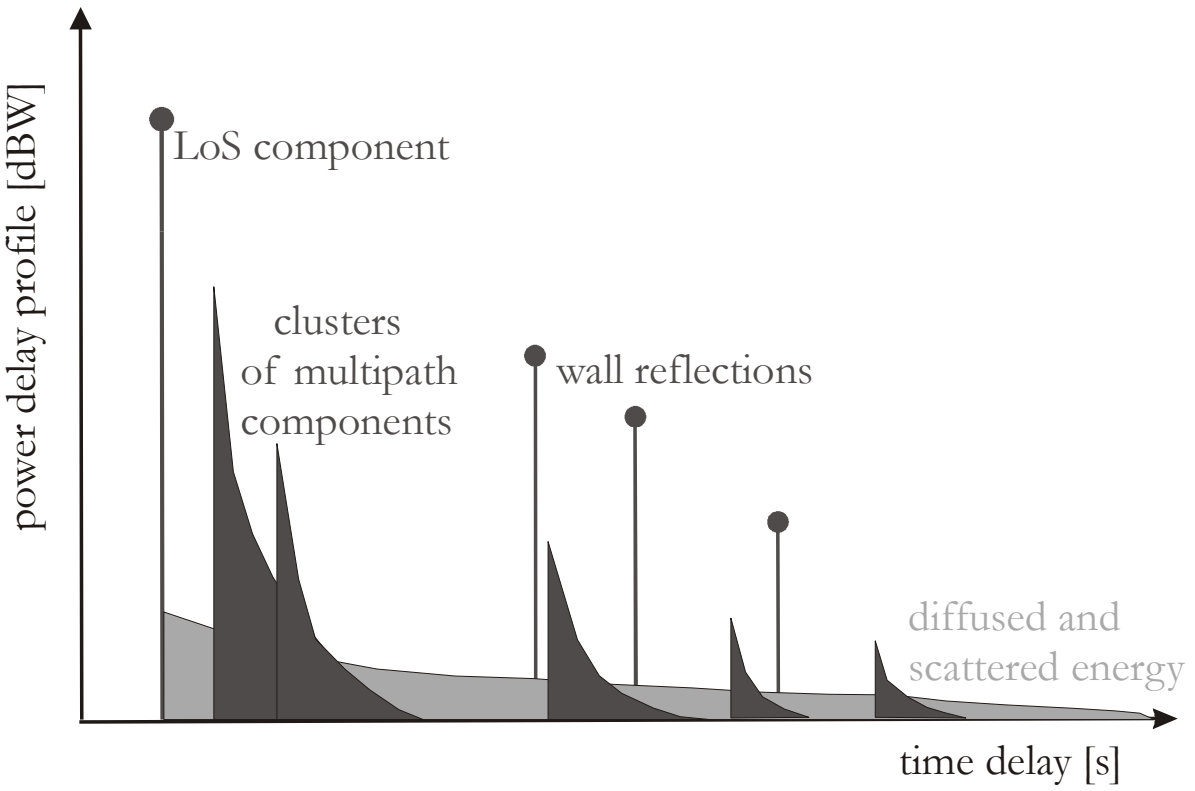

Fig. 2.3. The propagation phenomena shown on the schematic power delay profile of a radio channel.

The proper modelling of MIMO channels was one of the main research areas of the COST 273 project that has been recently ended. As a result of the activities of the group directed by A. Molisch, a new generic model was proposed and described in the final report of the COST project [12]. The model was designed for mobile MIMO systems in general, so the macro- and microcells typical for cellular networks were considered as well as picocells and ad-hoc structures suited for WLANs. This model can substitute ETSI 3GPP spatial channel model [2]. In both cases, the similar modelling approach is adopted, but the COST model describe more propagation environments and is more extended. The core of the COST 273 model is the same for all analysed environments what facilitates its implementation. Its main goal is to generate the double-directional impulse response for all the MIMO subchannels. The cluster nature of the propagation and observed correlation between DoDs and DoAs are taken into consideration. The clusters consist of the radio rays propagating from the Tx to the Rx antenna by many ways. LoS propagation, the single interaction with the closely or remotely located objects and some paths with multiple reflections are modelled. The diffused background energy is also incorporated. As the mobile channel is modelled, the stochastic occurrence of some elements is assumed, e.g. LoS component or some clusters can exist only for a short period of time. Both signal polarisations, as well as the effect of cross polarisation discrimination are analysed. The model is based on the external parameters characterising the described environments. These parameters were determined during the project measurements or were taken from the open literature. The model was implemented in Matlab and is free available [71].

2.2.2. Deterministic models

When the specific location of the wireless system should be analysed, stochastic channel models do not suffice to follow all the topology details of the system and the environment. This fact motivates for developing the deterministic methods of radio propagation prediction where the data about the specific location of the system and the objects in its vicinity can be applied.

The most accurate deterministic models are field-theoretical. The amplitude and the phase of radio signal can be calculated by solving Maxwell's equations with appropriate boundary conditions. These boundary conditions are the results of the existence of walls and other obstacles in the radio propagation environment. However, this approach is very difficult computationally. Thus, it is usually applied only to the analysis of the electromagnetic field in a small area, e.g. in the near field of a designed antenna. Instead, the group of the models based on geometric optics is widely used [20, 48, 52]. These models approximate the propagation of the electromagnetic waves using optical phenomena, like reflection, refraction and diffraction. Usually, the propagation media, e.g. the air and the walls are assumed to be homogeneous, isotropic and linear. Consequently, the radio rays are assumed to propagate along the straight lines. When the wall or other obstacle is encountered, the wave is split into two waves, the reflected one and the transmitted one, with appropriate angles and attenuation coefficients. To enhance the model accuracy, the diffraction on the edges and wedges can be considered. It allows calculating the signal power in shadow regions. The importance of diffraction effect decreases with the increasing frequency, e.g. it is negligible at 60 GHz. These models are also referred as the algorithms because of their deterministic nature.

Geometric optics based models are very well suited for the design of indoor wireless systems. An indoor environment can be described as a set of walls, floors, ceilings and furniture with many flat surfaces. The geometric optics can be easy applied. For an outdoor environment, these algorithms are hardly applicable, except of typical urban cases, particularly street canyons.

The radio propagation can be described with geometric optics only if the two following conditions are met. First, the wavelength should be much smaller than the dimensions of the walls. Second, according to the Fraunhofer criterion, the wavelength should be large in comparison to the size of irregularities on the surface of walls or other reflectors:

$$\sigma \leq \frac{\lambda}{32\cos\theta}, \tag{2.7}$$

where σ is the root mean square of the height of the irregularities on the surface and θ is the incident angle.

For the radio frequencies used in indoor WLANs ($2 \div 6\,\text{GHz}$) the above criterion is well met – the wavelength is equal to $5 \div 15\,\text{cm}$ and the inner side of the walls is rather smooth. In the case of UMTS system (2 GHz) working in an urban environment it could be more questionable, as outer sides of walls and the vegetation have rather rough surfaces. Then, the scattering effects should also be considered.

There are many geometric optics based algorithms [20]. The first one, called shadowing, is based on the calculation of the wave front generated by a transmit antenna and, then, reflected by walls. This algorithm is easy to imagine but, as well as solving Maxwell's equations, expensive computationally. There is also a group of methods based on ray launching. The radio wave transmitted by a Tx antenna is divided into the rays with the specific spatial separation. The spatial separation of the rays increases linearly with the distance, so the rays are split if it is found necessary. Also, the rays are split when a reflection occurs – the reflected and transmitted rays are created. These rays which reach the receive antenna are summed up, considering their amplitudes and phases.

In this thesis, the ray tracing with the method of images is used to predict the radio propagation [52]. In this algorithm, possible paths between transmit and receive antennas are sought. The images of the transmit antenna are created to check if the rays can reflect from the walls and reach the receive antenna. The basic idea of the method of images can be understood with the aid of Fig. 2.4. The antenna $T^{|}$ is the image of the transmit antenna T relative to the wall B. The straight line between $T^{|}$ and receive antenna R crosses the wall B, so the path between T and R with the single reflection from wall B is possible and this ray exists. The analysis of the multiple reflections is similar. To check the path between T and R with double reflection (the walls A and B), the image of T relative to the wall A should be created, and then, the image of this image relative to the wall B should be determined. The result is the antenna $T^{||}$. Next, the straight line between $T^{||}$ and R is checked. This line crosses the wall $A^{|}$ (the image of the wall A relative to the wall B) and wall B, so this ray also exists.

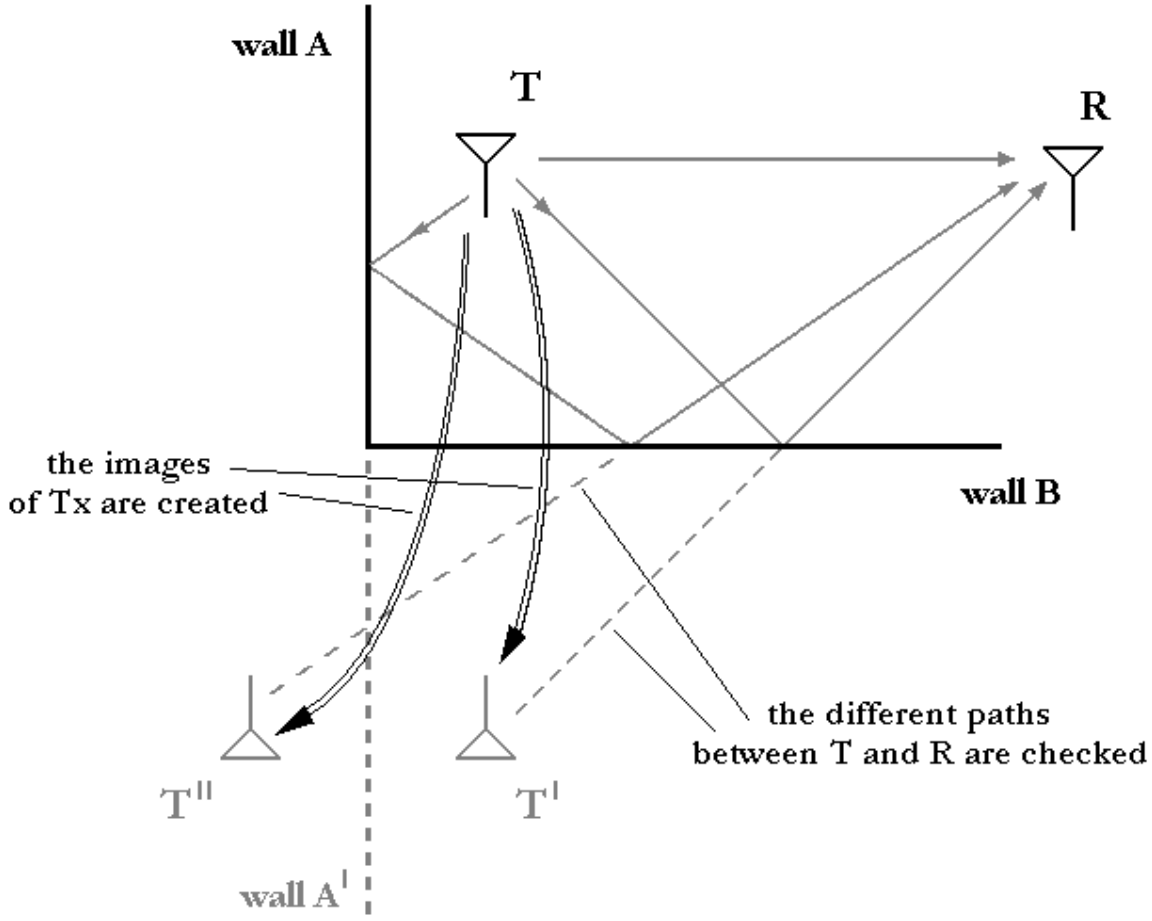

Fig. 2.4. The illustration of the method of images.

The 3-D ray tracing algorithm with the method of images can be applied to determine the possible paths between each Tx and Rx antenna pair. The transfer function h_{ij} between j-th Tx antenna and i-th Rx antenna can be computed as:

$$h_{ij} = h_{ij1} + h_{ij2} + ... + h_{ijk}, \tag{2.8}$$

where h_{ijx} is the element of the transfer function associated with the ray propagating by x-th path between j-th transmit antenna and i-th receive antenna, k is the number of the considered radio paths between transmit and receive antennas. The elements h_{ijx} consist of the real and imaginary parts, so they should be summed with the respect to their amplitude and phase. To calculate the full channel transfer matrix $\boldsymbol{H}$, the transfer functions between all the Tx antennas and all the Rx antennas should

be calculated. As the system is assumed to be narrowband, each h_{ijx} can be calculated as:

$$h_{ijx} = G_{ijx} \cdot P_{ijx} \cdot \frac{\exp(-j2\pi\, l_{ijx})}{l_{ijx}} \cdot \prod_{r=1}^{k} R_{ijxr}\,, \tag{2.9}$$

where G_{ijx} is the factor that incorporates the effects of transmit and receive antenna gain, P_{ijx} is the result of the projection of the wave polarization vector on the receive antenna polarization vector, l_{ijx} is the length of the path divided by the wavelength and R_{ijxr} is the reflection coefficient for r - th reflection.

When the reflected ray, i.e. the path with at least one reflection is analysed, each reflection should be carefully considered. For each reflection, the wave polarization vector should be resolved into two components: perpendicular ($\perp$) and parallel ($||$) to the plane of incidence. The assumption is made that the walls, the floor and the ceiling are dielectric and their relative permeability is equal to 1. In this situation, the reflection coefficients for both vectors have the following values [60]:

$$R_{\perp} = \frac{\cos\theta - \sqrt{\varepsilon_r - \sin^2\theta}}{\cos\theta + \sqrt{\varepsilon_r - \sin^2\theta}}, \tag{2.10}$$

$$R_{\parallel} = \frac{\varepsilon_r \cdot \cos\theta - \sqrt{\varepsilon_r - \sin^2\theta}}{\varepsilon_r \cdot \cos\theta + \sqrt{\varepsilon_r - \sin^2\theta}}, \tag{2.11}$$

where ε_r is the dielectric constant and θ is the angle of incidence. After multiplication by the reflection coefficients, both vectors should be added. Some issues concerning the accuracy of this ray tracing algorithm are discussed in the chapter 3, where it is applied to the calculations of the capacity in the indoor environment.

In some cases, the ray tracing algorithm may be more useful to analyse a MIMO propagation channel than any measurements – even if there is a possibility to take them. If beamforming techniques are planned and the distribution of DoDs and DoAs is required, such an information can be easily obtained from the ray tracing data. To extract the DoD and DoA distributions from measurements, the additional techniques, like MUSIC or ESPRIT, must be applied.

2.3. Time-varying radio channels

When a radio channel is observed in the long time perspective, some changes in its state can occur. Three main situations are usually distinguished what results in three different channel modelling approaches. First, the radio channel can be stationary. It means that the radio channel is static – it can be described by the same channel transfer matrix despite the passage of time. This case is rather theoretic in the era of the modern wireless systems, since the user terminals and the objects in the propagation environment change their positions frequently.

In the second case, the changes in the radio channel are slow. Mobile terminals are moving leisurely, e.g. carried by pedestrians. They can even have fixed positions, but there are some small changes in their vicinity. Such a radio channel is called quasi-stationary. It varies so slowly that is can be assumed stationary during a long time period. After this period, some modifications should be applied to the channel characteristics to properly model the channel variations. Then, the channel is stationary during the next time period. Such an assumption simplifies the analysis of the channel variations. The radio channel is de facto treated as stationary. The pace of the variations is modelled by the length of the time period. If the time period is sufficiently long, e.g. the duration of thousand transmitted symbols, the time wasted for the channel estimation can be neglected – it is described in details in the next section. The quasi-stationary channels are sufficient to describe the indoor radio propagation, e.g. in WLANs, where the mobility of the terminals is limited.

In the third case, the channel variations are rapid. The assumption about quasi-stationarity cannot be held. Some changes in the channel characteristics happen between each two transmitted symbols. This situation is probable in the cellular networks where people can move very quickly with their mobile phones, e.g. by a car or a fast train.

As mentioned in the chapter 1, in the first papers about MIMO systems it was assumed that the radio channel was stationary or quasi-stationary. This assumption

is the result of the fact that the actual channel state information should be known at the receiver. In a fast varying MIMO channel, it can be the serious problem.

To investigate fast varying radio channels, the changes in the channel transfer matrix should be appropriately modelled. As fast varying Rayleigh channels are the subject of the analysis in the chapter 4, the simple model describing this type of the channel will be now presented.

The variations of the channel can be modelled by the correlation coefficient C between the transfer functions in the two periods of time when the two subsequent symbols are transmitted:

$$C = E\left\{h_i \cdot h_{i+1}^*\right\}, \tag{2.12}$$

where h_i is the transfer function in the time of transmission of i-th symbol. Functions h_i and h_{i+1} should be zero-mean unit-variance circularly symmetric complex joint Gaussian random variables. Thus, h_{i+1} can be calculated on the basis of h_i as:

$$h_{i+1} = C \cdot h_i + \sqrt{1-C^2} \cdot g_{i+1}, \tag{2.13}$$

where g_{i+1} is auxiliary zero-mean unit-variance circularly symmetric complex joint Gaussian random variable independent of h_i.

The equation (2.13) allows generating the sequence of random variables. Moreover, the correlation between two subsequent random variables is equal to *C*. It can be quickly proven, as this correlation is equal to:

$$E\left\{h_i \cdot h_{i+1}^*\right\} = E\left\{C \cdot h_i \cdot h_i^* + \sqrt{1-C^2} \cdot h_i \cdot g_{i+1}^*\right\} = C \cdot E\left\{h_i^2\right\} + \sqrt{1-C^2} \cdot E\left\{h_i \cdot g_{i+1}^*\right\} = C \tag{2.14}$$

Furthermore, h_{i+1} is the random variable with the same distribution as h_i and g_{i+1}. $\mathrm{Re}\{h_{i+1}\}$ is the sum of $\mathrm{Re}\{h_i\}$ and $\mathrm{Re}\{g_{i+1}\}$ with appropriate coefficients. They are Gaussian random variables, so $\mathrm{Re}\{h_{i+1}\}$ is also Gaussian random variable [19]. The analogous statement for $\mathrm{Im}\{h_{i+1}\}$ is also truth. Also, h_{i+1} has the same mean value and variance as h_i and g_{i+1}. The mean of $\mathrm{Re}\{h_i\}$ and the mean of $\mathrm{Re}\{g_{i+1}\}$ are both equal to 0, so the mean of $\mathrm{Re}\{h_{i+1}\}$ is also equal to 0. If the variance of $\mathrm{Re}\{h_i\}$ (and the variance of $\mathrm{Re}\{g_{i+1}\}$) is denoted as σ_i^2, the variance of $\mathrm{Re}\{h_{i+1}\}$ is equal to:

$$\sigma_{i+1}^2 = E\left\{\mathrm{Re}^2\{h_{i+1}\}\right\} = E\left\{\left(C\cdot\mathrm{Re}\{h_i\} + \sqrt{1-C^2}\cdot\mathrm{Re}\{g_{i+1}\}\right)^2\right\}$$

$$\sigma_{i+1}^2 = E\left\{C^2\cdot\mathrm{Re}^2\{h_i\} + C\cdot\sqrt{1-C^2}\cdot\mathrm{Re}\{h_i\}\cdot\mathrm{Re}\{g_{i+1}\} + (1-C^2)\cdot\mathrm{Re}^2\{g_{i+1}\}\right\}$$

$$\sigma_{i+1}^2 = C^2\cdot\sigma_i^2 + C\cdot\sqrt{1-C^2}\cdot E\left\{\mathrm{Re}\{h_i\}\cdot\mathrm{Re}\{g_{i+1}\}\right\} + (1-C^2)\cdot\sigma_i^2$$

$$\sigma_{i+1}^2 = C^2\cdot\sigma_i^2 + C\cdot\sqrt{1-C^2}\cdot 0 + (1-C^2)\cdot\sigma_i^2$$

$$\sigma_{i+1}^2 = \sigma_i^2 \qquad (2.15)$$

Again, the similar derivation can be followed for the imaginary parts of these random variables.

In the MIMO Rayleigh channel, the subchannels are independent from each other, so the variations of each subchannel are also modelled independently according to the equations (2.12)÷(2.14). The reasonable assumption is that correlation coefficient is equal for all the subchannels.

The above mentioned model allows describing the pace of the channel variations by the single parameter C. According to the Jakes' model, this parameter can be associated with the velocity of the mobile terminal [37]:

$$C = J_0\left(\frac{2\pi f v \tau}{c}\right), \qquad (2.16)$$

where f is the carrier frequency, v is the velocity of the terminal, τ is the time duration of one symbol and c is the speed of light. Hence, the larger the velocity of the terminal and the time duration of each symbol, the greater the pace of the channel variation is. It is particularly significant in a narrowband channel or in OFDM systems, where there are many parallel narrowband transmissions.

As an example, an OFDM system operating at the carrier frequency of 2 GHz is considered, where the bandwidth allocated for the one carrier is equal to 10 kHz. Thus, the time duration of one symbol is 100 μs. The values of C and the related velocities v are presented in Table 2.1.

The equation (2.13) is the basis of modelling the radio channel variations in the chapter 4. The MIMO Rayleigh channels with C equal to 0.999, 0.99 and 0.9 are simulated. It will be shown that the transmission in the radio channels with $C < 0.9$ is impossible with $\mathrm{BER} < 10^{-2}$.

Table 2.1.

The values of the correlation coefficient and the related velocities of the mobile terminal for f = 2 GHz and τ = 100 μs.

C	v [km/h]
0.999	54
0.99	172
0.9	551

2.4. Channel estimation

In MIMO systems, the channel transfer matrix $\boldsymbol{H}$ is usually assumed to be known at the receiver, sometimes also at the transmitter. Behind this assumption, there is a need for channel estimation algorithms where the channel matrix could be calculated.

The common method for all wireless systems is sending the training sequence, also called pilot signal, among the data symbols. The training sequence consists of the symbols known at the receiver. The receiver performs the operation of calculating the channel transfer matrix. Contrary to the data decoding, the channel coefficients are calculated on the basis of known data symbols. These channel coefficients are later used to decode the data symbols.

In a MIMO (n,m) system, the channel estimation is more difficult than in a SISO system, because of many entries in the channel transfer matrix which should be estimated. Generally, in narrowband systems, where the transfer function of each subchannel can be described as a single complex value, at least n training vectors should be transmitted to estimate the matrix $\boldsymbol{H}$ properly. In wideband systems, where the transfer function of each subchannel is the sum of many taps, the estimation process is even more complicated.

Naturally, there are some errors of the channel estimation because of the radio noise. To increase the estimation accuracy, the power of training sequence can be enlarged, even at the cost of the power of the data symbols. Also, its length can be

expanded. It allows performing the channel estimation multiple times and taking the average value.

Having the channel state information known at the transmitter is more complex. If the transmission is performed in the same frequency band in both directions, as in time division duplex, it does not present a challenge. The matrix $\boldsymbol{H}$ estimated at the receiver is actual also for the transmission in the opposite direction. But, in frequency division duplex systems, such an assumption cannot be held. The matrix $\boldsymbol{H}$ estimated at the receiver must be retransmitted to the transmitter in the feedback channel. It involves the delay, hence it is generally not applicable when the radio channel is fast varying. It is also possible to retransmit some general simplified information about the radio channel instead of full channel transfer matrix. This limited information can also help to adapt the transmitted signal to the propagation conditions. Besides, the recent research in this subject leads to the surprising conclusion that the time needed for the transfer of the channel state information to the transmitter is decreasing with the number of Tx antennas [50].

The training sequences limit the spectral efficiency of the system. The data rate is decreased, because the time is wasted for the transmission of known symbols. When radio channel is varying slowly, it is a minor problem. In this case, the radio channel can be assumed quasi-stationary and, in consequence, invariant during a long time period. The channel estimation performed once per this period is enough to effectively track the channel. If this period is long, the time wasted for the training sequence is negligible. In these systems, the assumption about perfect channel knowledge, even at the transmitter, is reasonable. If the power of training symbols can be different than the power of data symbols, the optimal length of the training sequence (in symbols) is equal to the number of transmit antennas [30]. If these two power levels are required to be equal, the optimal length of training sequence may be larger. As the larger number of transmit antennas implies the need of longer training sequences, huge number of transmit antennas can be even sub-optimal for the system performance.

When the radio channel is fast varying, this problem is even more serious. It is impossible to assume channel invariance, how ever short would be the considered

period. The optimal length of training sequence can be different than suggested in [30]. If the training sequence is lengthened from its minimal value, there are three consequences of that fact:

a. the influence of the noise in the transmission is reduced,
b. the estimation becomes less adequate because of the channel variations,
c. there is less time for the transmission of data.

Hence, there is a tradeoff between (a) and (c), especially when the average SNR is low. The channel can be estimated more accurately, but the spectral efficiency decreases in the result. Moreover, in the really fast varying channels, long training sequences can cause errors. Known symbols that are sent at the beginning become outdated at the end of the sequence (b). These arguments allow concluding that the common approach to the channel estimation is not successful in fast varying channels.

2.5. Radio channel in WLANs and mobile cellular networks

The design, implementation and operation of two most popular and rapidly developing wireless communication systems, i.e. WLANs and mobile cellular networks, differ mainly with respect to the propagation channel. WLANs are designed for the indoor environment with the limited mobility of terminals. Thus, the radio channel is invariant or it is varying slowly and it can be assumed quasi-stationary. On the other hand, the cellular networks are operating in the wide spectrum of propagation conditions. People use their mobile phones in their homes – in this case the propagation channel is quasi-stationary. However, the phone call must be also possible from a car or a train – this radio channel can be fast varying.

The structure of both WLANs and mobile cellular networks is similar: the main base station or the access point is communicating with multiple mobile terminals. However, the analysis and the design of these networks must be different because of the propagation channel. In the indoor quasi-stationary channels of WLANs, the channel estimation is not a serious problem. The propagation

environment can be accurately described by the geometric dimensions of walls and furniture. The very exact site-specific models are possible. Thus, the capacity of the system can be modelled in variety of situations. On this basis, the system can be designed, optimised and its potential can be measured.

Many papers appeared where the capacity of the MIMO systems working in indoor environment was investigated. The capacity of indoor MIMO systems in many configurations was measured [4, 17, 53, 54, 56, 57, 66] or modelled [10, 16, 72, 78], mainly with deterministic ray tracing methods. It was shown that the capacity given by the Rayleigh model is the upper bound for real systems and, generally, is not achievable [10, 54]. The correlation between the MIMO subchannels, e.g. caused by small Tx and Rx antenna separation, limits the capacity [57].

The interesting comparison of LoS and NLoS conditions was reported in [4, 53, 56]. When the MIMO channels with the same average SNR at the receiver are compared, the NLoS conditions allow achieving higher capacity than in LoS case. It is caused by rich multipath propagation and small correlation between the subchannels in the NLoS case. However, in the MIMO channel with LoS possible, the average SNR at the receiver in much higher than in NLoS case. When these two effects are summed up, the LoS case appears to give higher capacity. MIMO multiplexing techniques are especially advantageous in high SNR region, where the sophisticated methods based on the detailed channel knowledge are possible [78]. However, the MIMO channel capacity does not increase infinitely with the number of antennas [10].

In this thesis, the detailed optimisation of the indoor MIMO WLAN is discussed. The mobile terminals configuration is usually independent from the network designer. Moreover, their optimisation or upgrade is more difficult and expensive than the adaptation of the access point (AP). Thus, the different configurations of the access point are analysed to maximise the system capacity. The position of the AP and the parameters of its antennas are considered. Also, the advantages of the asymmetrical configuration with the access point equipped with the huge number of dipole antennas are investigated. The research is performed with

the deterministic method of ray tracing. The analysis and the results of the calculations are widely presented in the chapter 3.

In the second case, the fast varying radio channels of mobile cellular networks should be analysed. In these non-stationary channels, the new problems arise: the actual channel state information must be constantly available at the receiver. As the frequent training sequences conflict with high spectral efficiency, the new ideas are necessary. The solution for this dilemma could be the blind detection techniques [73, 75]. However, their performance is lower than in the case of the standard detection, because they base on the channel statistics and the properties of the transmitted signal, only. The differential space-time block codes [69] were also proposed. Nevertheless, even in the stationary channels, it was shown that this solution performs with the 3 dB penalty in comparison to the case of perfect channel knowledge at the receiver.

In this thesis, the new algorithm, called Iterative Channel Estimation (ICE), is proposed. ICE allows for the channel estimation on the basis of the decoded data symbols. Thus, the time is not wasted for the frequent transmission of known symbols. The training sequences are still required, but they can occur rarely. ICE performs very well for space-time block codes [44, 47]. It can also be used with other coding techniques, but the transmitted vectors with data symbols should be linearly independent from each other. The whole algorithm is presented with details in the chapter 4. The results of the simulations verifying its performance are also included.

Research is the process of going up alleys to see if they are blind.

Marston Bates

Chapter 3

Capacity of indoor slow varying radio channels

In the indoor environment, the topology is generally more simple than in the outdoor case. The majority of the objects can be described geometrically as a set of flat surfaces. Moreover, these surfaces are more regular and the scattering is less important as compared to the urban or rural environment. Thus, the site-specific models can be built and effectively applied to the radio system planning.

Indoor radio channels, where the mobility of the radio terminals is limited, are generally quasi-stationary or even stationary. Such a channel is considered as constant during a period of time. Hence, the issues of channel estimation are not very important, as it was explained in the section 2.4. Instead of that, the detailed analysis of a radio system in the specific propagation environment can be carried out.

In this chapter, the performance of an indoor MIMO system working in the quasi-stationary radio channel is evaluated by the 3-D ray tracing algorithm written in C++ language by the author of this thesis. The calculations of the system capacity are presented. The focus is on geometric optimisation of the network. The position of the access point and the separation between the antennas are analysed and optimised. Different antennas are compared and the influence of their directivity and

half-power beamwidth is discussed. The concept of the antennas with dynamically shaped patterns is also investigated. During this analysis, some key points are shown how the capacity in a MIMO system working in the indoor environment can be increased.

3.1. Description of analysed WLAN network

The analysis and numerical calculations are performed for the WLAN network placed in a single room of the dimensions $10\text{m} \times 15\text{m} \times 3\text{m}$. It could be an office working room, a computer laboratory, a schoolroom, a small conference or a lecture hall. Some calculations are also performed for a room of the dimensions $3.75\text{m} \times 40\text{m} \times 3\text{m}$, which could be a long corridor. Both rooms have the same surface areas. The comparison of these two cases allows analysing the impact of the shape of the room on the system capacity.

The walls, the ceiling and the floor are assumed to be dielectric with the dielectric constant equal to 5 and relative permeability equal to 1. It is characteristic for wood material or some type of glass. The network consists of the access point (AP) and the user terminals (UTs). The UTs, e.g. personal computers, laptops, printers or PDAs, are evenly distributed in the whole room at the height of 75 cm, which can be the height of the desks where people are working with their devices. Six hundred positions of UTs are considered. For each UT position, the capacity in the radio channel between the AP and the UT is calculated. Then, the average value is taken over 600 cases. The multiple access protocols are not considered. The AP is situated under the ceiling, on the desk among the UTs or on the wall.

The whole analysis is performed with the aid of the 3-D ray tracing algorithm based on the methods of images, described in the section 2.2.2. In the calculations, the people, the furniture and the other equipment in the room are ignored. This assumption simplifies the analysed model and can be found a little bit unrealistic. However, in this thesis, the ray tracing calculations are only the basis to draw general conclusions about the indoor MIMO WLAN system. No specific network is analysed.

Furthermore, the ray tracing algorithm would be much more time-consuming, if the furniture and the people were also taken into account.

The carrier frequency is 2.4 GHz. The bandwidth of the system is assumed to be narrow so the inter-symbol interference caused by delay spread can be ignored. The AP as well as all the UTs have 4 antennas, so the radio channel between the AP and each of the UTs is the MIMO (4,4) channel. These 4 antennas are arranged in the square. In most of calculations, the separation between these antennas (the side of the square) is equal to 2 wavelengths (25 cm). Generally, the larger separation increases the capacity, what is shown more precisely in the section 3.8.1. From the other side, it is very uncomfortable for the users to have the huge AP and UTs. In the opinion of the author, 25 cm is the acceptable size of the AP. It is also possible separation for laptops, printers and computers. However, in the case of some devices, e.g. PDAs, the separation must be smaller. Thus, the results for the smaller antenna separation are also presented.

For the convenience, in the next sections of this thesis, the AP is often described as a transmitter and the UTs – as receivers. However, it should be noted that the radio transmission in this MIMO system is fully symmetric and duplex. The capacity is the same during the transmission in both directions. The transmitter power is fixed during the calculations, but it is chosen to obtain the average SNR at the Rx antennas equal to 20 dB. To achieve it, an initial experiment was carried out – it is described in the next section.

The main goal of the research reported here is to compare the WLAN performance in different configurations. The main criterion is average capacity of the channels between each of the UTs and the AP in the single-user communication. The coding scheme and modulation are not specified and the capacity is calculated as an upper bound of spectral efficiency in the communication channel. The radio channel is quasi-stationary and it is assumed that the channel transfer matrix is known at both sides of the link. In this case, the optimal transmission is performed by singular value decomposition and waterfilling the power at the transmitter. However, this technique requires much more complexity at the AP and at the UTs to calculate the eigenvalues of the channel transfer matrix. In the richly scattered environment and

with the high SNR, the equal power strategy in nearly optimal [29]. Thus, despite of the full CSI, it is assumed that equal power strategy is applied. In this case, the capacity of the MIMO channel is given by Eq. (1.4).

One could remark that the WLAN network is analysed in very specific conditions. To avoid this charge, the calculations are also performed for other than these basic parameters specified above. These calculations and its analysis are reported in the section 3.8. However, these parameter modifications do not change the general conclusions about the discussed MIMO system.

3.2. Isotropic antennas

In the first stage of the experiment, the ray tracing calculations are performed for the hypothetic isotropic antennas. Two main concepts of AP placement are considered: under the ceiling, 2.9 m above the floor level – so called CEIL case or on the desk among the UTs – DESK case. With other AP positions, e.g. on the wall, the achieved capacity is much lower. The antenna arrays are placed horizontally, their polarization is perpendicular to the floor surface.

Optimal position of AP is investigated. This is the position where the average capacity for the channels between AP and all UTs is maximal. Average signal-to-noise-ratio (SNR) at each receiver antenna is assumed to be 20 dB. However, to compare different cases fairly, the transmitter should have the same power in all cases. Therefore, the initial experiment was made. AP was being moved along the diagonal of the room in CEIL case and the average SNR at the UT antennas was accordingly calculated. Then, the power of the transmitter was corrected to achieve average SNR of 20 dB. This power level is kept for all experiments reported in this section and the subsequent one. The diagonal of the room in CEIL case was chosen as it seems to be representative for all positions of the AP under the ceiling. It should be expected that the average SNR is bigger in the DESK case and, in the consequence, the capacity of the system is higher. It is reported further.

For CEIL case, the capacity for the channel between the AP and each of the UTs is calculated [43, 45]. The average value is gained. Different positions of AP are considered, always 2.9 m above the floor level. The obtained capacities are between 10.0 and 17.9 bit/s/Hz. The maximal capacity is achieved for AP placed near the middle of the ceiling. It can be easily understood since in such a situation the average path from the AP to the UTs is the shortest. Besides, when the AP is in the corner of the room, the angle of departure of the transmitted signals is limited what results in decreasing the channel matrix rank. The difference between the minimal and maximal values indicates that the position of AP plays a key role in the performance of the system. For comparison, the capacity for the SISO system with the same SNR is 6.7 bit/s/Hz.

The results for DESK case are better: the maximal capacity is 19.7 bit/s/Hz. The best AP position is also near the middle of the room. Fig. 3.1 gives the capacity of the system as a function of the position of the AP, when the AP is being moved along the 18 meters long diagonal of the ceiling – both cases considered above are presented. The fast fluctuations of the capacity are caused by multipath fading. This phenomenon is covered in the section 3.7.

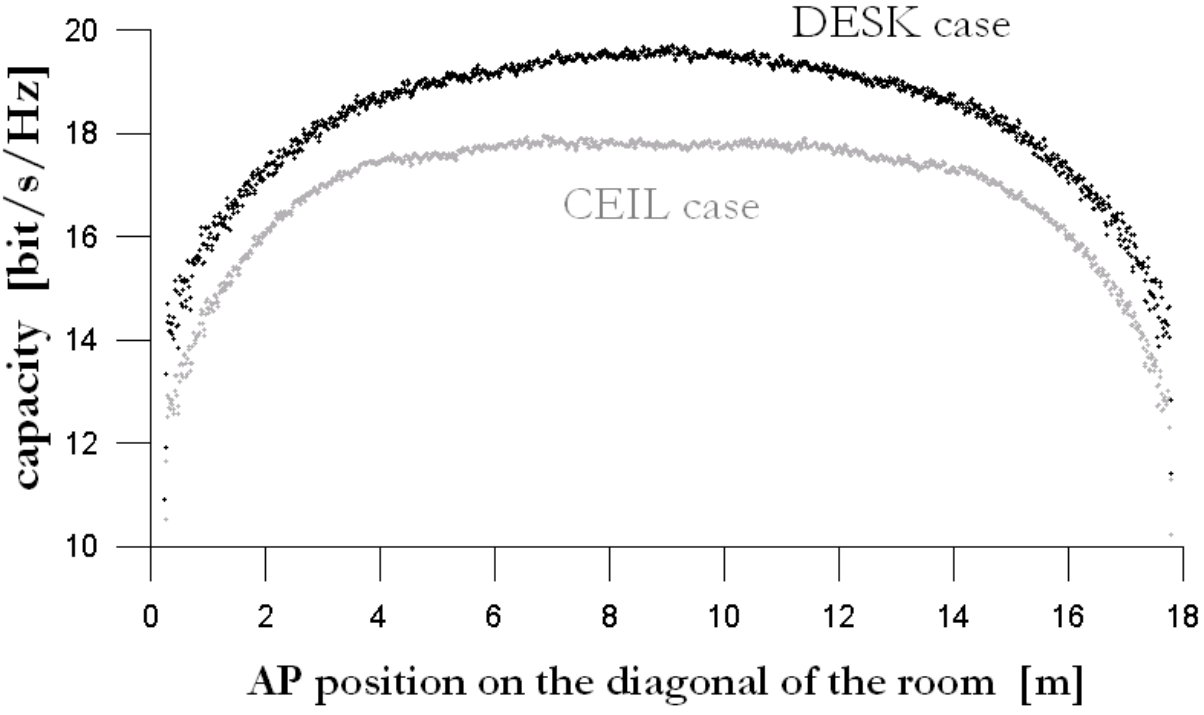

Fig. 3.1. The average capacity of the system as a function of the position of AP.

It should be noted that the advantage of DESK case over CEIL case is caused by higher average SNR at the Rx antennas, as it was defined in Eq. (1.6). In the calculations presented above, the difference is 5.6 dB. The reason is obvious: the average radio paths between the AP and UT antennas are shorter, so the average attenuation of the paths is smaller. In Fig. 3.2, the capacity of the system in DESK case is presented, but the transmitter level is reduced by 5.6 dB, to keep the same average SNR as in CEIL case. The obtained capacity is smaller than for CEIL case. It means that in DESK case the elements of channel transfer matrix $\boldsymbol{H}$ are more correlated (Eq. 1.4). Again, it can be explained by shorter radio paths: the LoS component became stronger in comparison to the other radio rays, reflected from the walls. In the real situation, when the transmitter power is fixed, better results can be achieved in DESK case (Fig. 3.1). This leads to the conclusion that high SNR is more important factor than the small correlation between the elements of the matrix $\boldsymbol{H}$. It is also confirmed by the measurements made in Bristol [53] and in Aalborg [4, 56].

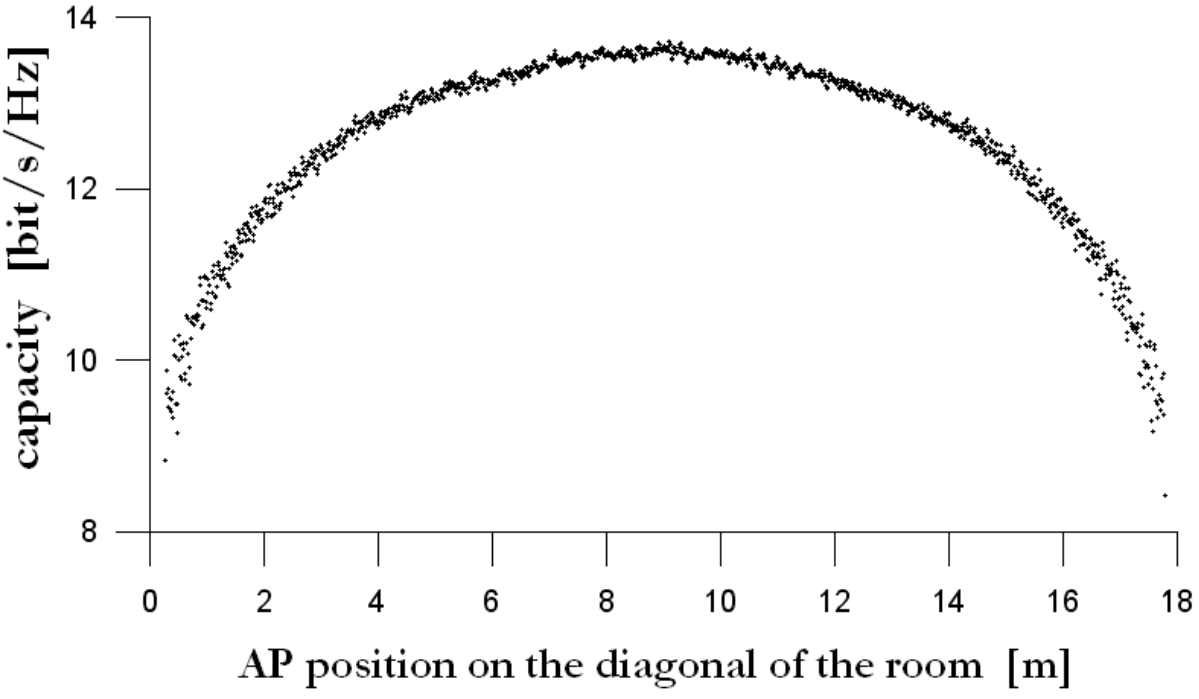

Fig. 3.2. The capacity of the system as a function of the position of AP in DESK case. The transmitter power is reduced to achieve the average SNR equal to 20 dB.

For small communication devices like PDAs or mobile phones, the antenna separations must be smaller than 2λ. Thus, the calculations analogous to presented above are made for UT antenna separation (d_{UT}) equal to 0.5λ. The antenna separation at the AP (d_{AP}) is still 2λ. The results for CEIL and DESK cases are presented in Fig. 3.3. The maximal capacities are equal to 13.7 and 15.7 bit/s/Hz, respectively. These results are worse than the ones for separation equal to 2λ, despite of the same transmitter power. It is because of higher correlation between the elements of matrix $\boldsymbol{H}$. The detailed analysis of the influence of antenna separation on the capacity is provided in the section 3.8.1.

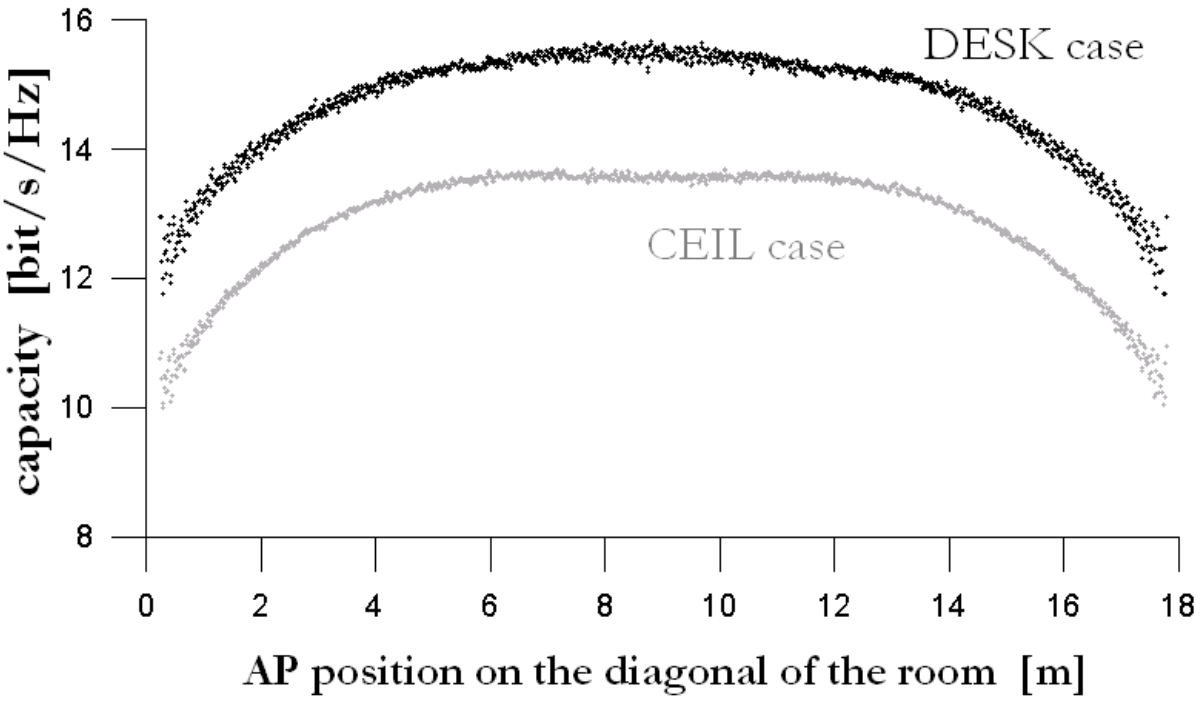

Fig. 3.3. The capacity of the system as a function of the position of AP for d_{UT} equal to 0.5λ.

3.3. Large separation between AP antennas

The antenna separation seems to be one of the key parameters to achieve the independent radio paths between transmit and receive antennas and, in consequence, the high system capacity. Antenna separation at the UTs is limited by the small dimensions of the terminals. However, there is no such limits in the case of

the AP. Could it be advantageous to divide the AP and mount the AP antennas totally separately? There are some drawbacks of this idea. First, such an installation can be hardly acceptable for the users of the WLAN network. There are four devices instead of one which must be placed in the room. In both cases, CEIL and DESK, there is also the problem with installing the cables. Furthermore, the long waveguides which are required to feed the radio signal from the transceiver to the antennas involve the high signal attenuation. The last drawback is not critical, but, to keep the needed transmitter power, the total power consumption at the AP must be higher.

The idea of large separation between the AP antennas is verified in the numerical calculations. In the previous section it was concluded that the AP in the middle of the room (in both CEIL and DESK cases) results in the best system performance. On the basis of these conclusions the following calculation are performed. The AP is installed in the middle of the room but its antennas are drawn aside, as it is presented in Fig. 3.4. Four situations are considered: CEIL and DESK cases, both for d_{UT} equal to 2λ and 0.5λ. The results are documented in figures 3.5 and 3.6, respectively.

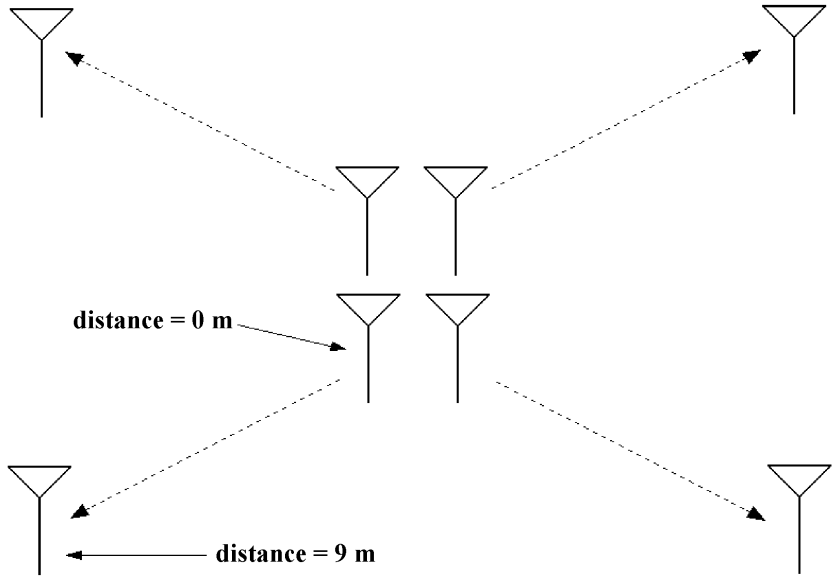

Fig. 3.4. The scheme of drawing aside the antennas. The distance between the antennas and the middle of the room is increasing.

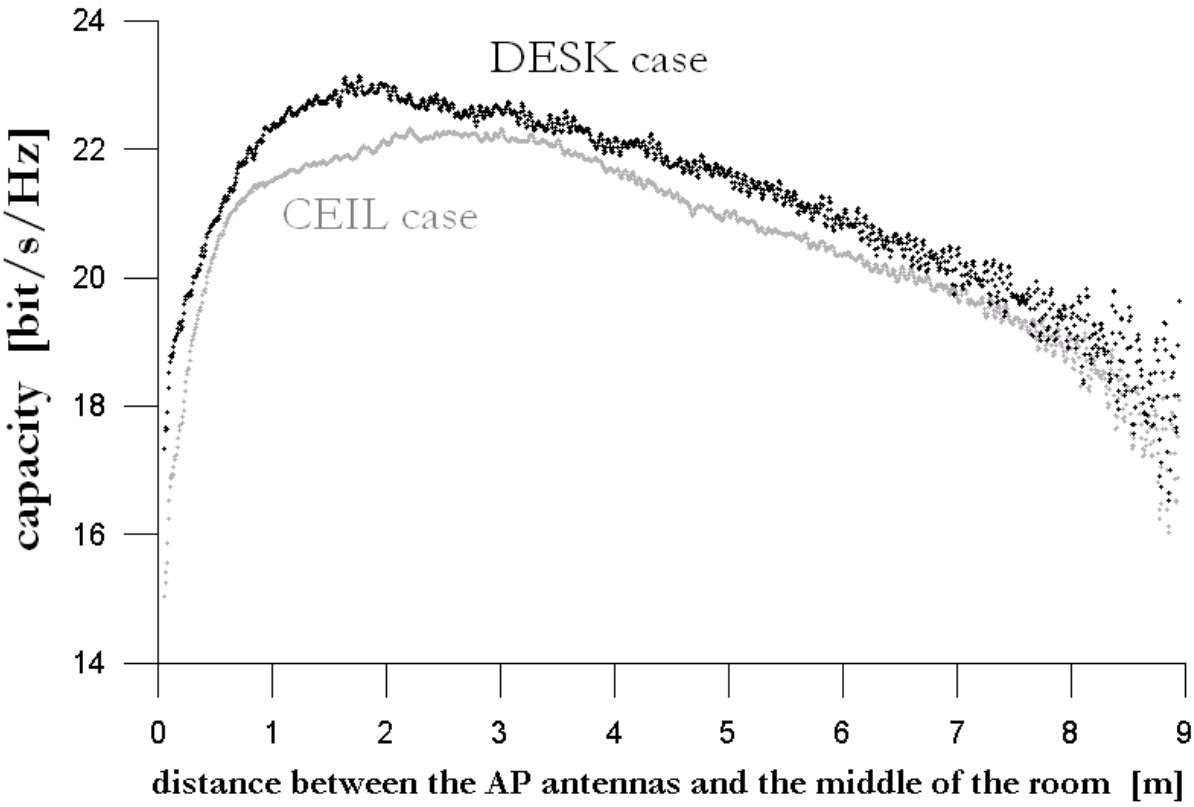

Fig. 3.5. The capacity of the system as a function of the distance between the AP antennas and the middle of the room. These antennas are drawn aside from the middle (distance = 0 m) to the corners (distance = 9 m). The d_{UT} is equal to 2λ.

With AP antennas drawn aside, the capacity of 23.1 bit/s/Hz ($d_{UT} = 2\lambda$) and 21.4 bit/s/Hz ($d_{UT} = 0.5\lambda$) can be achieved. The reason for such good results is decreasing correlation between the elements of matrix $\boldsymbol{H}$. This concept is attractive for all cases: CEIL and DESK, d_{UT} equal to 2λ and 0.5λ. When $d_{UT} = 0.5\lambda$, the maximal capacity is achieved not until the distance between the AP antennas and the middle of the room is about 4 meters. For the case of $d_{UT} = 2\lambda$, the distance of 2 meters is enough. This is again caused by the fact that the correlation between the elements of matrix $\boldsymbol{H}$ is higher when $d_{UT} = 0.5\lambda$. Surprisingly, for $d_{UT} = 0.5\lambda$, the larger capacity can be achieved in CEIL case than in DESK case. A certain attempt of its explanation is as follows. There are two factors that result in high correlation between the subchannels of the MIMO system in the DESK case: the small antenna separation at the UTs and the short average distance between the AP and the UTs. In

this case, these two factors added together are more important than high average SNR.

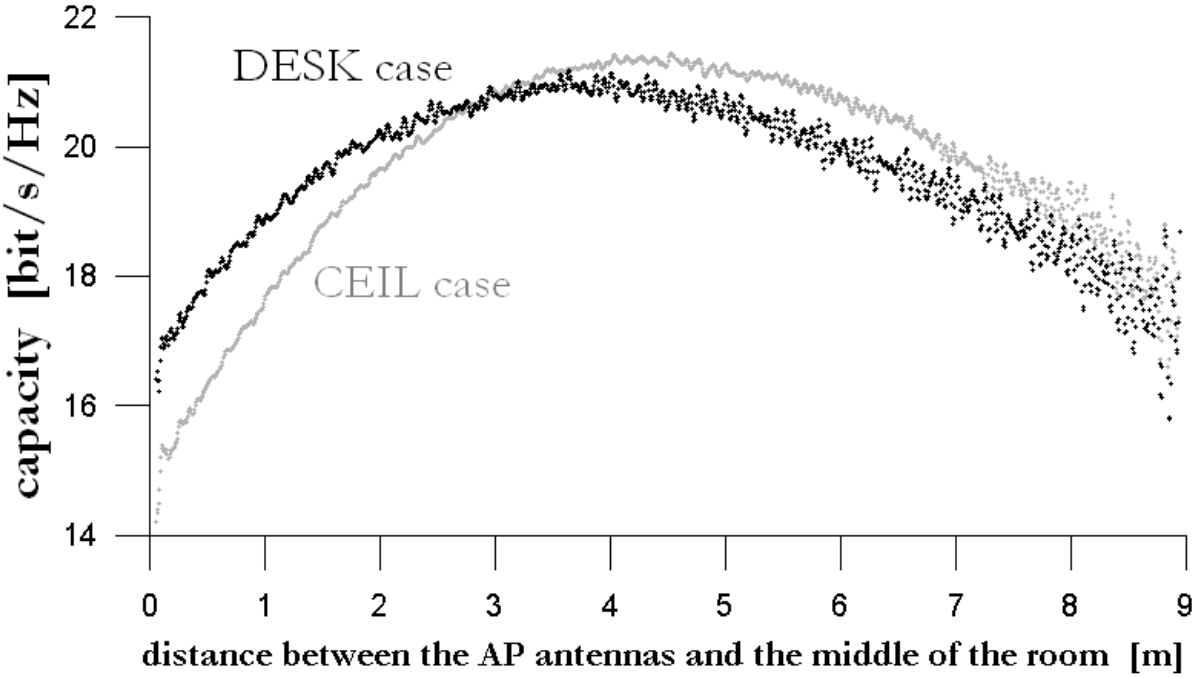

Fig. 3.6. The capacity of the system as a function of the distance between the AP antennas and the middle of the room. The d_{UT} is equal to 0.5 λ.

Generally, with such an asymmetrical configuration – large AP antenna separation and small separation at the UTs – it is possible to obtain very good system performance. However, because of the drawbacks discussed earlier, such a concept for indoor WLAN will rather not became popular.

3.4. Concept of directional antennas

The natural question arises: does the directional antennas can boost the system performance in such a stationary and multipath environment like indoor one? Does the directional antennas can help decrease the correlation between the subchannels of the MIMO system?

Let us consider the example of AP with four sector antennas (Fig. 3.7). One can suggest that (because of the strong multipath propagation) signals transmitted by each of the AP antenna are strong at each of the receive antenna. Moreover, these signals are uncorrelated as they propagate with other paths. However, only the second statement is true. The reflections from the walls cause the radio signal to attenuate. In the consequence, the signal from e.g. antenna B is hardly received at the UT (Fig. 3.7). Such an AP with sector antennas can be efficient only for the case of very small antenna separations, where the correlation between the subchannels in the MIMO system is very large.

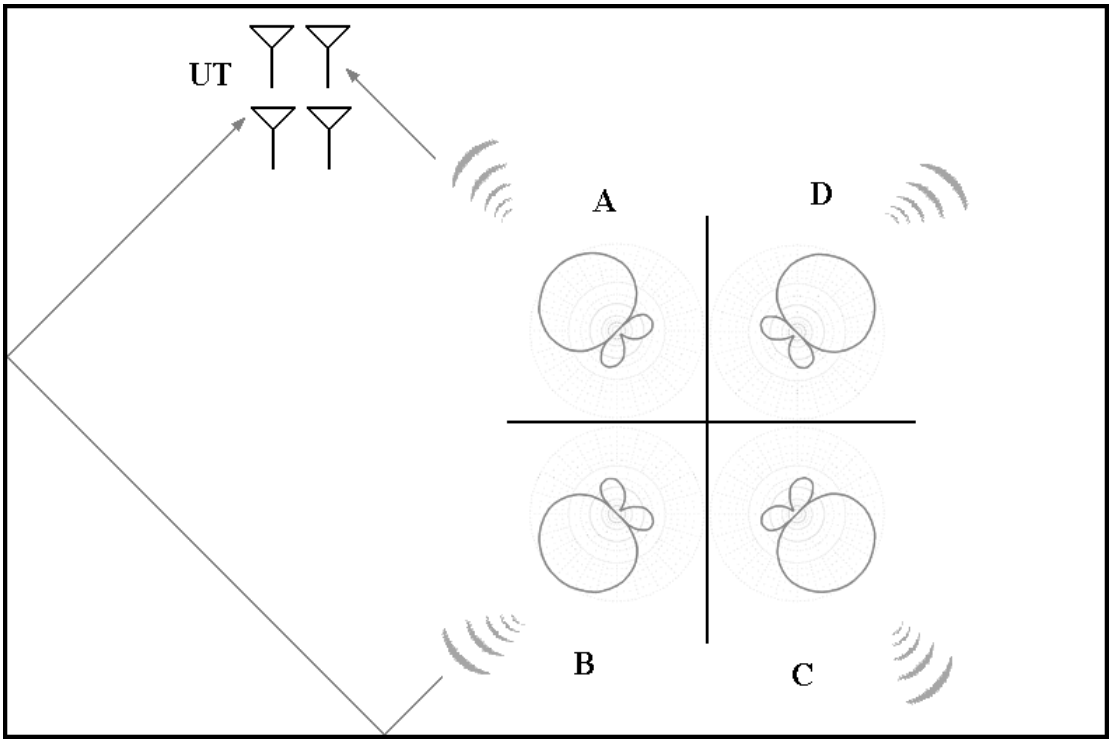

Fig. 3.7. An example of radio propagation in the MIMO (4,4) system. The AP has four sector antennas A, B, C and D, the sketches of their radiation patterns are also presented.

On the other hand, the directional antennas in MIMO WLAN can be effectively used in a well known manner: to strengthen the power transmitted in the direction of the UTs. The results of the calculations supporting these theories are presented in the next section.

3.5. Capacity of WLAN with directional antennas

The capacity of the WLAN with directional antennas is studied as a function of the directivity of the AP antennas [46]. Three different types of the AP antennas are considered: 1, 2 and 4 centre-fed thin quarter-wavelength dipoles organized in the linear array. The separation between dipoles is always 0.25λ. The excitation amplitude of all the dipoles is the same and the phase difference between the two adjacent ones is constant and equal to 90°. The parameters of these antennas are compared in Table 3.1. The UT antennas are single quarter-wavelength dipoles all the time. The separation between AP antennas and between UT antennas is always 2λ. The position of the AP is horizontal. The axes of all the dipoles are always perpendicular to the floor what determines their polarisation.

It should be noted that the antennas used for the numerical experiments are only the examples. Designing the antennas is beyond the scope of this thesis. The problems of antennas efficiency and mismatching in feeding the antennas are also omitted. The author is interested in the effects of using the antennas with specific directivity and half-power beamwidth.

Table 3.1.

The parameters of the three types of antennas used in the numerical experiments.

Antenna type	A1	A2	A3
Number of dipoles	1	2	4
Directivity [dBi]	1.86	4.86	7.24
Elevation θ_{3dB} [deg.]	86.8	84.2	77.0
Azimuth θ_{3dB} [deg.]	360	179.4	113.6

To choose the power of the AP, one more initial experiment was made, analogous to the one reported in the section 3.1. All the AP and UT antennas were assumed to be single quarter-wavelength dipoles. Again, AP was being moved along

the diagonal of the ceiling and the power of the transmitter was chosen to achieve average SNR of 20 dB. This power level is kept for all further experiments.

Similarly to the case of isotropic antennas, the location of the AP is crucial for the capacity of the WLAN with MIMO antennas. The ray tracing results presented below show that it is possible to achieve nearly twice as large capacity choosing the proper place for the AP.

The results for single quarter-wavelength dipole antennas with directivity equal to 1.86 dBi are presented in Fig. 3.8. The AP is being moved along the diagonal and the largest capacity can be achieved when the AP is near the centre of the room. The maximal obtained capacities are equal to 18.6 and 22.3 bit/s/Hz in CEIL and DESK cases, respectively. For comparison, with the AP in the corner, the capacity is less than 13 bit/s/Hz.

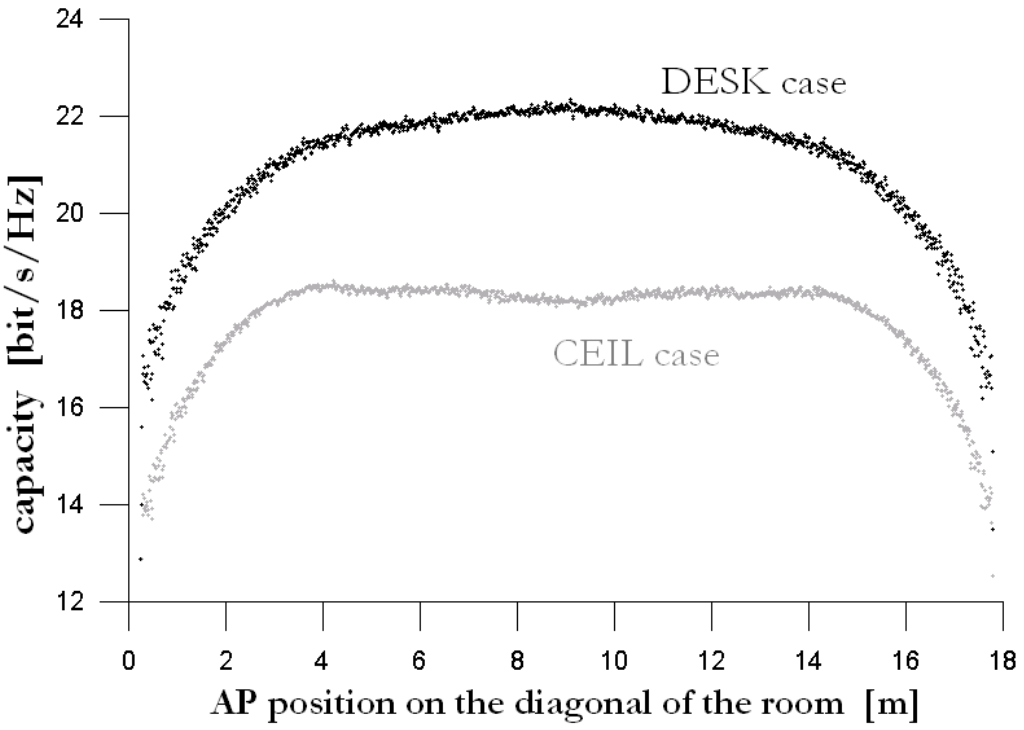

Fig. 3.8. The average capacity of the system with the AP equipped with the single dipole antennas.

Assuming the AP to be situated in the middle of the room (both CEIL and DESK cases), the capacity does not increase when the antennas with higher directivities are used. If such AP antennas were pointed in different, nearly

orthogonal directions, the transmitted signals would be less correlated. From the other side, the half-power beamwidth (θ_{3dB}) would be small in this case. Therefore, the signal received by the UTs scattered in the room would be strongly attenuated.

The linear arrays of dipoles can be effectively used when the AP is installed in the vertical position on the shorter wall of the room. All the antennas are pointed towards the middle of the room. Fig. 3.9 shows the capacities in this case for three different types of the AP antennas, described in Table 3.1. The capacity of 19.8 bit/s/Hz can be achieved with the antennas with maximal gain equal to 7.24 dBi. The capacity results for the AP located on the wall and in the middle of the room are compared in Table 3.2.

Table 3.2.

The maximal capacities [bit/s/Hz] achieved in three different AP positions for three antenna types.

AP position	A1	A2	A3
Under the ceiling	18.6	18.3	17.8
On the desk	22.3	21.9	21.2
On the wall	16.3	19.1	19.8

3.6. MIMO-MRC system

The arrays of dipoles can be used more effectively if their antenna patterns are shaped dynamically. This adaptation of the antenna patterns is performed by maximal ratio combining (MRC) algorithm. In order to avoid the complexity at the UTs, the MRC algorithm is applied only at the AP, during the transmission in both directions. It is possible due to the full CSI. Now, each AP antenna consists of 2, 4 or 6 dipoles. All the dipoles are placed in the square $2\lambda \times 2\lambda$ to keep the size of the AP unchanged. The separation between the dipoles is 0.5λ, which value is confirmed to be optimal [74]. The basic idea of antenna arrangements at the AP can be understood with the aid of Fig. 3.10.

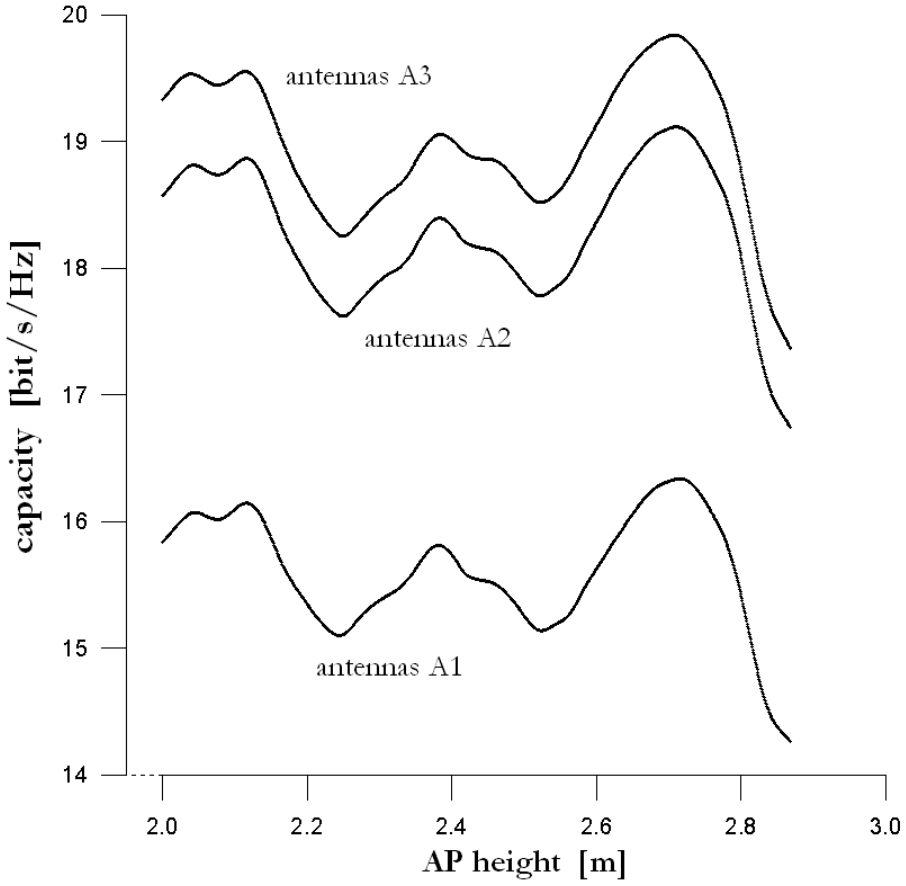

Fig. 3.9. The average capacity of the system when the AP is installed vertically on the wall and is being moved up along the axis of the wall.

MRC is one of the diversity techniques and it is sometimes called beamforming or linear combining. The antenna radiation patterns are adapted for the transmission between the AP and the particular UT. In the consequence, the channel gain is higher. It can be performed at the transmitter or at the receiver. However, the channel knowledge is needed at this side of the channel where this technique is applied.

If the receiver has k antennas and the transmitter has only 1 antenna, receive beamforming (MRC at the receiver side) can be applied by multiplying the k received signals by MRC coefficients and adding them together. The MRC coefficients are given by [74]:

$$MRC_i = \frac{h_i^*}{\sqrt{|h_1|^2 + |h_2|^2 + ... + |h_k|^2}}, \quad i = 1, 2, \ldots, k \tag{3.1}$$

where h_k is the transfer function between the transmit antenna and the k-th receive antenna. If there are k transmit antennas and only 1 receive antenna, the analogous technique, called transmit beamforming, can be applied.

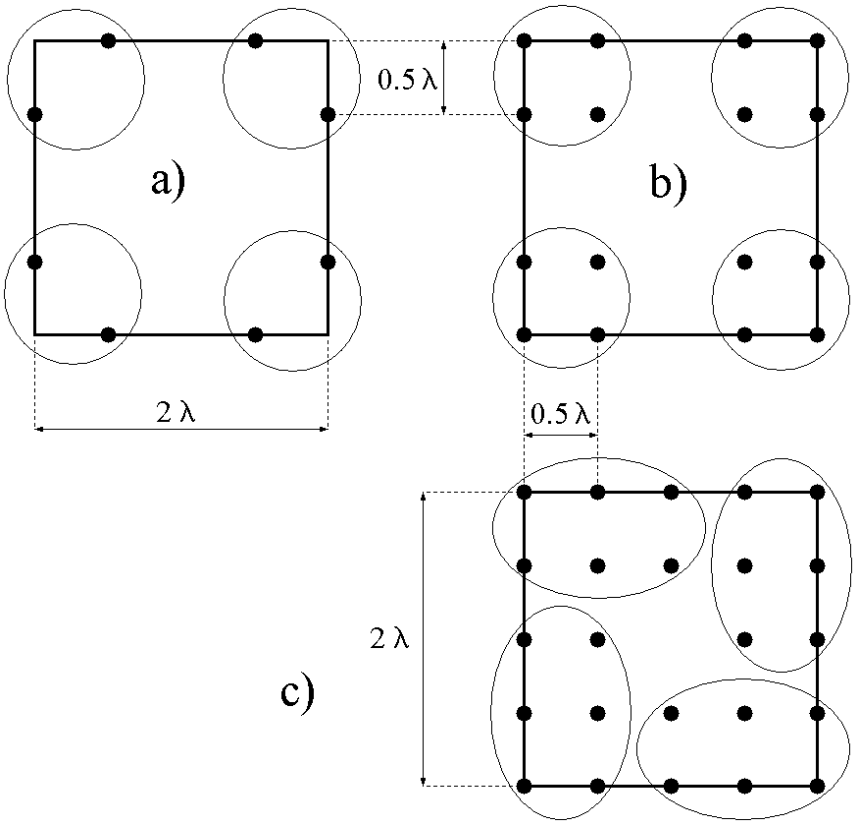

Fig. 3.10. The idea of the placement of the dipoles at the AP when MRC technique is used. Each AP antenna consists of 2 dipoles (a), 4 dipoles (b) or 6 dipoles (c). The ellipses shows how the dipoles are grouped to form the AP antennas.

Now, the MRC technique is implemented in the MIMO (4,4) system. Each of 4 AP antennas is, in fact, the antenna array of k dipoles. The MRC algorithm is performed between the four pairs: the array of dipoles at the AP and the antenna at the given UT. Therefore, the gains in four parallel channels are increased.

According to the information theory results [74], the transmit and receive beamforming techniques are equally efficient. Since the full CSI is assumed, the beamforming can be performed at the AP all the time, regardless whether the AP transmits or receives. Such a solution increases the capacity of the system without adding the complexity to the UTs. Because of the MIMO-MRC combination, the AP

has the huge amount of $4 \cdot k$ dipoles. However, very good results can be obtained when all the AP dipoles are placed in the 25cm×25cm ($2\lambda \times 2\lambda$) square. In this situation, the size of the AP is not enlarged.

The results of the system capacity for MIMO-MRC combination are presented in figures 3.11 and 3.12. First, the AP is at the height of the desks and is being moved along the diagonal of the room (Fig. 3.11). The cases of for 2, 4 and 6 dipoles at each AP antenna are compared. With the MRC technique and maximal number of dipoles, the capacity of even 26.5 bit/s/Hz can be achieved. It is nearly 20% more than in the best situation of all cases with directional antennas. The analogous calculations for the AP installed on the wall are documented in Fig. 3.12. The results are a little worse. The advantage of this position of the AP reported in the section 3.5 was based on the directional antennas consisting of even 4 dipoles. Now, the additional dipoles are used to perform the MRC algorithm, so this advantage is lost. However, the results for the AP on the wall with MRC algorithm exceed the corresponding ones reported in the section 3.5.

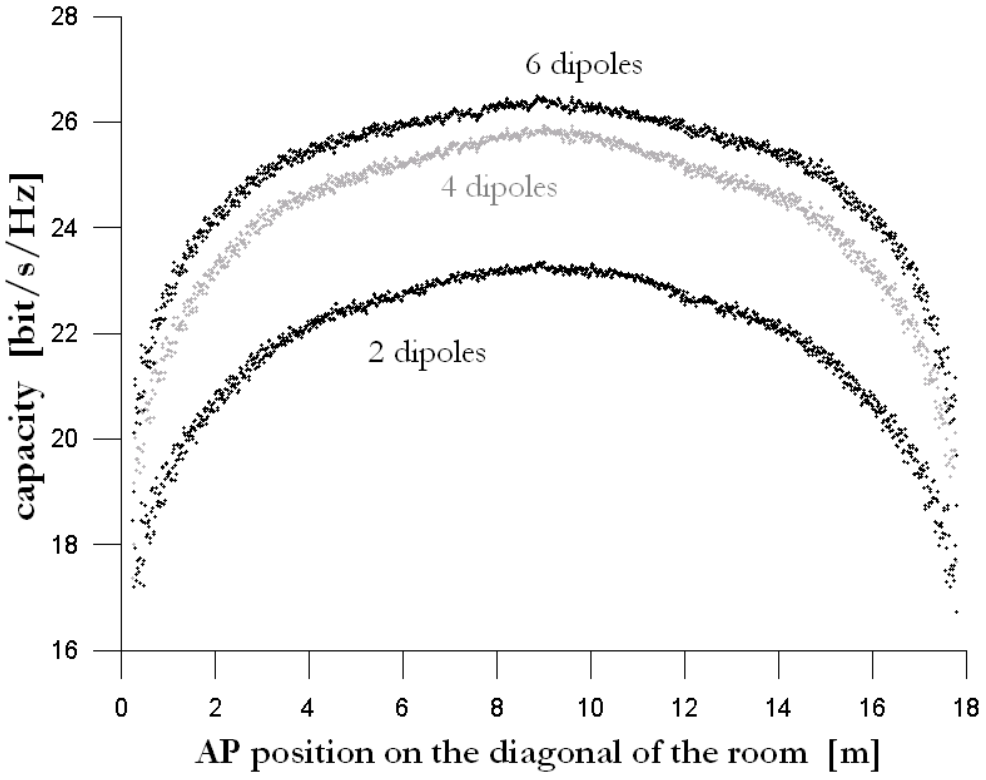

Fig. 3.11. The average capacity of the system in the DESK case.
The AP antennas consist of 2, 4 or 6 dipoles and perform MRC algorithm.

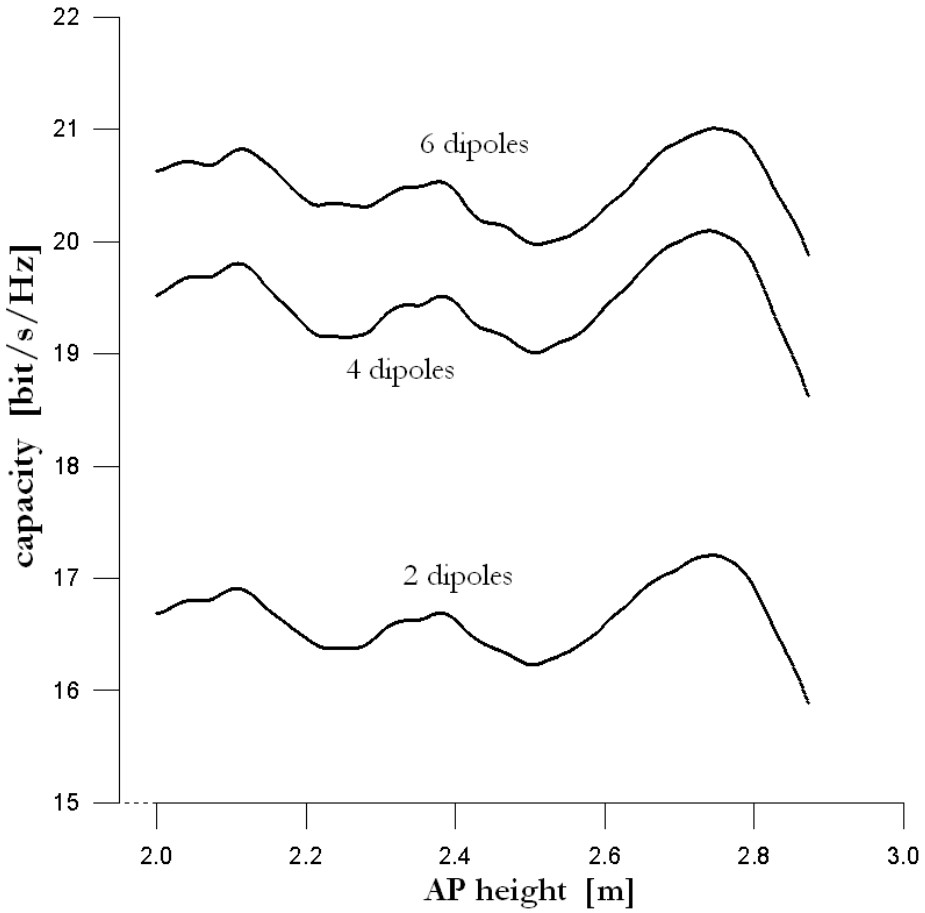

Fig. 3.12. The average capacity of the system. The AP is installed vertically on the wall and is being moved up along the axis of the wall. The AP antennas consist of 2, 4 or 6 dipoles and perform MRC algorithm.

The AP with adaptive antennas performing MRC seems to be a very flexible structure. Such an AP can effectively cooperate with UTs equipped with different number of antennas. When a UT has only 2 antennas, the whole set of AP dipoles can be divided into two groups and the MRC algorithm can be performed in these groups. The same strategy can be applied for the transmission with a UT with only 1 antenna. In this case, all AP dipoles form single antenna and dynamically shape its pattern. Every dipole at the AP is used all the time.

3.7. Impact of multipath propagation

It should be emphasized that the effective exploitation of multiple antennas is possible because of radio wave reflections and the multipath propagation. If the radio wave propagated only by line-of-sight path, the signals from different transmit antennas would be highly correlated, what was explained in the section 2.1. The multipath propagation results in decreasing the correlation between the received signals and also in strengthening the received power. In Fig. 3.13, the impact of the multipath propagation on the system capacity is shown. The capacity is calculated with the AP being moved along the diagonal of the room under the ceiling and different number of reflections being considered. The capacity is nearly the same for the cases of up to 2, 3 and 4 reflections, because the power of the radio rays reflected 3 or 4 times is very small. The multipath fading (caused by constructive or destructive interference of radio waves) can be already observed with only single reflections taken into account. It should be noted that LoS is very strong component. When LoS is blocked (the lower grey curve in Fig. 3.13), the capacity decreases significantly. Thus, the radio channel between the AP and the UTs can be treated as Rician: it is Rayleigh channel with a strong LoS component.

The multipath fading can be observed in the figures despite the fact that the plotted capacity is the average value over the 600 UTs. For the comparison, the capacity of the radio channel between the AP and the single UT is shown in Fig. 3.14. The fluctuations of the capacity are much higher.

3.8. Influence of other parameters

The above presented results and conclusions could be found not reliable if the WLAN was analysed in the specific conditions, only. To avoid this charge, some other parameters describing this WLAN are also considered. Influence of Tx and Rx antenna separations, SNR, the dielectric constant of the walls and the room

dimensions is investigated in the next sections. However, these results do not change the overall conclusions about the discussed indoor MIMO system.

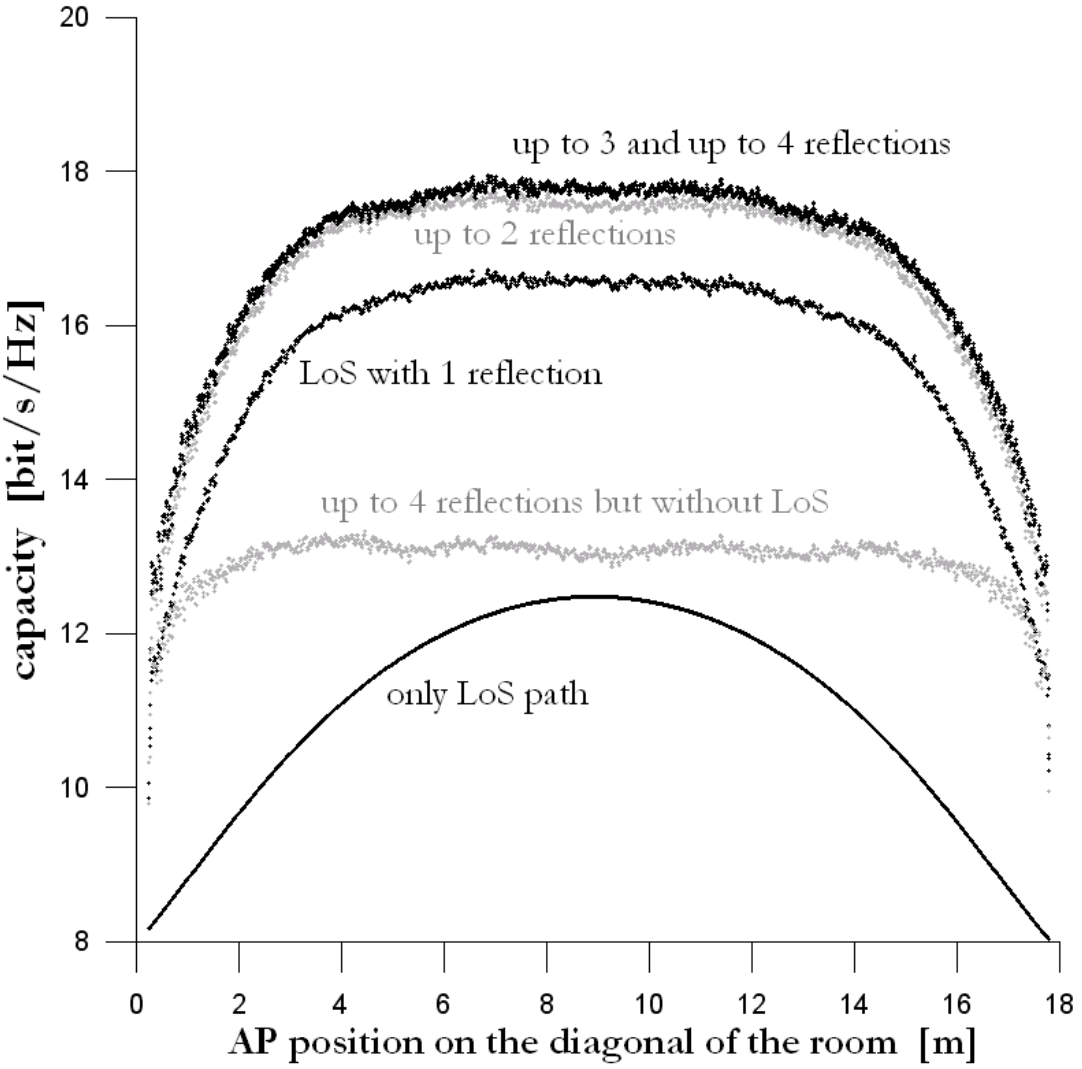

Fig. 3.13. The average capacity of the system in the CEIL case with different number of reflections considered: only LoS, without LoS, LoS with up to 1, 2, 3 and 4 reflections.

3.8.1. Antenna separation

The results for the antenna separations d_{AP} and d_{UT} equal to 0.5λ and 2λ were presented in the section 3.2. Also, the idea of drawing aside the AP antennas were discussed. Here, the extended calculations of the influence of the antenna separation on the system capacity are included.

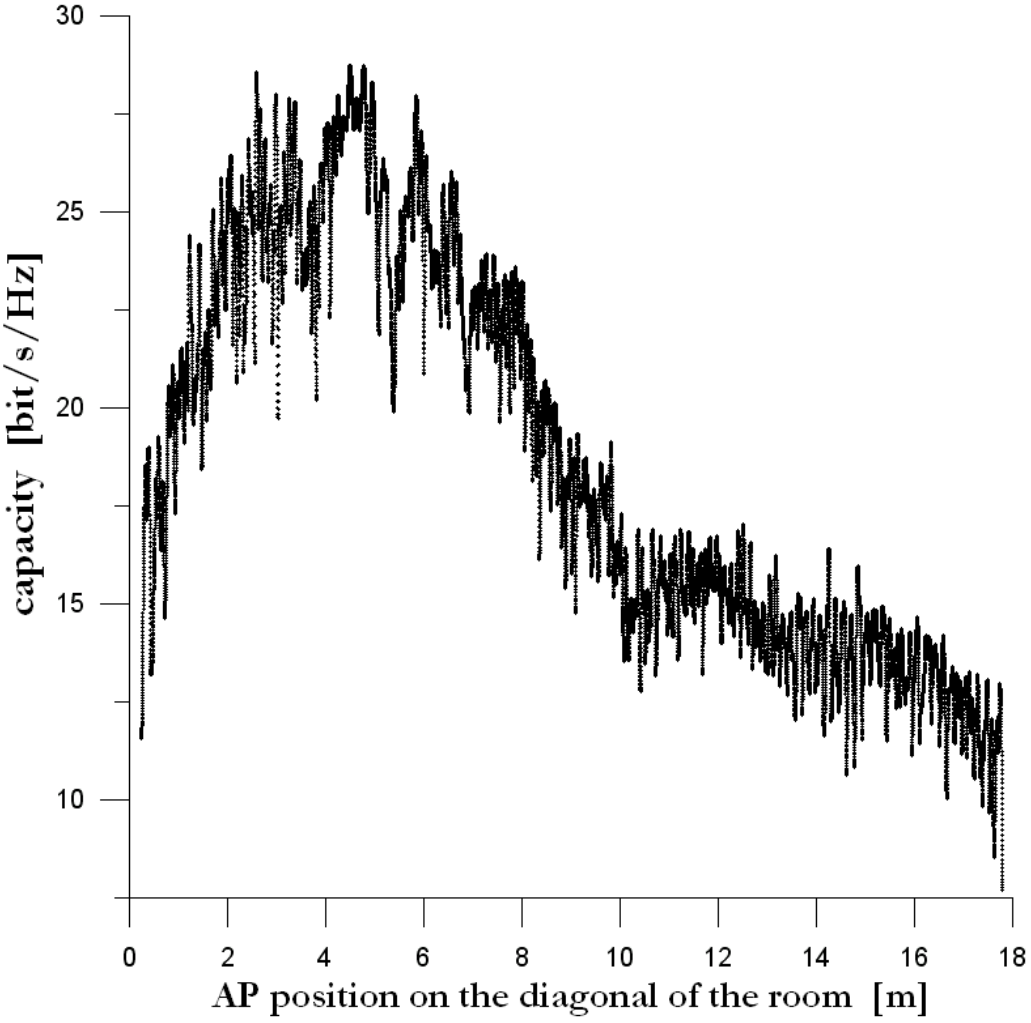

Fig. 3.14. The capacity of the radio channel between the AP and the single UT. The position of the UT is chosen arbitrary in the midway between the middle and the corner of the room.

Early papers about MIMO systems [22] suggest that antenna separations should be at least 0.5λ. Later experiments [40] show that smaller values of antenna separation are also acceptable. The indoor WLAN analysed in this thesis operates in the radio channel with strong LoS component. Because of that, the elements of matrix $\boldsymbol{H}$ are correlated even for antenna separations equal to 2λ. The capacity of the WLAN with MIMO antennas could be increased if d_{AP} and d_{UT} were larger. The results presented in Fig. 3.15 confirm the advantage of large antenna separations. However, the huge AP is troublesome and hardly acceptable to the users. At the UTs, large separation is usually impossible because of the dimensions of the terminals.

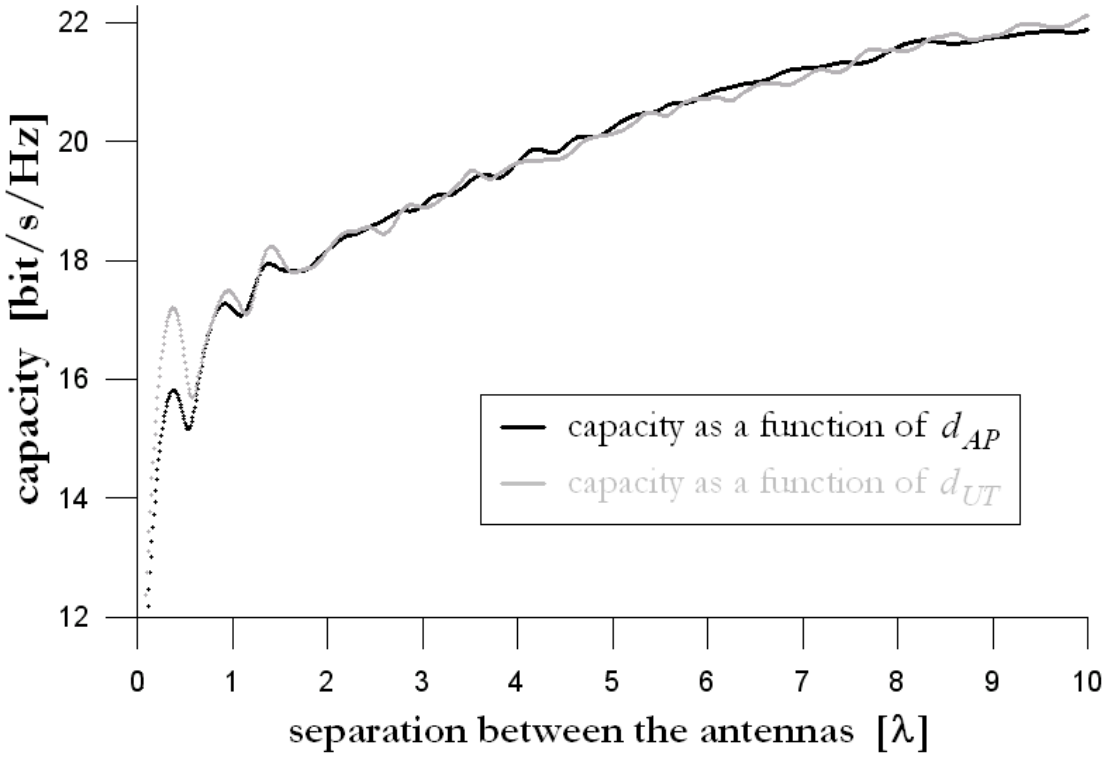

Fig. 3.15. The average capacity of the system as a function of d_{AP} or d_{UT}. When d_{AP} is changed, d_{UT} is equal to 2λ and vice versa. The AP with 4 single dipoles is installed under the middle of the ceiling.

3.8.2. Signal-to-noise ratio

The impact of SNR is a simple consequence of Eq. (1.4). In high SNR region, the identity matrix $\boldsymbol{I}_m$ can be neglected. Because of 4 antennas at each side of the radio link, the average capacity increases by nearly 4 bit/s/Hz with the SNR increasing each 3 dB. It is confirmed with the aid of calculations presented in Fig. 3.16: when SNR increases by 7.5 dB, the capacity is nearly 10 bit/s/Hz larger. This relationship is true only if SNR is high. Otherwise, the above approximation cannot be done. Moreover, in the case of low SNR, the assumed equal power strategy is inefficient.

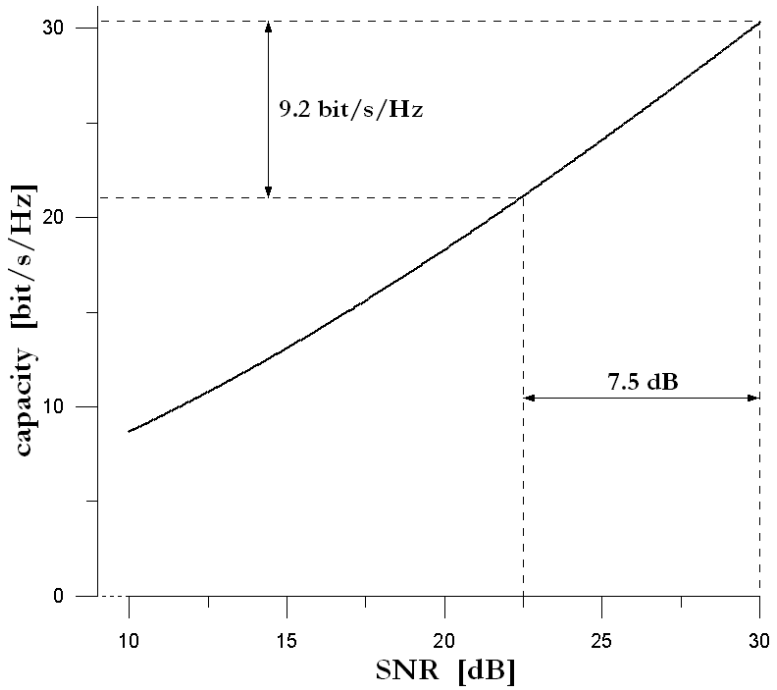

Fig. 3.16. The capacity of the system as a function of average SNR. The AP is placed in the arbitrary chosen point under the ceiling: midway between the middle and the corner.

3.8.3. Dielectric constant of the walls

For both radio wave polarisations, the amplitudes of the reflection coefficients increase with ε_r (equations 2.10 and 2.11). In the consequence, the power of reflected radio waves also increases, as well as the signal power at the receive antennas. Furthermore, the LoS component is relatively weaker and the elements of matrix $\boldsymbol{H}$ are less correlated. Because of these factors, one can expect that high ε_r results in large system capacity.

In Fig. 3.17, the system capacity as a function of ε_r is considered in two situations. First, the AP is placed under the ceiling, in midway between the middle and the corner. The AP antenna separation is equal to 2λ, so the elements of matrix $\boldsymbol{H}$ are correlated. Second, the AP antennas are drawn aside, also to the midway between the middle and the corners. In the second case, the correlation between the element of matrix $\boldsymbol{H}$ is very small. In all cases, all the antennas are single quarter-wavelength dipoles.

As it was expected, in both cases the system capacity increases with ε_r. However, in the uncorrelated case, the influence of ε_r is minor. For $2 \le \varepsilon_r \le 10$, what

is appropriate for the straight majority of the wall materials, a very weak dependence is observed. These results suggest that the calculations presented earlier ($\varepsilon_r = 5$) are also correct for a room made of other materials. It is encouraging for future experiments. From the other hand, in correlated case, the influence of ε_r is significant and cannot be neglected. It allows concluding that the influence of ε_r on the system capacity is mainly in decreasing the correlation between the elements of matrix $\boldsymbol{H}$.

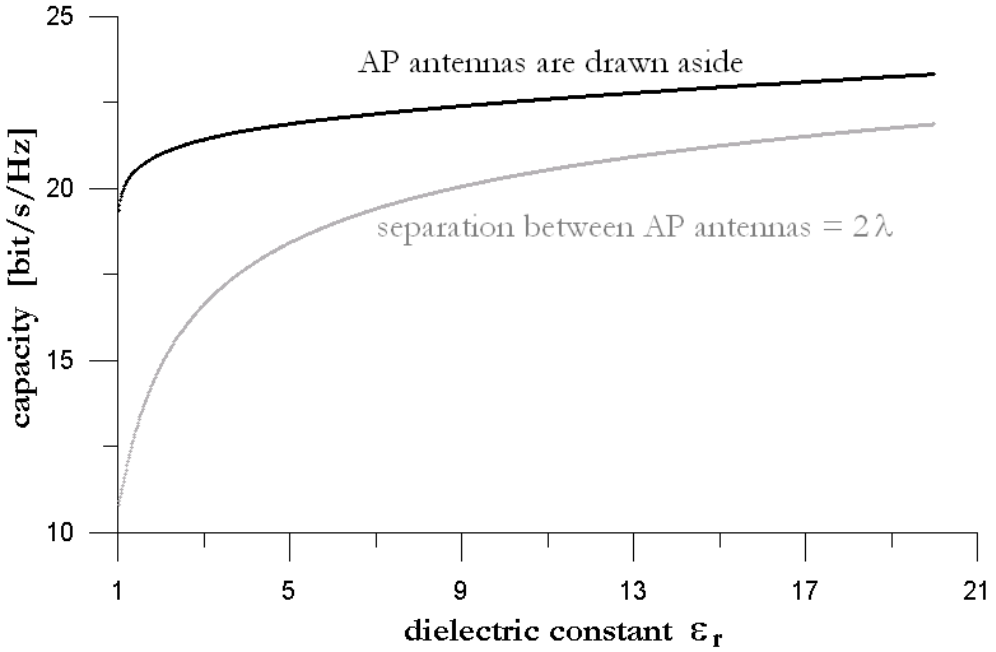

Fig. 3.17. The capacity as a function of the dielectric constant of the room walls, floor, and ceiling. Transmitter antennas are drawn aside and have optimal positions. Receiver antennas separation is 0.5λ.

3.8.4. Room dimensions

The calculations analogous to the ones mentioned in the section 3.5 are performed for the room of dimensions $3.75\text{m} \times 40\text{m} \times 3\text{m}$ what could be a hallway or a corridor. That room has the same surface area as the schoolroom analysed earlier. The same transmitter power level is also kept. The system capacity is considered for three different types of AP antennas as described in Table 3.1.

The values of the capacity do not differ widely from the results for the schoolroom. When the AP is near the middle of such a hallway, the most effective antennas are single dipoles. The capacities of 16.8 bit/s/Hz for CEIL case and 20.2

bit/s/Hz for DESK case can be achieved. If the AP is installed on the shorter wall, the antennas with gain of 7.24 dBi are more efficient than single dipoles – the maximal capacity is 17.6 bit/s/Hz. Generally, the results for the hallway are worse in comparison to the ones obtained for the schoolroom, because of the longer radio paths.

If the dimensions of the room are scaled up, the calculated capacity of the system decreases. It concerns all the discussed cases. The reason is obvious: the bigger the room is, the longer the radio paths and the more attenuated the signals.

3.9. Reliability and accuracy of ray tracing algorithm

To verify the reliability and the accuracy of the ray tracing algorithm used for the calculations, some additional experiments are performed. The problems of the number of reflections, the distribution of the UTs in the analysed room and the mutual coupling in the antenna arrays are considered below.

3.9.1. Number of reflections

There is an infinity of possible paths between each transmit and each receive antenna, because a radio ray can reflect from the walls infinitely. However, when the ray tracing algorithm is used, the number of considered reflections must be limited. Thus, only the paths with N_{ref} or less reflections are tracked. Such a limitation is reasonable, since the rays with more reflections are more attenuated. The laboratory measurements and their comparison with ray tracing results [76] show that N_{ref} equal to 3 gives the good accuracy. In this thesis, N_{ref} is equal to 4, for achieving even more exact results. The accuracy of the calculations with up to 4 wall reflections is also confirmed by the results presented in [10]. However, the differences between the results with $N_{ref} = 3$ and $N_{ref} = 4$ are negligible. The example of such a comparison is illustrated in Fig. 3.18. In this case, the average capacity for the AP placed under the ceiling and being moved along the diagonal of the room is shown.

For each AP position, the difference between the capacities in these two cases can be calculated as:

$$\Delta = \left| C\left(N_{ref} = 3\right) - C\left(N_{ref} = 4\right) \right| \tag{3.2}$$

The average and maximal differences are equal to 0.05 and 0.23 bit/s/Hz, respectively. These differences are similar for other cases analysed in the previous sections of these chapter. It allows concluding that the differences between the results with $N_{ref} = 4$ and $N_{ref} = 5$ are even smaller and the choice of $N_{ref} = 4$ provides the good accuracy of the calculations.

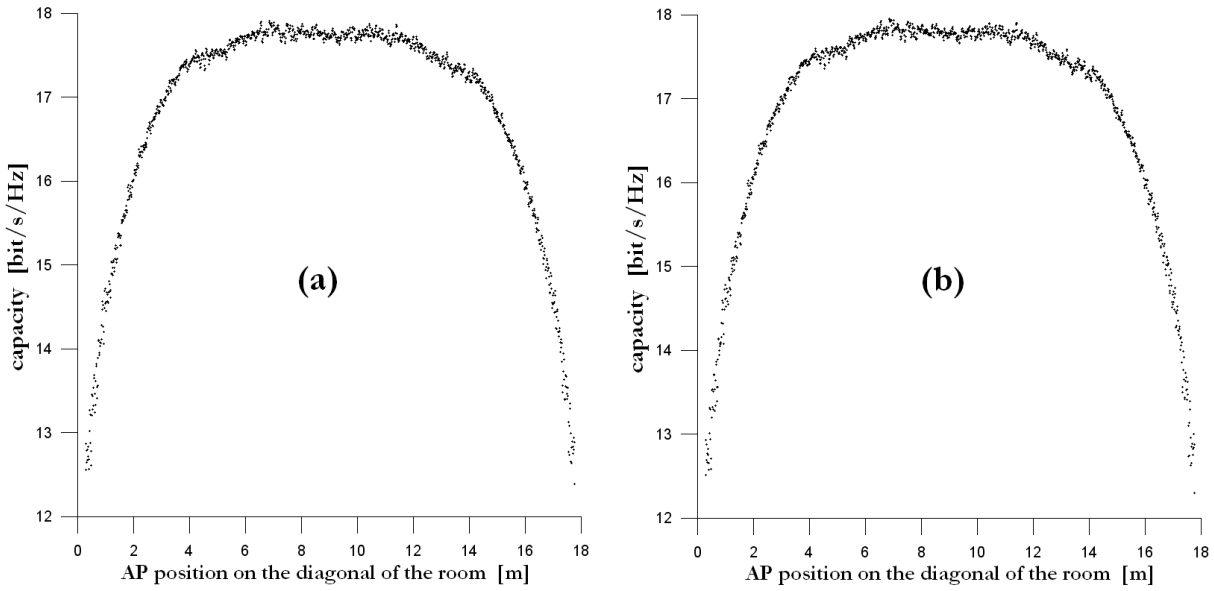

Fig. 3.18. The comparison of the average capacity calculated with $N_{ref} = 3$ (a) and $N_{ref} = 4$ (b). The AP is placed under the ceiling and is being moved along the diagonal of the room.

3.9.2. Location of the access point and the user terminals

In the richly scattered environment, even a small shift of the Tx or Rx antennas results in changes of the radio channel capacity. It is caused by constructive and destructive interferences of multipath components arriving to Rx antennas by multiple paths. It is clearly visible in the figures describing the average system capacity when the AP is being moved.

The shifts of the UTs positions can also effect the changes of the channel capacity. In all the above mentioned calculations, 600 UT positions in the analysed

room were considered. These positions were evenly distributed at the height of 75cm. To check if these evenness does not distort the results, the additional experiment is conducted. Each UT is horizontally shifted by the random distance, not more than 1 wavelength and then the capacity C_r is calculated. This value is compared with the capacity C_e when the UTs are evenly distributed. As a result, the difference between the capacities in these two cases can be calculated, similarly to Eq. (3.2):

$$\Delta_2 = \left| C_e - C_r \right|. \tag{3.3}$$

The average difference Δ_2 is below 0.07 bit/s/Hz and the maximal value is equal to 0.3 bit/s/Hz. This experiment shows that the considered inaccuracy is not very significant.

3.9.3. Mutual coupling

In the sections 3.4 ÷ 3.6, the ray tracing algorithm is used to analyse the radio propagation between the arrays of dipoles. The field patterns of the linear arrays of dipoles can be calculated from the simple theoretic formulas as a superposition of the patterns of each dipole with the appropriate normalization [42]. However, this method ignores the mutual coupling between the dipoles. The smaller the separation between the dipoles, the stronger the impact of this phenomenon is. In this thesis, the smallest considered separation is equal to 0.5λ.

To evaluate the impact of mutual coupling, the tests were done. The field patterns of the three types of AP antennas presented in Table 3.1 were again generated with EZNEC [18], the tool for modelling the antennas. The patterns from EZNEC and the analytical ones were used to calculate the capacity of the system for each type of the AP antenna. The differences were less than 0.03 bit/s/Hz in all cases, so the mutual coupling was ignored in further calculations. The mutual coupling also exists between the whole antennas at the AP and at the UTs. However, the separation between these antennas is much larger – usually 2λ, so the influence of mutual coupling can be neglected.

3.10. Conclusions

The first thesis of this dissertation states that:

The throughput in slow varying radio channels of indoor MIMO systems can be significantly increased when the locations and the antennas of the access point are carefully chosen.

In this chapter, this thesis was proved.

The MIMO WLAN systems are expected to operate in an indoor stationary or quasi-stationary environment. Even in such a simple case, when all the network is placed in a single room, there is a strong dependence of the system capacity on the radio channel and propagation. There are two main factors that have the positive effect on the system capacity: the high SNR and the small correlation between the subchannels of the MIMO system. To keep the SNR high, the average paths between the AP and the UTs should be as short as possible. Because of that, the AP should be located in the middle of the room: under the ceiling or on the desk among the UTs. The concept of AP with dynamically shaped antenna patterns is also very promising. The MRC algorithm can be applied to adapt the antenna patterns to the transmission between the AP and the particular UT. Since the radio channel is rather quasi-stationary and the full CSI can be assumed, the MRC algorithm can be performed at the AP all the time, avoiding the complexity of the UTs.

From the other side, the correlation between the subchannels of the MIMO system should be as small as possible. This correlation decreases as the separation between the AP antennas or between UT antennas increases. However, the antenna separation cannot be very large because of the limited dimensions of the AP and UTs. As an alternative, the AP can be divided into four parts. Very good results can be obtained if the AP antennas are mounted totally separately.

The calculations presented in this chapter show that the radio channel is crucial for the indoor MIMO WLAN performance. The understanding of the radio propagation in the quasi-stationary channel is a key to the proper indoor MIMO system design.

Anyone who considers arithmetical methods of producing
random digits is, of course, in a state of sin.
John von Neumann

Chapter 4

Estimation of fast varying radio channels

It is widely expected that MIMO systems will be applied in a new generation of mobile communication networks. In such networks, the radio channel can quickly change its characteristics because of the movement of a fast mobile terminal. Thus, in MIMO mobile communication systems, one faces fast varying radio channel which has to be estimated sufficiently often.

When the radio channel is varying fast, the procedure of the channel estimation encounters the number of difficulties. The radio channel cannot be assumed stationary or even quasi-stationary. The crucial question is: how often the channel transfer matrix should be estimated? On the one hand, the frequency of channel estimation should be high to track the channel variations. The faster the time variations are in the radio channel, the more frequent channel estimation should be. On the other hand, the frequent channel estimations result in less time for the data transmission. This problem is especially important in OFDM systems, because of the long duration of each transmitted symbol.

In the case of fast varying radio channels, one more important question arises: how long the training sequences should be? There are some suggestions in [30], but they concern stationary of quasi-stationary channels. Generally, there are three consequences of lengthening training sequences. First, the influence of the noise in the transmission is reduced. It is because of averaging the channel transfer matrix coefficients over the large number of values. Second, the estimation becomes less adequate because of channel variations during the estimation process. At last, to keep the same ratio between the data and training sequence transmission periods, the data transmission period must be proportionally longer, too. It results in a strong divergence between the estimated and real channel transfer matrices near the end of the data transmission period.

The two aforementioned questions are considered in this chapter. The new algorithm, Iterative Channel Estimation (ICE), is presented. ICE enables radio channel estimation during the data transmission. Thus, the channel is tracked frequently and the time is not wasted for numerous training sequences. ICE is designed for STBC codes, one of the most popular coding techniques for MIMO systems. Nevertheless, it could be also applied to some other coding schemes.

The effectiveness of the proposed algorithm is verified by the Monte-Carlo simulations. As these simulations require very long sequence of random numbers, the choice of appropriate pseudo-random number generator is discussed. Then, ICE performance is evaluated for BPSK and QPSK modulations. The influence of the length of the training sequence on the channel estimation effectiveness is also analysed.

4.1. Iterative Channel Estimation algorithm

In the most of modern radiocommunication systems, especially in mobile cellular networks, the whole transmission can be divided in two parts. First, the training sequence is transmitted – there are symbols which are known at the receiver. Then, the matrix $\boldsymbol{H}_{est}$ is estimated on the basis of the training sequence. The second

part is the data transmission. The symbols are decoded with the assumption that $\boldsymbol{H}_{est}$ is still a good approximation of the actual channel transfer matrix $\boldsymbol{H}$. However, when the radio channel is non-stationary, the difference between $\boldsymbol{H}_{est}$ and $\boldsymbol{H}$ is growing during the transmission. Near the end of the transmission of data, this difference may be quite significant. This is the obvious reason for a large BER. Of course, it is possible to transmit training sequence more often, but the capacity of the radio channel decreases, as a result.

The new proposed solution is the algorithm called Iterative Channel Estimation [44, 47]. ICE is designed for STBC codes. This algorithm enables the radio channel estimation on the basis of transmitted and decoded data. Thus, the radio channel can be estimated frequently without wasting time for training sequences. The concept of ICE is as follows.

In MIMO (n,m) system with STBCs, the transmission on a single block can be described as:

$$\boldsymbol{Y} = \boldsymbol{H} \cdot \boldsymbol{X} + \boldsymbol{N}, \tag{4.1}$$

where the elements of the $n \times p$ matrix $\boldsymbol{X}$ represent the transmitted symbols from space-time block coding scheme, $\boldsymbol{H}$ is the $m \times n$ channel transfer matrix, $\boldsymbol{N}$ is the $m \times p$ matrix of additive white Gaussian noise, $\boldsymbol{Y}$ is the $m \times p$ matrix of received signals and p is the number of vectors with data symbols transmitted in each block. The radio channel is assumed to be narrowband, so is can be treated as frequency-flat.

When the data symbols have been decoded from the matrix $\boldsymbol{X}$, the received signals can be multiplied by the matrix $\boldsymbol{X}^H$. The result is:

$$\boldsymbol{Y} \cdot \boldsymbol{X}^H = \boldsymbol{H} \cdot \boldsymbol{X} \cdot \boldsymbol{X}^H + \boldsymbol{N} \cdot \boldsymbol{X}^H. \tag{4.2}$$

For STBCs, the following statement can be written [68]:

$$\boldsymbol{X} \cdot \boldsymbol{X}^H = \sum_{i=1}^{k} \left| x_i \right|^2 \cdot \boldsymbol{I}_n = A \cdot \boldsymbol{I}_n, \tag{4.3}$$

where x_i is the $i-$th symbol from k different ones transmitted in a single block (see the section 1.4.1). $\boldsymbol{I}_n$ is the $n \times n$ identity matrix and A is the constant which is equal to the sum of the powers of all transmitted symbols. After substitution (4.3) into (4.2):

$$\boldsymbol{Y} \cdot \boldsymbol{X}^{H} = A \cdot \boldsymbol{H} + \boldsymbol{N} \cdot \boldsymbol{X}^{H} . \tag{4.4}$$

So, the multiplication of the matrix of the received signals and the matrix of the estimated transmitted signals (transpose and conjugate) gives the channel transfer matrix $\boldsymbol{H}$ disturbed by noise. If all the symbols of the constellation have the same power (e.g. BPSK, QPSK, but not M-QAM), A equals to the number of symbols transmitted in one block.

The equations presented above show that it is possible to estimate the channel transfer matrix $\boldsymbol{H}$ iteratively after decoding of each block with data symbols. Moreover, the estimation is a very simple process – multiplication of the received signals and conjugate transmitted ones. The accuracy of the estimation is affected by the two factors: average SNR at each receive antenna and the dynamics of the channel variations. With the SNR decreasing, more data blocks are decoded with errors. In consequence, when ICE is used, the radio channel is estimated incorrectly what can result in the error propagation. On the other hand, when fast channel variations occur, the estimated matrix $\boldsymbol{H}_{est}$ is inadequate to decode the next data blocks. Generally, the transmission without ICE results in larger BER. The influence of the above mentioned factors is described in details in the section 4.3, with the results of the simulations.

4.2. Data transmission with ICE algorithm

Now, the whole data transmission process with ICE algorithm will be presented. As in typical radiocommunication systems, the transmission consists of two alternating parts: training and data sequences. But, after the transmission of each block of data, the matrix $\boldsymbol{H}$ is re-estimated with ICE algorithm. In the consequence, the radio channel is tracked systematically.

For multiple-input single-output (MISO) systems with n transmit antennas, the minimum length of training sequence is n vectors of symbols [30]. The channel transfer matrix $\boldsymbol{H}$ has n elements and to solve a set of equations with n variables, n equations are needed. These equations should be linearly independent, so the

training sequence should also contain linearly independent vectors. For MIMO systems with n transmit antennas and m receive antennas, the minimum training sequence is also equal to n. In this case, the channel transfer matrix has $n \times m$ elements, but there are $n \times m$ equations also, because of m simultaneously received signals. The optimal length of the training sequence in MIMO systems can be longer than n – it will be shown in the section 4.3, with the results of the simulations. It is assumed that the training and data symbols are transmitted with the same power.

For the ICE algorithm, both training and data symbols should be organised in blocks. The length of training sequence is equal to T blocks and data sequence – D blocks. The proposed algorithm is designed for STBCs what determines the structure of data symbols. The training sequence does not need to be organised in STBC blocks, but there should be the blocks containing at least n orthogonal vectors of symbols. Such a single block can be the basis for estimating the matrix $\boldsymbol{H}$ independently. In the case of training sequence arranged in STBC blocks, the receiver can treat all the blocks (training and data) in the same way. From the other side, there is a drawback of such a solution: for some STBC codes the number of transmitted vectors p is higher than number of the transmit antennas n. In this case training sequence is lengthened over its minimum value and cannot be shortened. For the most popular STBC – Alamouti code, n equals to p, so this drawback disappears.

The presentation of ICE starts with easiest case, when the optimal length of training sequence is equal to one block. The whole part of the transmission contains one training block and D data blocks. The transmission begins with the training block and the channel transfer matrix $\boldsymbol{H}_{est}$ is estimated. Then, the first data block B_1 is sent. This block is decoded on the basis of $\boldsymbol{H}_{est}$. When this block is already known, the radio channel can be estimated again with no need of training sequence. The decoded block becomes the new training sequence and the new estimated channel transfer matrix $\boldsymbol{H}^{\mathrm{I}}_{est}$ is calculated. This new $\boldsymbol{H}^{\mathrm{I}}_{est}$ is the basis for decoding the next data block B_2. Again, the known block B_2 is treated as the training sequence and the subsequent matrix $\boldsymbol{H}^{\mathrm{II}}_{est}$ is calculated. The next data block B_3 is transmitted and so

on. After the transmition of D data blocks, the new training block is sent and the whole process restarts.

Now, the generalised algorithm is considered: the optimal length of training sequence is equal to T blocks. To initiate the transmission, the whole training sequence (T blocks) is sent and $\boldsymbol{H}_{est}$ is estimated. $\boldsymbol{H}_{est}$ is the average of estimations performed on the basis of each of T training blocks. Next, the first data block B_1 is transmitted and decoded. Then, the channel transfer matrix $\boldsymbol{H}_{est}^{\mathrm{I}}$ is estimated on the basis of T last blocks – one decoded data block and $T-1$ training blocks. $\boldsymbol{H}_{est}^{\mathrm{I}}$ is used to decode the next data block B_2. After that, $\boldsymbol{H}_{est}^{\mathrm{II}}$ is calculated on the basis of decoded blocks B_1 and B_2 and last $T-2$ training blocks. $\boldsymbol{H}_{est}^{\mathrm{II}}$ allows decoding next data block B_3 and so on. Since B_T data block is transmitted, the channel transfer matrix is estimated only on the basis of data blocks. After transmitting of D data blocks, the new training sequence is sent and the whole process restarts.

The presented above algorithm for the MIMO (n,m) system with the training sequence length of T blocks and the data sequence length of D blocks can be described as a four step procedure:

Step 1. The training sequence – T blocks – is transmitted and the whole channel transfer matrix $\boldsymbol{H}_{est}$ is estimated.

Step 2. One block of data is transmitted and decoded with the estimated $\boldsymbol{H}_{est}$.

Step 3. The channel transfer matrix is estimated again on the basis of last T blocks. These blocks can contain either data or training symbols.

Step 4. After transmission of D blocks of data, the algorithm returns to *Step 1* and restarts counting the blocks. If D blocks of data are not transmitted yet, the algorithm goes to *Step 2*.

Generally, the ICE algorithm consists of two main parts performed one after another: steps *2* and *3* of the algorithm. The first one is the decoding of a data block using the most up-to-date channel transfer matrix $\boldsymbol{H}_{est}$. The second one is the

channel estimation on the basis of last T blocks. The ICE algorithm is also illustrated in Fig. 4.1.

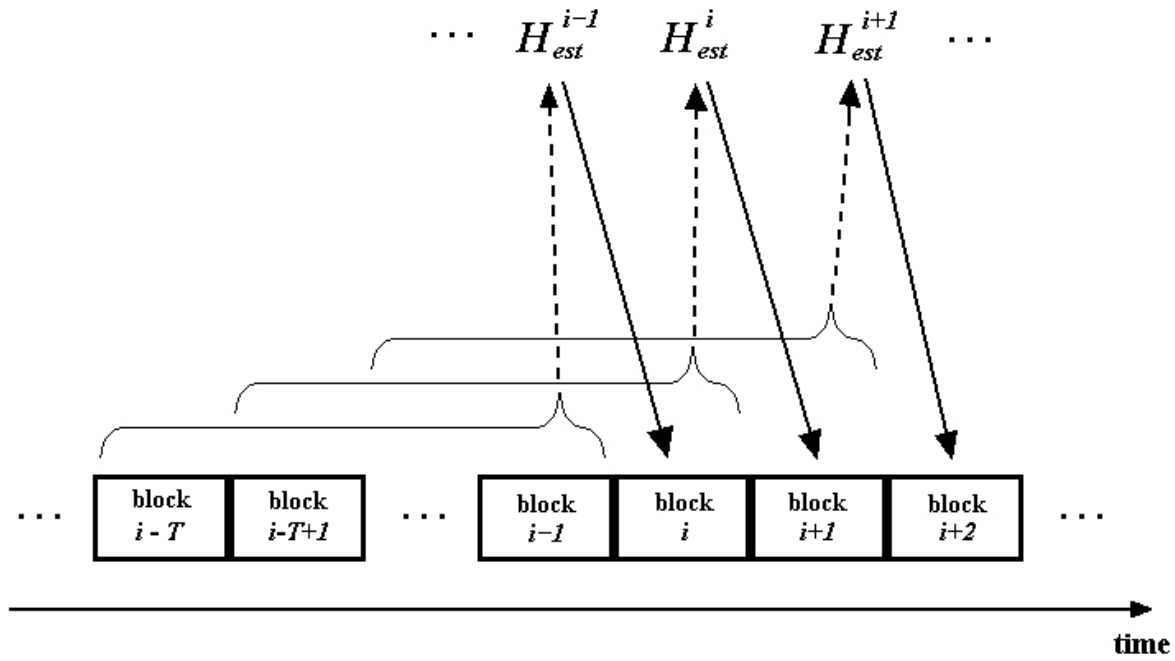

Fig. 4.1. The ICE algorithm consists of channel estimation (dashed lines) and data blocks decoding (continuous lines) performed in rotation.

It is desirable that the ratio T/D be as small as possible to maximize the system capacity. One could propose the ICE algorithm with the training sequence at the start and the infinitely long data sequence. The radio channel would be estimated on the basis of training sequence at the start. After that, ICE could be used and the channel estimation would be performed on the basis of decoded data blocks till the end of the transmission. However, there is serious drawback of such a conception: so called "domino effect" can happen. If only data blocks are transmitted and some subsequent blocks are decoded with errors, the radio channel will be estimated incorrectly. In the consequence, the next data blocks will be also decoded with errors, next channel estimations will be wrong and so on and so forth. It can cause the collapse of the whole transmission. To avoid this danger, the training sequence should be transmitted from time to time.

In the fast varying radio channel, the differential STBC scheme can be also used. It is also the scheme where a block of data symbols is decoded on the basis of

the previous one. However, even for stationary radio channels, the BER performance of the differential STBCs is 3 dB worse than in the case of the perfect channel knowledge [69]. ICE algorithm has not this penalty. If the channel is stationary, very long training sequence, e.g. 100 blocks, can be used. In Fig. 4.2, the BER performance of ICE in this case is shown. Even if the ratio T/D is as small as 0.01, the results are nearly the same as with the perfect channel knowledge. The results presented in Fig. 4.2 were obtained with Monte-Carlo simulations which are described in the section 4.3.1.

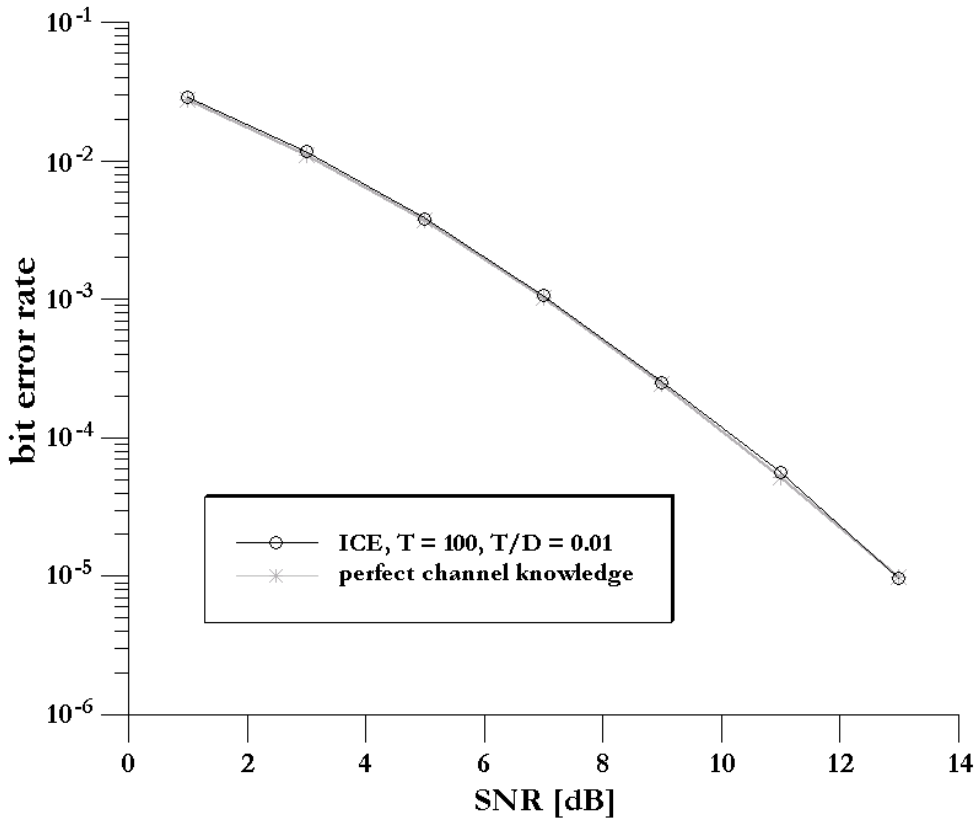

Fig. 4.2. BER performance for the transmission with ICE algorithm and BPSK modulation in the stationary radio channel compared to the case of perfect channel knowledge.

The ICE algorithm is designed for the codes where n orthogonal vectors of symbols are transmitted in each block. Then, the channel estimation algorithm is very simple, as presented in the section 4.1. Iterative Channel Estimation can be also applied for the transmission with other codes, not only with STBCs. To estimate the radio channel properly, n linearly independent vectors of symbols should be

received. If a code is used where there are n linearly independent vectors in each data block, the ICE algorithm can be applied. However, the radio channel estimation is more complicated in comparison to the case of orthogonal transmitted vectors: the set of n equations must be solved at the receiver.

If the transmission code is not the block one, the problem is even more difficult. The n consecutive vectors are not necessarily linearly independent. Thus, it should be assumed that there are n orthogonal vectors in r consecutive ones ($r \geq n$). Then, $\boldsymbol{H}$ can be estimated on the basis of these r vectors. However, even for $r >> n$, it is possible that there are less than n orthogonal vectors among r consecutive ones. Furthermore, the complexity of such an estimation is much higher than for STBCs, as these orthogonal vectors should be correctly chosen from the group of r ones.

4.3. Performance analysis of ICE algorithm

The Monte-Carlo simulations were made to verify the new method of channel estimation. The BER in MIMO (2,2) system with Alamouti transmission scheme and maximum-likelihood decoding was calculated. Two different modulations, BPSK and QPSK, were considered.

The radio channel was modelled as Rayleigh one. The channel variations were introduced by the different correlation coefficients C, as it was explained in the section 2.3. Every test was made for the wide range of SNR. Two types of transmission were likened:

a. standard transmission – the training sequence was sent and the channel transfer matrix $\boldsymbol{H}$ was estimated. Then, data symbols were sent and decoded on the basis of $\boldsymbol{H}$.
b. transmission with ICE algorithm – as described in the section 4.2.

In all cases, the training and data symbols were transmitted with the same power. The results were also compared with the case when the receiver had perfect knowledge about channel transfer matrix.

4.3.1. Simulation methodology

The simulation tool for BER performance analysis was written by the author of this thesis in C++. For both scenarios: with and without the ICE algorithm, BER was calculated for C equal to 0.999, 0.99 and 0.9. SNR ranged from 1 to 29 dB. Two modulation schemes were considered – BPSK and QPSK. The lengths of training sequences were equal to 1, 2, 5, 10 and 20 blocks. To compare these cases fairly, it was assumed that the system maintained the same capacity in all cases. The time for training sequences was always 10% of the total transmission time. This means that the sequences with data blocks were always 9 times longer than the training sequences and the effective capacity was 90% of maximal capacity. For the comparison, BER was also calculated for the case of the perfect channel knowledge, but these results are not novel: they can be found in [3].

The Monte-Carlo simulations of each BER value were made 10 times. Hence, the unbiased estimator of the mean BER was equal to:

$$\mu = \frac{1}{10}\sum_{i=1}^{10} \mathrm{BER}_\mathrm{i} \,, \tag{4.5}$$

where BER_i is the BER calculated in $i-\mathrm{th}$ simulation run. The value of μ is then treated as the calculated BER. To evaluate the accuracy of these simulations, the standard error of the mean BER was also computed:

$$\sigma_{\mathrm{BER}} = \sqrt{\frac{\sum_{i=1}^{10}\left(\mathrm{BER}_\mathrm{i} - \mu\right)^2}{90}} \,. \tag{4.6}$$

The calculated values of BER were even so small as 10^{-7}. To obtain the accurate results, the transmission of at least 10^8 blocks (10 series of 10^7 blocks) were simulated for each BER value. Also, it was assumed that at least 1000 erroneous bits had to occur in each simulation. Moreover, the ratio of standard error to the mean BER was not allowed to be higher than 0.1. Thus, some simulations were additionally extended to fulfil these conditions. Generally, the maximal transmission was $2\cdot 10^{10}$ blocks long. The mean values of BER for all the considered cases are presented and discussed in the next two sections. The standard errors of these mean values are listed in the tables in Appendix.

As the transmission of even $2 \cdot 10^{10}$ blocks should be taken into account, the appropriate pseudo-random number generator (PRNG) should be chosen. For the simulation of the transmission of one block, 12 complex joint Gaussian random variables and two uniformly distributed random variables have to be generated (two 2×2 channel matrices, one 2×2 noise matrix and two transmitted symbols). One complex joint Gaussian random variable can be generated as two Gaussian random variables with appropriate mean value and variance. The popular method to generate the Gaussian random variable is the Box-Muller transformation (polar method) proposed in [8]. The polar method is also used in this thesis. It allows generating two Gaussian random variables (or one complex joint Gaussian random variable) on the basis of two uniformly distributed random variables. However, during this transformation, about 21% of variables have to be discarded what decreases the efficiency of this method. This allows concluding that approximately 33 uniformly distributed random variables are needed for the simulation of the transmission of a single block. Therefore, the reasonable assumption is that the PRNG should be able to create the sequence of $33 \cdot 2 \cdot 10^{10} \approx 2^{40}$ independent and uniformly distributed random numbers.

Very popular PRNGs are linear congruential generators. Non-linear PRNGs generate the random numbers very slowly. However, is was proven [15] that linear congruential PRNG could be used as a source of no more than L numbers:

$$L = 16 \cdot \sqrt[3]{N}, \tag{4.7}$$

where N is the period of the PRNG. So, if the needed sequence of random numbers is 2^{40} long, the linear congruential PRNG with the period of at least 2^{108} should be used.

The commonly used linear PRNGs have the periods of $2^{31}-1$ or $2^{48}-1$ and must be discarded. Instead of them, the generator called "Mersenne Twister" [51] was chosen for the simulations described in this thesis. This generator has the period equal to $2^{19937}-1$ and is faster than standard linear congruential PRNGs. It passed many tests for PRNGs, including the diehard test and the load test. Currently, "Mersenne Twister" is considered as one of the best PRNGs for fast and reliable random number generating.

4.3.2. BPSK modulation

The system with BPSK modulation was simulated. To show the wide range of channel variations, the radio channels with C equal to 0.999, 0.99 and 0.9 were considered. The smaller the coefficient C, the larger the channel variations are.

First, the simulations were performed for $C = 0.999$. The BER performance for the standard transmission and the transmission with ICE is shown in Figs. 4.3 and 4.4, respectively. The results for different lengths of training sequences are compared. In all figures, the case of perfect channel knowledge is also given as a reference.

Generally, when SNR is small, e.g. below 5 dB, using of longer training sequences gives better results. The estimation of the radio channel is inaccurate after the minimal training sequence. For the high channel correlation ($C = 0.999$), variations in radio channel are not very rapid. Thus, it is possible to estimate the radio channel more properly on the basis of the longer training. The changes of the channel transfer matrix caused by variations are negligible in comparison to deteriorations caused by a radio noise. However, for such a small SNR, BER is unacceptably high, more than 10^{-2}.

When SNR is growing, shorter training sequences become more effective. In this case, the radio channel could be well estimated after the very short training. The longer training gives no improvement. Quite the contrary: the long channel estimation is deteriorated by channel variations, even if they are very small. For the case of standard transmission, the training sequences $T = 10$ and $T = 20$ are inefficient for the whole range of SNR, so these cases were not shown at all.

The transmissions with and without ICE are compared in Fig. 4.5. For the standard transmission, the cases of $T = 2$ and $T = 1$ are chosen, as they allow achieving the best results for the average ($10 \div 15\,\mathrm{dB}$) and high ($20 \div 25\,\mathrm{dB}$) SNR, respectively. For the transmission with ICE, the cases of $T = 10$ and $T = 2$ are presented for the same reason.

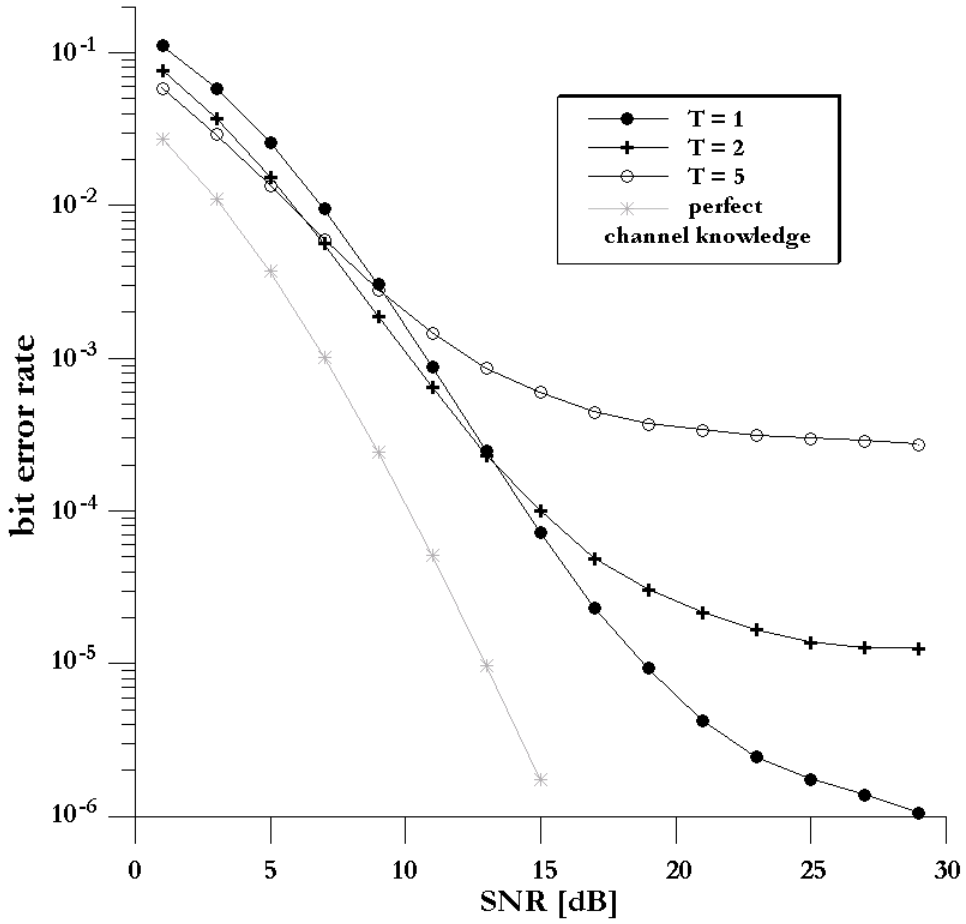

Fig. 4.3. BER performance for the standard transmission with BPSK modulation and channel correlation C = 0.999.

Generally, the ICE algorithm improves the BER performance for nearly whole range of SNR. If the criterion was to achieve $\mathrm{BER} < 10^{-3}$, the transmission with ICE could be realized with $\mathrm{SNR} = 9\,\mathrm{dB}$ in comparison to $\mathrm{SNR} = 11\,\mathrm{dB}$ in the case of standard transmission. The advantage of ICE is especially significant for high SNR. For $\mathrm{SNR} = 25\,\mathrm{dB}$, ICE can reduce BER about 16 times. Moreover, it is impossible to achieve $\mathrm{BER} < 10^{-6}$ without this algorithm.

Next, BER was calculated for $C = 0.99$. In Fig. 4.6, the results of these calculations for the standard transmission are shown. In this case, the variations in the radio channel are so fast that the training sequences longer than 2 blocks are totally inefficient. The best results are obtained for $T = 1$, but even in this case it is impossible to achieve $\mathrm{BER} < 10^{-3}$. Increasing SNR even to 50 dB does not improve the BER performance.

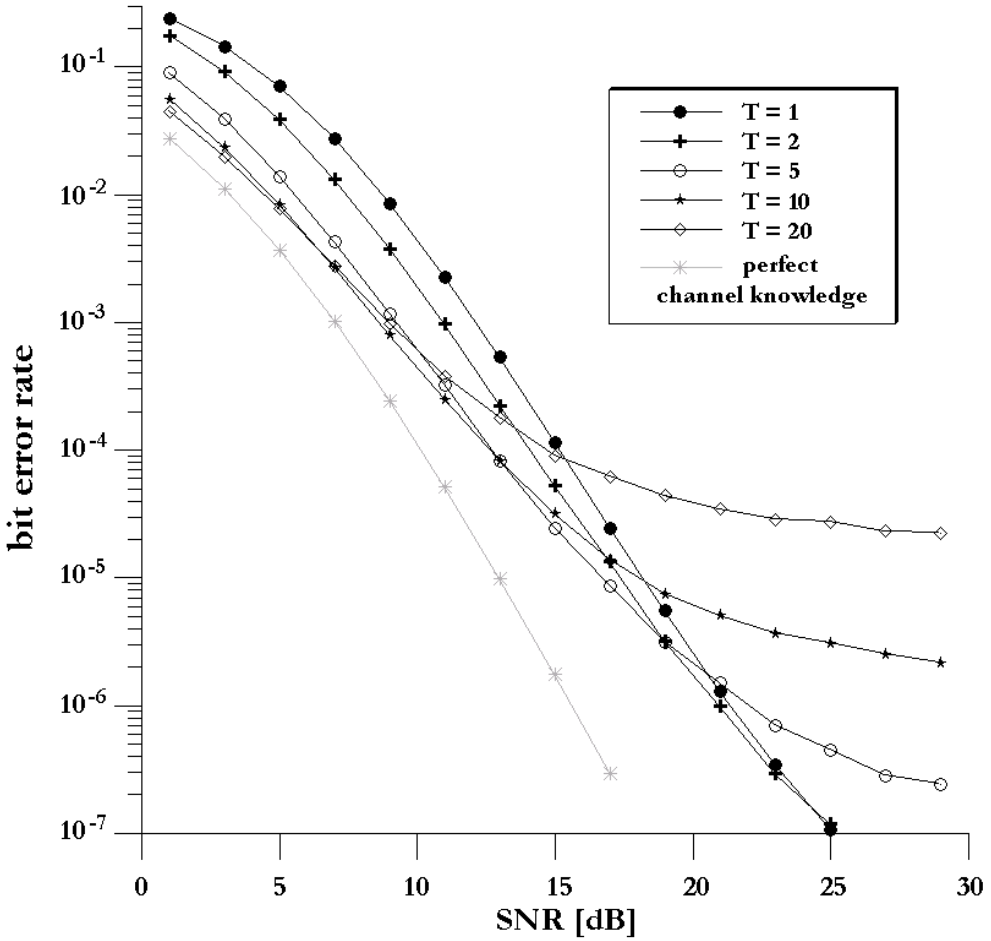

Fig. 4.4. BER performance for the transmission with ICE, BPSK modulation and channel correlation $C = 0.999$.

The results of the transmission with ICE are presented in Fig. 4.7. The training longer than $T = 1$ is effective only for $\mathrm{SNR} < 15\,\mathrm{dB}$ and the improvement is insignificant. To achieve $\mathrm{BER} < 10^{-3}$, $\mathrm{SNR} = 15\,\mathrm{dB}$ is sufficient. For $\mathrm{SNR} = 29\,\mathrm{dB}$, ICE algorithm reduces BER more than 80 times in comparison to the standard transmission.

Finally, the case with $C = 0.9$ was analysed. In the radio channel with such huge variations, BER performance is severely degraded. In the case of standard transmission with the optimal length of the training sequence, BER is not lower than 0.2 even for $\mathrm{SNR} = 50\,\mathrm{dB}$. When ICE is applied, BER equal to 0.05 can be achieved for the same SNR.

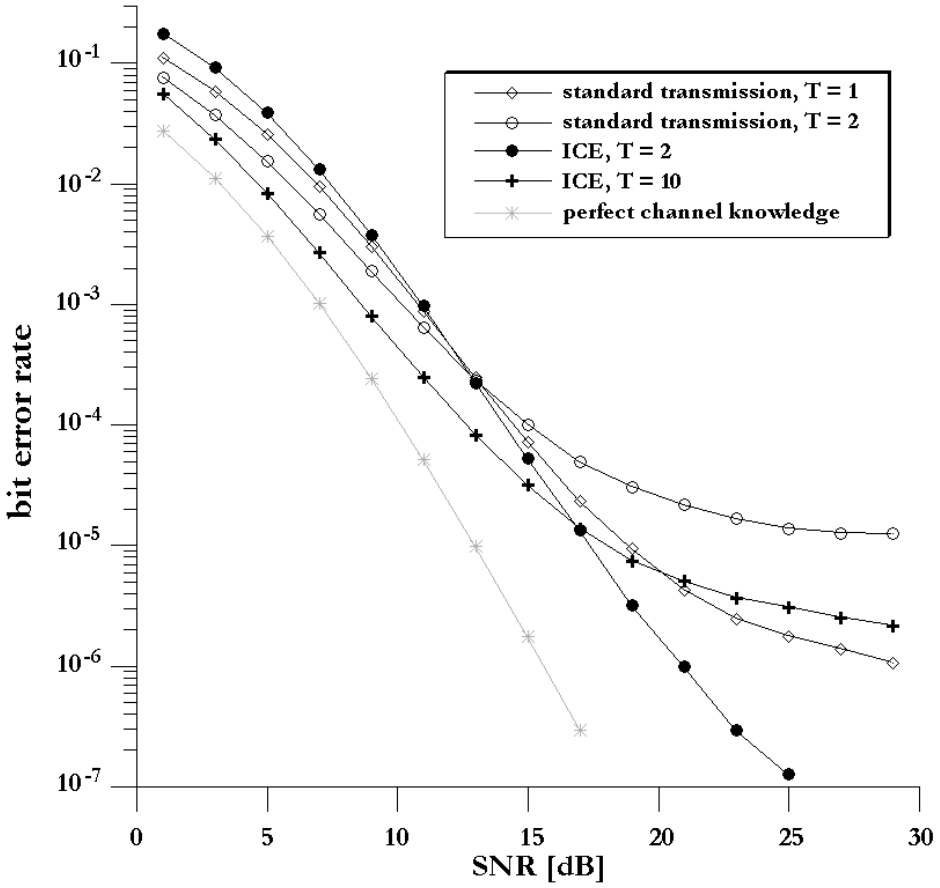

Fig. 4.5. The comparison of the chosen cases of the standard transmission and the transmission with ICE for $C = 0.999$ and BPSK modulation.

4.3.3. QPSK modulation

The ICE algorithm can be implemented successfully also for higher level modulations. The results of BER performance simulations for QPSK modulation are presented in Figs. 4.8 ÷ 4.10. These results are similar to the BPSK cases. The obtained BER values are a little worse. It can be easily understood, as the higher level modulation requires higher SNR to achieve the same BER.

The BER curves for $C = 0.999$ are depicted in Figs. 4.8 and 4.9, for the standard transmission and ICE algorithm, respectively. When SNR is low, the improvement of ICE is not noticeable. However, ICE allows achieving $\mathrm{BER} < 10^{-3}$ with 2 dB lower SNR, i.e. 13 dB instead of 15 dB. When SNR is as high as 27 dB, $\mathrm{BER} < 10^{-6}$ can be obtained with ICE. For the standard transmission with the same SNR, BER is higher than 10^{-5}.

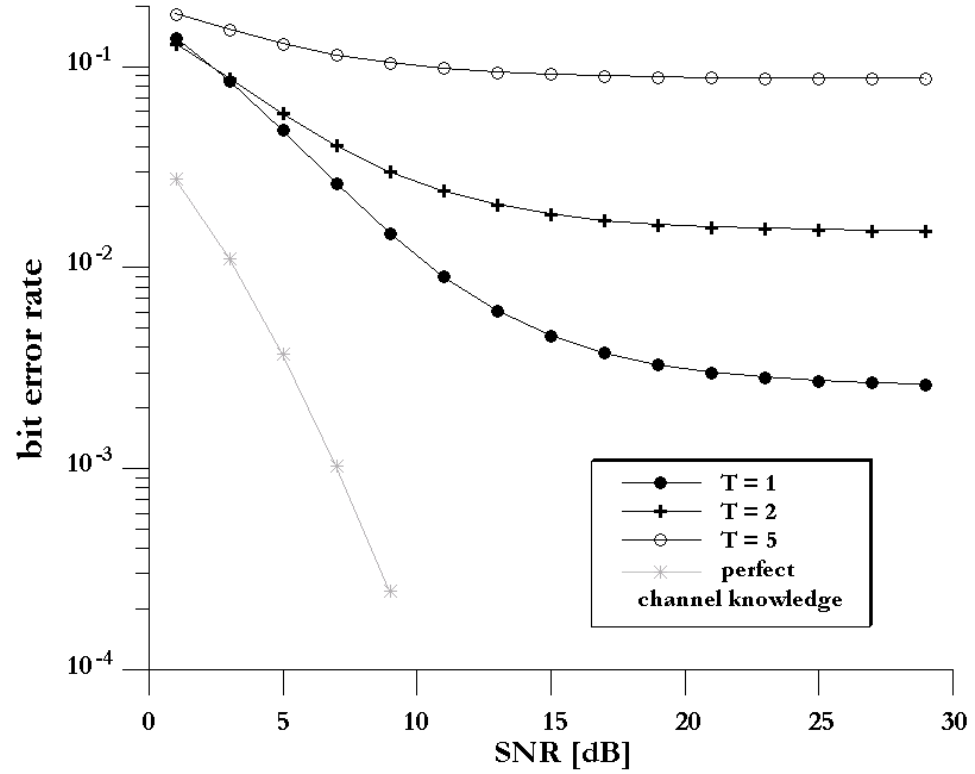

Fig. 4.6. BER performance for the standard transmission with BPSK modulation and channel correlation $C = 0.99$.

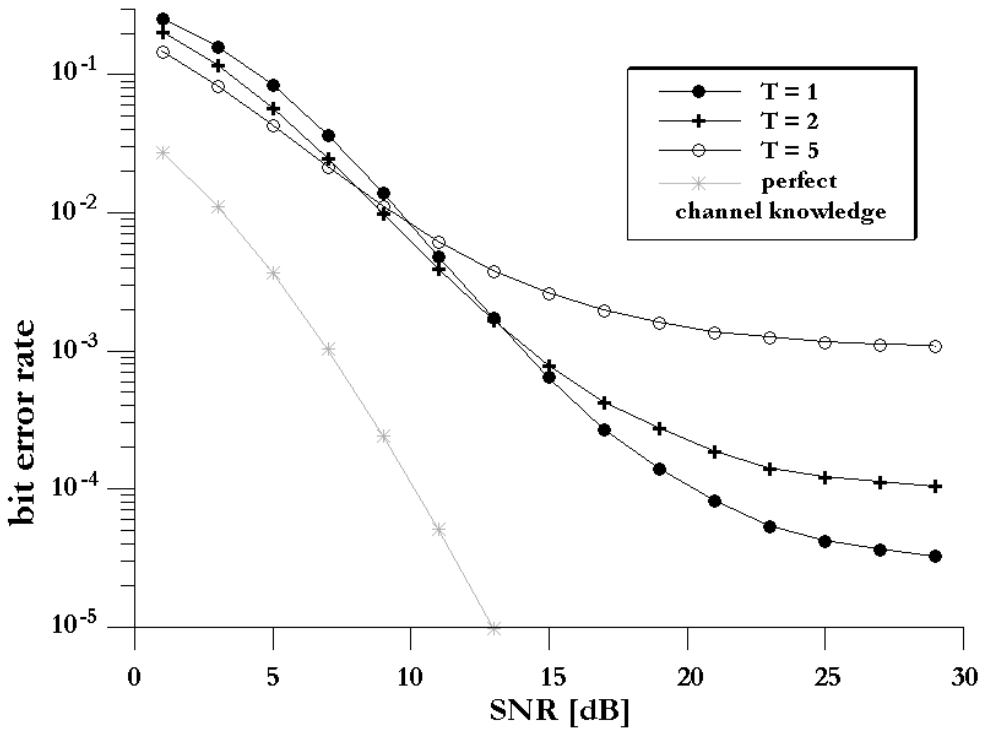

Fig. 4.7. BER performance for the transmission with ICE, BPSK modulation and channel correlation $C = 0.99$.

For the radio channels with $C = 0.99$, it was very difficult to achieve $\mathrm{BER} < 10^{-3}$. It was even impossible for standard transmission. ICE algorithm allowed achieving $\mathrm{BER} < 10^{-3}$ only for SNR higher than $21\,\mathrm{dB}$. In Fig. 4.10, the case of standard transmission with $T = 1$ is compared to the transmission with ICE with $T = 1$ or $T = 2$. Other lengths of training sequences are not effective.

4.3.4. Length of training sequence

The optimal length of training sequence T strongly depends on the channel correlation C. Moreover, C can vary during the transmission. The ICE algorithm is designed for the case of fast variations, mainly. In such a radio channel, short or even minimal length of training sequence seems to be optimal. It is shown in Figs. 4.7 and 4.10, where the ICE algorithm in the channel with $C = 0.99$ is discussed.

Also, if the transmission system requires very low BER and high average SNR is possible to obtain, minimal length of training sequence is preferable. Long training sequence is more suitable for the transmission in the slowly varying radio channel with low signal-to-noise ratio (Figs. 4.5 and 4.9).

4.3.5. MIMO systems with high number of antennas

If there are n transmit antennas in a MIMO system, the minimal length of training sequence is also n. If a system with higher n is used, e.g. 4 or 8, the training sequence should be proportionally longer. So, the channel estimations as well as the transmissions of the data blocks are also longer. Thus, the radio channel variations are more troublesome. For this reason, one can suppose the improvement of the system performance with the ICE algorithm is even larger for the higher number of transmit antennas.

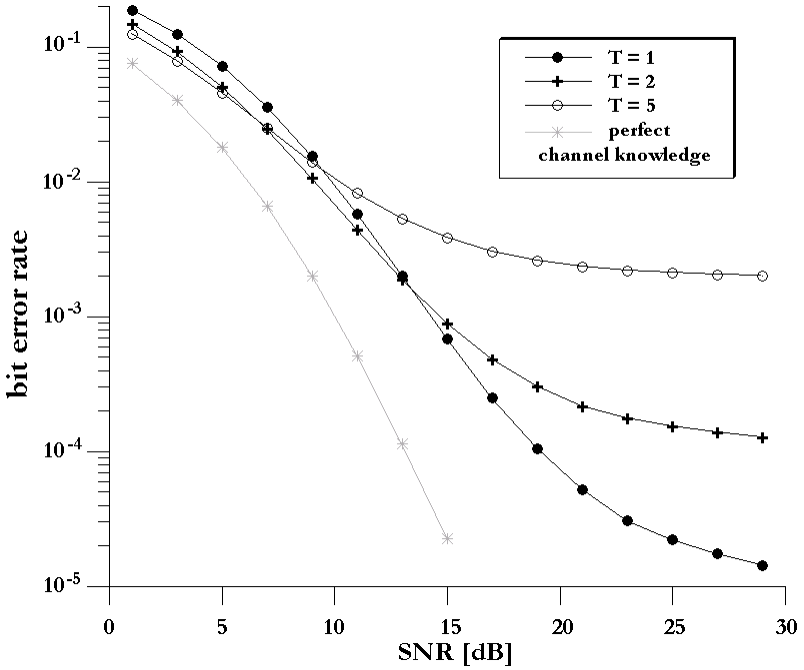

Fig. 4.8. BER performance for the standard transmission with QPSK modulation and channel correlation $C = 0.999$.

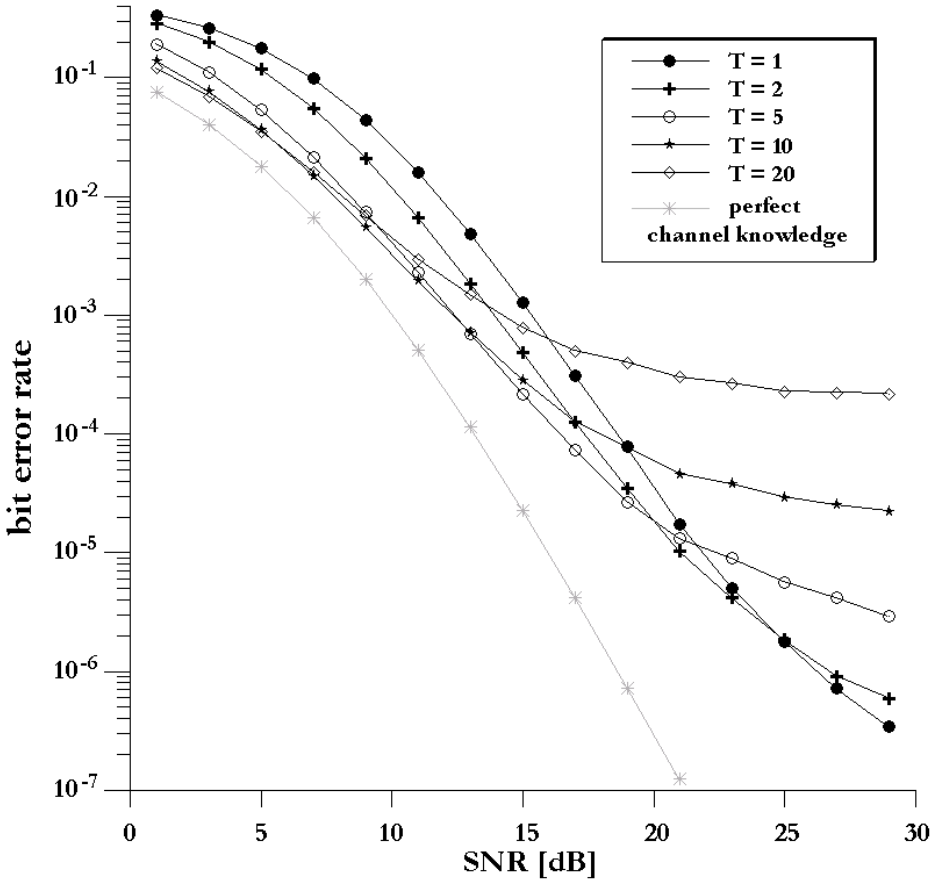

Fig. 4.9. BER performance for the transmission with ICE, QPSK modulation and channel correlation $C = 0.999$.

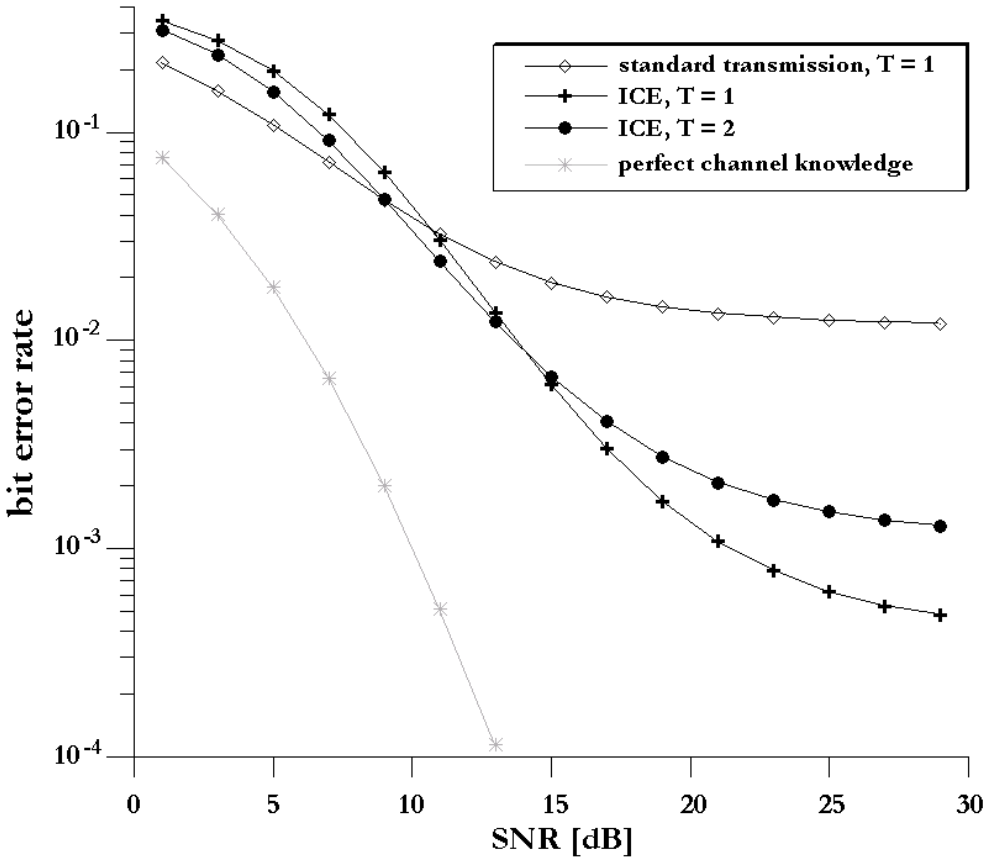

Fig. 4.10. The comparison of the chosen cases of the standard transmission and the transmission with ICE for $C = 0.99$ and QPSK modulation.

4.4. Conclusions

With the first ideas of MIMO systems, it was assumed that the radio channel is stationary or quasi-stationary. Nonetheless, MIMO systems were adapted to the standards of third generation cellular networks. When a mobile terminal is moving at a high speed, the radio channel is fast varying and cannot be assumed quasi-stationary. In this case, the key issue is the radio channel estimation. It should be performed sufficiently often to effectively track the channel variations. From the other side, the training sequence cannot consume too much time allotted for data transmission.

To break this stalemate, the new algorithm, Iterative Channel Estimation, was proposed. ICE allows the estimation of the channel transfer matrix simultaneously

with the data symbols transmission. The estimation is a very simple process – just the multiplication of signals. ICE is designed for the transmission in the radio channels with fast variations where an often channel estimation is needed. When ICE is implemented, BER is reduced in comparison to the standard transmission. The ICE algorithm is particularly efficient for high SNR values: for some cases BER is reduced even 50 times or more.

Thus, according to the second thesis of this dissertation, it is now proved that: **Iterative Channel Estimation algorithm allows decreasing the bit error rate in fast varying radio channels without frequent transmissions of training sequences.**

In this chapter, the problem of the length of training sequences for the fast varying radio channels was also considered. Generally, the faster variations in the radio channel, the shorter the training sequence should be. If SNR is high, the minimal length of training sequence is the optimal solution.

The future, according to some scientists,
will be exactly like the past, only far more expensive.
John Sladek

Summary

MIMO systems are perceived as a very promising technique which will help to overcome the problems of the limited throughput and the multipath fading in the next generation of mobile wireless networks. Is it especially important in the case of two most popular and rapidly developing wireless communication systems – WLANs and cellular networks. There are strong expectations that MIMO systems will play the key role in the future standards of these networks. So far, there is no rapid progress in the integration of MIMO systems into the telecommunication standards. Despite nearly ten years of the extensive research in this field, many problems still remain unsolved.

The cellular networks and WLANs differ mainly with respect to the radio propagation channel. The WLAN radio channel is stationary or quasi-stationary. In the case of the cellular networks, the radio channel can be even fast varying. In each instance, there are other challenges and possibilities when the MIMO systems are considered.

This PhD dissertation was focused on the efficient implementation of the MIMO systems in the wireless networks with different types of the radio channels. The following theses were formulated and proved:

1. The throughput in slow varying radio channels of indoor MIMO systems can be significantly increased when the locations and the antennas of the access point are carefully chosen.

2. Iterative Channel Estimation algorithm allows decreasing the bit error rate in fast varying radio channels without frequent transmissions of training sequences.

The results of the author's research were provided in two parts, described in the separate chapters. In each of these chapters, one of the abovementioned theses was proved and the novel achievements, concerning the slow and fast varying channels, were presented.

First, the example of the system in the quasi-stationary radio channel was considered. The performance of the indoor WLAN with multiple antennas was evaluated with the aid of the 3-D ray tracing algorithm. It was shown that the proper location of the access point could double the system capacity. The advantages of the directional and omnidirectional antennas were discussed. The concept of the access point with the adaptive antennas was verified. The influence of the antenna separation, the dimensions and the shape of the room and dielectric constant of the walls were also investigated. As a result, some important factors and design rules critical for the high system performance were presented.

In the second part of the research, the transmission in the fast varying channel was analysed. The problem of the accurate channel estimation was addressed. The new Iterative Channel Estimation algorithm was proposed. This method allows for the simultaneous data transmission and the channel estimation. Therefore, the time is not wasted for numerous training sequences and the channel state information can be accurate and frequently updated. This algorithm was designed for space-time block codes, but it can also be used with other coding schemes if only the vectors of the transmitted symbols are linearly independent from each other. ICE was verified by the Monte-Carlo simulations. It was shown that, in some cases, BER could be reduced even 80 times when ICE was applied.

There are some challenges in both slow and fast varying channels when wireless networks with multiple antennas are designed. Some of them were recognised and responded in this PhD thesis. However, many issues are unsolved and many of them are still hidden. Let's not limit our vision.

Appendix

The standard errors of mean bit error rates

In the chapter 4, the Monte-Carlo simulations of bit error rates during the transmission in time-varying radio channels were described. The mean BER values were depicted in figures 4.2 ÷ 4.10. For the clarity of the figures, the standard errors of mean BER values were omitted. They are presented in the tables below. For each table, the corresponding figures from the chapter 4 are mentioned. In any case, the standard error is not higher than 10% of the mean bit error rate. The bit error rates below 10^{-7} were not considered.

Table A.1

The mean BER values and their standard errors

for the case of perfect channel knowledge (supplement to figures 4.2÷4.10).

	BPSK modulation		QPSK modulation	
SNR [dB]	mean BER	standard error	mean BER	standard error
1	0.02743	7.33E-06	0.075398	1.14E-05
3	0.011115	6.06E-06	0.040248	8.97E-06
5	0.003695	5.26E-06	0.017962	5.82E-06
7	0.001022	1.95E-06	0.006607	5.92E-06
9	0.000244	7.79E-07	0.002005	2.45E-06
11	5.12E-05	5.25E-07	0.000511	1.48E-06
13	9.76E-06	1.70E-07	0.000114	3.70E-07
15	1.75E-06	2.27E-08	2.26E-05	2.39E-07
17	2.93E-07	4.74E-09	4.19E-06	3.00E-08
19	< 1E-07	-	7.22E-07	9.72E-09
21	< 1E-07	-	1.24E-07	1.22E-09

Table A.2

The mean BER values and their standard errors for the transmission with ICE algorithm and BPSK modulation in the stationary channel (supplement to Fig. 4.2).

SNR [dB]	mean BER	standard error
1	0.028657	0.00013
3	0.011654	6.90E-05
5	0.003841	3.82E-05
7	0.001061	1.23E-05
9	0.000249	4.40E-06
11	5.61E-05	2.75E-06
13	9.75E-06	3.75E-07

Table A.3

The mean BER values and their standard errors for the standard transmission with BPSK modulation in the radio channel with $C = 0.999$ (supplement to figures 4.3 and 4.5).

	$T = 1$		$T = 2$		$T = 5$	
SNR [dB]	mean BER	standard error	mean BER	standard error	mean BER	standard error
1	0.110861	5.63E-05	0.076371	5.05E-05	0.058201	3.59E-05
3	0.058484	2.22E-05	0.037156	3.04E-05	0.02924	3.29E-05
5	0.02583	2.37E-05	0.015404	1.67E-05	0.013455	1.55E-05
7	0.009517	1.18E-05	0.005612	7.53E-06	0.006001	1.35E-05
9	0.003033	5.43E-06	0.001886	8.00E-06	0.0028	1.20E-05
11	0.00088	4.52E-06	0.000646	3.50E-06	0.001464	5.44E-06
13	0.000248	1.28E-06	0.000232	2.79E-06	0.000858	5.59E-06
15	7.22E-05	1.04E-06	0.0001	1.79E-06	0.000596	3.16E-06
17	2.32E-05	5.60E-07	4.89E-05	4.93E-07	0.000443	4.68E-06
19	9.33E-06	4.07E-07	3.06E-05	7.02E-07	0.000367	4.34E-06
21	4.26E-06	4.19E-08	2.16E-05	5.59E-07	0.000336	3.12E-06
23	2.44E-06	5.24E-08	1.66E-05	4.01E-07	0.000311	3.52E-06
25	1.76E-06	6.46E-08	1.38E-05	2.14E-07	0.000297	5.32E-06
27	1.38E-06	4.17E-08	1.27E-05	2.56E-07	0.000286	4.75E-06
29	1.06E-06	4.41E-08	1.25E-05	3.44E-07	0.000272	4.66E-06

Table A.4

The mean BER values and their standard errors for the transmission with ICE and BPSK modulation, T = 1, 2 and 5, C = 0.999 (supplement to figures 4.4 and 4.5).

	$T = 1$		$T = 2$		$T = 5$	
SNR [dB]	mean BER	standard error	mean BER	standard error	mean BER	standard error
1	0.239638	6.08E-05	0.175741	6.07E-05	0.090028	6.72E-05
3	0.145176	7.15E-05	0.092335	6.15E-05	0.039027	7.81E-05
5	0.070717	5.42E-05	0.038773	4.53E-05	0.013945	4.77E-05
7	0.02748	2.14E-05	0.013216	2.76E-05	0.004248	2.90E-05
9	0.008606	1.42E-05	0.003802	2.07E-05	0.00118	1.17E-05
11	0.002282	1.02E-05	0.000972	6.70E-06	0.000323	6.41E-06
13	0.000534	5.21E-06	0.000223	3.52E-06	8.19E-05	2.08E-06
15	0.000115	3.14E-06	5.25E-05	1.75E-06	2.45E-05	1.50E-06
17	2.46E-05	1.02E-06	1.33E-05	9.63E-07	8.71E-06	5.78E-07
19	5.50E-06	1.62E-07	3.17E-06	1.64E-07	3.12E-06	2.34E-07
21	1.28E-06	7.26E-08	9.84E-07	6.00E-08	1.50E-06	1.40E-07
23	3.43E-07	7.55E-09	2.91E-07	1.74E-08	7.01E-07	3.69E-08
25	1.06E-07	3.75E-09	1.26E-07	4.24E-09	4.21E-07	2.73E-08
27	< 1E-07	-	< 1E-07	-	2.82E-07	2.28E-08
29	< 1E-07	-	< 1E-07	-	2.41E-07	1.56E-08

Table A.5

The mean BER values and their standard errors for the transmission with ICE and BPSK modulation, T = 10 and 20, C = 0.999 (supplement to figures 4.4 and 4.5).

	$T = 10$		$T = 20$	
SNR [dB]	mean BER	standard error	mean BER	standard error
1	0.055609	9.35E-05	0.044917	8.35E-05
3	0.023332	5.32E-05	0.019747	5.94E-05
5	0.008374	4.38E-05	0.007736	2.40E-05
7	0.002685	1.03E-05	0.002789	2.82E-05
9	0.000796	1.45E-05	0.000976	1.33E-05
11	0.000249	3.33E-06	0.000382	1.24E-05
13	8.22E-05	4.41E-06	0.000178	1.00E-05
15	3.16E-05	2.56E-06	8.99E-05	8.02E-06
17	1.37E-05	5.48E-07	6.18E-05	3.70E-06
19	7.47E-06	6.04E-07	4.40E-05	2.33E-06
21	5.05E-06	1.86E-07	3.45E-05	1.26E-06
23	3.68E-06	3.44E-07	2.86E-05	9.76E-07
25	3.05E-06	1.74E-07	2.74E-05	1.38E-06
27	2.52E-06	1.89E-07	2.31E-05	1.97E-06
29	2.15E-06	1.14E-07	2.24E-05	1.91E-06

Table A.6

The mean BER values and their standard errors for the standard transmission with BPSK modulation in the radio channel with $C = 0.99$ (supplement to Fig. 4.6).

	$T = 1$		$T = 2$		$T = 5$	
SNR [dB]	mean BER	standard error	mean BER	standard error	mean BER	standard error
1	0.137946	5.21E-05	0.129349	7.26E-05	0.182522	6.12E-05
3	0.084745	3.14E-05	0.086769	4.18E-05	0.15148	0.000105
5	0.048065	2.55E-05	0.057993	4.16E-05	0.128991	9.25E-05
7	0.026227	1.81E-05	0.040228	2.50E-05	0.113664	7.28E-05
9	0.014737	2.22E-05	0.029836	2.46E-05	0.103923	0.000144
11	0.00896	9.44E-06	0.023918	3.37E-05	0.09756	0.0001
13	0.006084	1.18E-05	0.020412	2.66E-05	0.09342	7.78E-05
15	0.004555	9.02E-06	0.018305	3.82E-05	0.090982	8.88E-05
17	0.003736	7.04E-06	0.017033	2.16E-05	0.089284	7.89E-05
19	0.003268	6.69E-06	0.016298	2.66E-05	0.08817	7.96E-05
21	0.002991	9.22E-06	0.015779	1.74E-05	0.087469	0.000103
23	0.00283	5.66E-06	0.01552	2.79E-05	0.087044	4.63E-05
25	0.002716	5.11E-06	0.01534	1.75E-05	0.086961	7.51E-05
27	0.002658	4.50E-06	0.01518	2.95E-05	0.086795	8.84E-05
29	0.002613	5.86E-06	0.015139	1.14E-05	0.086676	7.45E-05

Table A.7

The mean BER values and their standard errors for the transmission with ICE and BPSK modulation in the radio channel with $C = 0.99$ (supplement to Fig. 4.7).

	$T = 1$		$T = 2$		$T = 5$	
SNR [dB]	mean BER	standard error	mean BER	standard error	mean BER	standard error
1	0.252248	9.75E-05	0.201015	0.000104	0.144943	7.95E-05
3	0.159633	8.24E-05	0.11666	6.32E-05	0.082048	0.000107
5	0.083545	5.05E-05	0.05721	4.31E-05	0.042505	7.86E-05
7	0.036583	3.76E-05	0.024557	4.12E-05	0.021289	5.15E-05
9	0.013837	2.36E-05	0.009853	2.73E-05	0.011038	4.51E-05
11	0.004837	1.73E-05	0.003922	1.45E-05	0.006146	2.58E-05
13	0.001711	7.69E-06	0.00165	5.60E-06	0.003782	4.10E-05
15	0.000638	5.36E-06	0.000773	8.12E-06	0.00259	1.89E-05
17	0.000269	2.83E-06	0.00042	5.19E-06	0.001952	1.01E-05
19	0.000138	2.29E-06	0.000273	5.11E-06	0.001576	1.48E-05
21	8.14E-05	1.59E-06	0.000186	2.92E-06	0.001337	1.89E-05
23	5.34E-05	9.49E-07	0.00014	2.92E-06	0.001234	1.09E-05
25	4.14E-05	1.14E-06	0.000119	3.17E-06	0.001144	1.02E-05
27	3.61E-05	1.08E-06	0.000112	1.43E-06	0.001095	1.32E-05
29	3.22E-05	1.09E-06	0.000103	1.94E-06	0.001078	1.41E-05

Table A.8

The mean BER values and their standard errors for the standard transmission with QPSK modulation in the radio channel with $C = 0.999$ (supplement to Fig. 4.8).

	$T = 1$		$T = 2$		$T = 5$	
SNR [dB]	mean BER	standard error	mean BER	standard error	mean BER	standard error
1	0.188017	5.72E-05	0.14814	5.64E-05	0.124	3.90E-05
3	0.124601	3.54E-05	0.092395	3.41E-05	0.078356	4.65E-05
5	0.072399	2.68E-05	0.050668	2.78E-05	0.045593	2.74E-05
7	0.036086	1.64E-05	0.024444	2.25E-05	0.02518	2.64E-05
9	0.015456	1.02E-05	0.010642	1.34E-05	0.013942	2.83E-05
11	0.005814	7.27E-06	0.004419	7.93E-06	0.008204	6.90E-06
13	0.002006	4.19E-06	0.001876	7.61E-06	0.005323	1.75E-05
15	0.000684	2.08E-06	0.000888	3.24E-06	0.003852	7.21E-06
17	0.000248	1.15E-06	0.000477	1.90E-06	0.003039	1.13E-05
19	0.000106	7.89E-07	0.000302	2.45E-06	0.002597	8.89E-06
21	5.24E-05	7.26E-07	0.000215	1.42E-06	0.002354	9.40E-06
23	3.06E-05	4.46E-07	0.000176	1.99E-06	0.002199	7.41E-06
25	2.21E-05	4.19E-07	0.000153	1.13E-06	0.002104	6.83E-06
27	1.74E-05	3.99E-07	0.000138	1.69E-06	0.002048	8.44E-06
29	1.43E-05	2.55E-07	0.000126	1.24E-06	0.002	9.83E-06

Table A.9

The mean BER values and their standard errors for the transmission with ICE and QPSK modulation, $T = 1$, 2 and 5, $C = 0.999$ (supplement to Fig. 4.9).

	$T = 1$		$T = 2$		$T = 5$	
SNR [dB]	mean BER	standard error	mean BER	standard error	mean BER	standard error
1	0.331583	6.49E-05	0.284116	6.49E-05	0.190439	6.34E-05
3	0.25925	3.25E-05	0.200108	0.00011	0.111291	0.000125
5	0.175677	6.16E-05	0.116878	3.48E-05	0.053399	5.85E-05
7	0.098171	2.40E-05	0.054895	5.06E-05	0.021299	4.31E-05
9	0.044134	2.50E-05	0.020849	4.23E-05	0.007351	3.29E-05
11	0.015976	1.80E-05	0.006634	2.14E-05	0.002296	1.10E-05
13	0.004857	8.91E-06	0.001845	1.22E-05	0.000696	8.33E-06
15	0.001283	5.48E-06	0.00049	4.62E-06	0.000216	3.19E-06
17	0.000309	3.01E-06	0.000126	2.37E-06	7.32E-05	2.57E-06
19	7.74E-05	1.57E-06	3.49E-05	9.18E-07	2.67E-05	1.32E-06
21	1.74E-05	5.98E-07	1.02E-05	8.69E-07	1.31E-05	1.01E-06
23	5.00E-06	3.31E-07	4.14E-06	1.82E-07	8.95E-06	6.35E-07
25	1.78E-06	4.17E-08	1.84E-06	8.62E-08	5.63E-06	2.96E-07
27	7.18E-07	9.92E-09	9.05E-07	5.24E-08	4.14E-06	1.98E-07
29	3.40E-07	5.32E-09	5.90E-07	1.87E-08	2.90E-06	2.10E-07

Table A.10

The mean BER values and their standard errors for the transmission with ICE and QPSK modulation, T = 10 and 20, C = 0.999 (supplement to Fig. 4.9).

	$T = 10$		$T = 20$	
SNR [dB]	mean BER	standard error	mean BER	standard error
1	0.137491	7.71E-05	0.119951	8.68E-05
3	0.076389	0.000108	0.068946	0.00012
5	0.036342	4.47E-05	0.034912	9.05E-05
7	0.014942	3.83E-05	0.015926	5.68E-05
9	0.00549	4.00E-05	0.006856	5.27E-05
11	0.001943	1.03E-05	0.002961	2.75E-05
13	0.000708	1.07E-05	0.001489	1.93E-05
15	0.000283	5.69E-06	0.00078	2.33E-05
17	0.000126	5.89E-06	0.0005	1.08E-05
19	7.70E-05	3.39E-06	0.000396	1.41E-05
21	4.59E-05	1.51E-06	0.000301	1.47E-05
23	3.78E-05	1.80E-06	0.000266	1.05E-05
25	2.90E-05	1.56E-06	0.000227	4.35E-06
27	2.51E-05	1.58E-06	0.000221	7.72E-06
29	2.22E-05	1.44E-06	0.000216	4.77E-06

Table A.11

The mean BER values and their standard errors for the transmission with QPSK modulation, C = 0.99 (supplement to Fig. 4.10).

	standard transmission $T = 1$		ICE algorithm $T = 1$		ICE algorithm $T = 2$	
SNR [dB]	mean BER	standard error	mean BER	standard error	mean BER	standard error
1	0.215725	5.31E-05	0.34203	5.34E-05	0.309111	6.73E-05
3	0.157701	3.18E-05	0.275086	4.35E-05	0.234732	7.74E-05
5	0.108453	3.17E-05	0.196689	3.93E-05	0.156405	7.58E-05
7	0.07153	2.43E-05	0.121258	3.84E-05	0.090953	7.23E-05
9	0.047136	2.56E-05	0.064353	4.74E-05	0.047764	5.10E-05
11	0.032349	1.91E-05	0.030373	3.17E-05	0.023922	3.20E-05
13	0.023815	1.42E-05	0.013575	1.31E-05	0.012249	3.07E-05
15	0.018926	1.11E-05	0.006166	1.23E-05	0.006686	2.23E-05
17	0.016098	1.40E-05	0.003034	8.77E-06	0.004068	1.43E-05
19	0.014433	8.41E-06	0.001687	4.98E-06	0.002753	1.17E-05
21	0.013442	1.32E-05	0.00108	3.27E-06	0.002063	1.17E-05
23	0.012829	1.29E-05	0.000782	3.80E-06	0.001702	1.18E-05
25	0.012447	1.19E-05	0.000617	4.56E-06	0.001498	1.20E-05
27	0.012206	8.64E-06	0.000526	3.77E-06	0.00136	1.46E-05
29	0.012046	1.31E-05	0.000482	4.03E-06	0.001279	1.12E-05

Bibliography

[1] 3GPP, Multiple Input Multiple Output (MIMO) antennae in UTRA, TR 25.876, *3GPP Technical Specifications*, 2005.

[2] 3GPP, Spacial channel model for Multiple Input Multiple Output (MIMO) simulations, TR 25.996, *3GPP Technical Specifications*, 2003.

[3] S. Alamouti, Space block coding: A simple transmitter diversity technique for wireless communications, *IEEE Journal on Selected Areas in Communications*, vol. 16, no. 8, pp. 1451–1458, October 1998.

[4] J. B. Andersen, J. O. Nielsen, G. Bauch and M. Herdin, The Large Office Environment - Measurement and Modeling of the Wideband Radio Channel, *IEEE International Symposium on Personal, Indoor and Mobile Radio Communications PIMRC*, September 2006.

[5] C. Berrou, A. Glavieux, and P. Thitimajshima, Near Shannon Limit Error-Correcting Coding and Decoding: Turbo-codes, *IEEE International Conference on Communications ICC*, pp. 1064–1070, May 1993.

[6] C. Berrou and A. Glavieux, Near Optimum Error Correcting Coding and Decoding: Turbo-codes, *IEEE Transactions on Communications*, vol. 44, no. 10, pp. 1261–71, October 1996.

[7] E. Bonek, The MIMO Radio Channel, *Antenna 06 Nordic Antenna Symposium*, pp. 23-34, May 2006.

[8] G. E. P. Box and M. E. Muller, A note on the generation of random normal deviates, *Annals of Mathematical Statistics*, vol. 29, no. 2, pp. 610-611. June 1958.

[9] S. ten Brink, G. Kramer and A. Ashikhmin, Design of Low-Density Parity-Check Codes for Modulation and Detection, *IEEE Transactions on Communications*, vol. 52, no. 4, pp. 670-678, April 2004.

[10] A. Burr, Evaluation of the capacity of the MIMO channel in a room using ray tracing, *International Zurich Seminar on Broadband Communications, Access, Transmission, Networking*, pp. 28-1-28-6, February 2002.

[11] G. Caire and S. Shamai (Shitz), On the achievable throughput of a multiantenna Gaussian broadcast channel, *IEEE Transactions on Information Theory*, vol. 49, no. 7, pp. 1691-1706, July 2003.

[12] L. M. Correia, *Mobile Broadband Multimedia Networks*, Academic Press, 2006.

[13] M. H. M. Costa, Writing on dirty paper, *IEEE Transactions on Information Theory*, vol. 29, no. 3, pp. 439–441, May 1983.

[14] C. Dubuc, D. Starks, T. Creasy and Y. Hou, A MIMO-OFDM Prototype for Next-Generation Wireless WANs, *IEEE Communications Magazine*, vol. 42, no. 12, pp. 82- 87, December 2004.

[15] P. L'Ecuyer and R. Simard, On the Performance of Birthday Spacings Tests with Certain Families of Random Number Generators, *Mathematics and Computers in Simulation (selected papers from the 1999 IMACS Seminar on Monte Carlo Methods)*, vol. 55, no. 1-3, pp. 131-137, February 2001.

[16] M.S. Elnaggar, S. Safavi-Naeini and S. K. Chaudhuri, Site-specific indoor MIMO capacity using adaptive techniques, *IEEE Antennas and Propagation Society International Symposium*, pp. 426- 429, July 2005.

[17] C. H. Y. Eugene, K. Sakaguchi and K. Araki, Experimental and analytical investigation of MIMO channel capacity in an indoor line-of-sight (LOS) environment, *IEEE International Symposium on Personal, Indoor and Mobile Radio Communications PIMRC*, pp. 295- 300, September 2004.

[18] EZNEC Antenna Software, http://www.eznec.com, 2006.

[19] W. Feller, *An Introduction to Probability Theory and Its Applications*, Wiley, 1968.

[20] S. Fortune, Algorithms for prediction of indoor radio propagation, *Technical Report Document, Bell Laboratories*, 1998.

[21] G. J. Foschini, Layered space–time architecture for wireless communication in a fading environment when using multielement antennas, *Bell Labs Technical Journal*, pp. 41–59, Autumn 1996.

[22] G. J. Foschini and M. J. Gans, On limits of wireless communications in a fading environment when using multiple antennas, *Wireless Personal Communications*, vol. 6, pp. 311–335, March 1998.

[23] G. J. Foschini, G. D. Golden, R. A. Valenzuela and P. W. Wolniansky, Simplified Processing for High Spectral Efficiency Wireless Communication Employing Multi-Element Arrays, *IEEE Journal on Selected Areas in Communications*, vol. 17, no. 11, pp. 1841-1852, November 1999.

[24] G. J. Foschini, D. Chizhik, M. J. Gans, C. Papadias and R. A. Valenzuela, Analysis and Performance of Some Basic Space–Time Architectures, *IEEE Journal on Selected Areas in Communications*, vol. 21, no. 3, pp. 303-320, April 2003.

[25] R. G. Gallager, *Low Density Parity Check Codes, Monograph*, M.I.T. Press, 1963.

[26] H. E. Gamal, A. R. Hammons, Jr., A new approach to layered space-time coding and signal processing, *IEEE Transactions on Information Theory*, vol. 47, no. 6, pp. 2321-2334, September 2001.

[27] D. Gesbert, M. Shafi, D. Shiu, P. J. Smith and A. Naguib, From Theory to Practice: An Overview of MIMO Space–Time Coded Wireless Systems, *IEEE Journal on Selected Areas in Communications*, vol. 21, no. 3, pp. 281-302, April 2003.

[28] G. D. Golden, G. J. Foschini, R. A. Valenzuela and P. W. Wolniansky, Detection algorithm and initial laboratory results using V-BLAST space-time communication architecture, *Electronics Letters*, vol. 35, no. 1, pp. 14-16, January 1999.

[29] A. J. Goldsmith and P. P. Varaiya, Capacity of Fading Channels with Channel Side Information, *IEEE Transactions on Information Theory*, vol. 43, no. 6, pp. 1986-1992, November 1997.

[30] B. Hassibi and B. M. Hochwald, How much training is needed in multiple-antenna wireless links?, *IEEE Transactions on Information Theory*, vol. 49, no. 4, pp. 951–965, April 2003.

[31] S. Haykin, M. Sellathurai, Y. de Jong and T. Willink, Turbo-MIMO for Wireless Communications, *IEEE Communications Magazine*, vol. 42, no. 10, pp. 48-53, October 2004.

[32] L. He and H. Ge, A New Full-Rate Full-Diversity Orthogonal Space-Time Block Coding Scheme, *IEEE Communications Letters*, vol. 7, no. 12, pp. 590-592, December 2003.

[33] R. W. Heath, Jr. and A. J. Paulraj, Switching Between Diversity and Multiplexing in MIMO Systems, *IEEE Transactions on Communications*, vol. 53, no. 6, pp. 962-968, June 2005.

[34] B. M. Hochwald and S. ten Brink, Achieving Near-Capacity on a Multiple-Antenna Channel, *IEEE Transactions on Communications*, vol. 51, no. 3, pp. 389-399, March 2003.

[35] R. A. Horn and C. R. Johnson, *Matrix Analysis*, Cambridge University Press, 1985.

[36] IEEE 802.11, The Working Group Setting the Standards for Wireless LANs, http://www.ieee802.org/11, 2006.

[37] W. C. Jakes, *Microwave Mobile Communications*, Wiley, 1994.

[38] M. A. Jensen and J. W. Wallace, A Review of Antennas and Propagation for MIMO Wireless Communications, *IEEE Transactions on Antennas and Propagation*, vol. 52, no. 11, pp. 2810-2824, November 2004.

[39] M. A. Jensen and J. W. Wallace, MIMO Wireless Channel Modeling and Experimental Characterization, Chapter I in the book *Space-Time Processing for MIMO Communications* edited by A. Gershman and N. Sidiropoulos, Wiley, 2005.

[40] V. Jungnickel and V. Pohl, Capacity of MIMO Systems With Closely Spaced Antennas, *IEEE Communications Letters*, vol. 8, no. 7, pp. 361-363, August 2003.

[41] J. P. Kermoal, L. Schumacher, K. I, Pedersen, P. E. Mogensen and F. Frederiksen, A Stochastic MIMO Radio Channel Model With Experimental Validation, *IEEE Journal on Selected Areas in Communications*, vol. 20, no. 6, pp. 1211-1226, August 2002.

[42] J. D. Kraus and R. J. Marhefka, *Antennas for All Applications*, McGraw-Hill, 2002.

[43] P. Kulakowski and W. Ludwin, Ray Tracing Technique for Capacity Analysis of MIMO System in a Single Room (in Polish), *National Conference on Radiocommunication, Radio and Television KKRRiT*, pp. 165-168, Warsaw 2004.

[44] P. Kulakowski and W. Ludwin, An Estimation Algorithm of the Channel Transfer Function Matrix for a MIMO System with Alamouti Coding Scheme (in Polish), *National Conference on Radiocommunication, Radio and Television KKRRiT*, Cracow, 2005.

[45] P. Kulakowski and W. Ludwin, Performance Analysis of Multiple-Input Multiple-Output System for Wireless Network in an Office Room, *AEU – International Journal of Electronics and Communications*, vol. 60, no. 3, pp. 240-243, March 2006.

[46] P. Kulakowski and W. Ludwin, The Capacity Evaluation of WLAN MIMO System with Multi-Element Antennas and Maximal Ratio Combining, *IEEE International Symposium on Personal, Indoor and Mobile Radio Communications PIMRC*, September 2006.

[47] P. Kulakowski and W. Ludwin, Iterative MIMO Channel Estimation for Space-Time Block Codes, submitted to *IEEE Transactions on Communications*.

[48] P. Kyritsi and D. Chizhik, Capacity of Multiple Antenna Systems in Free Space and Above Perfect Ground, *IEEE Communications Letters*, vol. 6, no. 8, pp. 325-327, August 2002.

[49] V. K. N. Lau and Y. K. R. Kwok, *Channel Adaptive Technologies and Cross Layer Designs for Wireless Systems with Multiple Antennas*, Wiley, 2006.

[50] T. L. Marzetta and B. M. Hochwald, Fast transfer of channel state information in wireless systems, *IEEE Transactions on Signal Processing*, vol. 54, no. 4, pp. 1268-1278, April 2006.

[51] M. Matsumoto and T. Nishimura, Mersenne Twister: A 623-dimensionally equidistributed uniform pseudorandom number generator, *ACM Transactions on Modeling and Computer Simulation*, vol. 8, no. 1, pp.3-30, January 1998.

[52] J. McKown and R. Hamilton, Ray tracing as a design tool for radio networks, *IEEE Network Magazine*, vol. 5, no. 6, pp. 27–30, November 1991.

[53] D. P. McNamara, M. A. Beach, P. Karlsson and P. N. Fletcher, Initial characterisation of multiple-input multiple-output (MIMO) channels for space-time communication, *IEEE Vehicular Technology Conference VTC Fall*, pp. 1193-1197, September 2000.

[54] A. F. Molisch, M. Steinbauer, M. Toeltsch, E. Bonek and R. S. Thoma, Capacity of MIMO Systems Based on Measured Wireless Channels, *IEEE Journal on Selected Areas in Communications*, vol. 20, no. 3, pp. 561-569, April 2002.

[55] S. Nanda, R. Walton, J. Ketchum, M. Wallace and Steven Howard, A High-Performance MIMO OFDM Wireless LAN, *IEEE Communications Magazine*, vol. 43, no. 2, pp. 101-109, February 2005.

[56] J. O. Nielsen, J. B. Andersen, G. Bauch, M. Herdin, Relationship Between Capacity and Pathloss for Indoor MIMO Channels, *IEEE International*

Symposium on Personal, Indoor and Mobile Radio Communications PIMRC, September 2006.

[57] H. Ozcelik, M. Herdin, H. Hofstetter and E. Bonek, Capacity of Different MIMO Systems Based on Indoor Measurements at 5.2 GHz, *IEE European Personal Mobile Communications Conference EPMCC*, pp. 463-466, April 2003.

[58] K. I. Pedersen, J. B. Andersen, J. P. Kermoal and P. Mogensen, A Stochastic Multiple-Input-Multiple-Output Radio Channel Model for Evaluation of Space-Time Coding Algorithms, *IEEE Vehicular Technology Conference VTC Fall*, pp. 893-- 897, September 2000.

[59] T. S. Rappaport, *Wireless Communications*, Prentice Hall, 1996.

[60] Recommendation ITU-R P.1238-2, Propagation data and prediction methods for the planning of indoor radiocommunication systems and radio local area networks in the frequency range 900 MHz to 100 GHz, *ITU Recommendations*, Geneva, 2001.

[61] T. Richardson and R. Urbanke, The Renaissance of Gallager's Low-Density Parity-Check Codes, *IEEE Communications Magazine*, vol. 41, no. 8, pp. 126-131, August 2003.

[62] A. Richter, *Estimation of Radio Channel Parameters: Models and Algorithms, PhD Thesis*, Ilmenau University of Technology, 2005.

[63] A. A. M. Saleh and R. A. Valenzuela, A Statistical Model for Indoor Multipath Propagation, *IEEE Journal on Selected Areas in Communications*, vol. 5, no. 2, pp. 128-137, February 1987.

[64] C. E. Shannon, A Mathematical Theory of Communication, *The Bell System Technical Journal*, vol. 27, pp. 379–423 and 623–656, July and October, 1948.

[65] M. Steinbauer, A. Molisch and E. Bonek, The Double-Directional Radio Channel, *IEEE Antennas and Propagation Magazine*, vol. 43, no. 4, pp. 51-63, August 2001.

[66] R. Stridh, K. Yu, B. Ottersten and P. Karlsson, MIMO Channel Capacity and Modeling Issues on a Measured Indoor Radio Channel at 5.8 GHz, *IEEE Transactions on Wireless Communications*, vol. 4, no. 3, pp. 895-903, May 2005.

[67] V. Tarokh, N. Seshadri and A. R. Calderbank, Space–Time Codes for High Data Rate Wireless Communication: Performance Criterion and Code Construction, *IEEE Transactions on Information Theory*, vol. 44, no. 2, pp. 744-765, March 1998.

[68] V. Tarokh, H. Jafarkhani and A. R. Calderbank, Space–Time Block Codes from Orthogonal Designs, *IEEE Transactions on Information Theory*, vol. 45, no. 5, pp. 1456-1467, July 1999.

[69] V. Tarokh and H. Jafarkhani, A Differential Detection Scheme for Transmit Diversity, *IEEE Journal on Selected Areas in Communications*, vol. 18, no. 7, pp. 1169-1174, July 2000.

[70] I. E. Telatar, Capacity of Multi-antenna Gaussian Channels, *AT&T Bell Laboratories, Technical Memorandum*, June 1995.

[71] The COST 273 MIMO Channel Model Implementation, http://www.ftw.at/cost273, 2006.

[72] E. Tila, E. R. Shepherd and S. R. Pennock, Theoretic capacity evaluation of indoor micro- and macro-MIMO systems at 5 GHz using site specific ray tracing, *Electronics Letters*, vol. 39, no. 5, pp. 471-472, May 2003.

[73] L. Tong and S. Perreau, Multichannel Blind Identification: From Subspace to Maximum Likelihood Methods, *Proceedings of the IEEE*, vol. 86, no. 10, pp. 1951-1968, October 1998.

[74] D. Tse and P. Viswanath, *Fundamentals of Wireless Communication*, Cambridge University Press, 2005.

[75] J. K. Tugnait and B. Huang, Blind Estimation and Equalization of MIMO Channels via Multidelay Whitening, *IEEE Journal on Selected Areas in Communications*, vol. 19, no. 8, pp. 1507-1519, August 2001.

[76] R. A. Valenzuela, S. Fortune and J. Ling, Indoor Propagation Prediction Accuracy and Speed Versus Number of Reflections in Image-Based 3-D Ray-Tracing, *IEEE Vehicular Technology Conference VTC*, pp. 539-543, May 1998.

[77] B. Vucetic and J. Yuan, *Space-Time Coding*, Wiley, 2003.

[78] J. W. Wallace and M. A. Jensen, MIMO capacity variation with SNR and multipath richness from full-wave indoor FDTD simulations, *IEEE Antennas and Propagation Society International Symposium*, pp. 523- 526 vol. 2, June 2003.

[79] W. Weichselberger, M. Herdin, H. Ozcelik and E. Bonek, A Stochastic MIMO Channel Model With Joint Correlation of Both Link Ends, *IEEE Transactions on Wireless Communications*, vol. 5, no. 1, pp. 90-100, January 2006.

[80] J. H. Winters, On the Capacity of Radio Communication Systems with Diversity in a Rayleigh Fading Environment, *IEEE Journal on Selected Areas in Communications*, vol. 5, no. 5, pp. 871-878, June 1987.

[81] H. Yang, A Road to Future Broadband Wireless Access: MIMO-OFDM-Based Air Interface, *IEEE Communications Magazine*, vol. 43, no. 1, pp. 53-60, January 2005.

[82] K. Yu, M. Bengtsson, B. Ottersten, P. Karlsson, D. McNamara and M. Beach, Measurement Analysis of NLOS Indoor MIMO Channels, *IST Mobile Communications Summit*, pp. 277-282, September 2001.

[83] K. Yu, M. Bengtsson, B. Ottersten, D. McNamara, P. Karlsson and M. Beach, A Wideband Statistical Model for NLOS Indoor MIMO Channels, *IEEE Vehicular Technology Conference VTC Spring*, pp. 370-374 vol.1, May 2002.

[84] K. Yu and B. Ottersten, Models for MIMO Propagation Channels, A Review, *Journal on Wireless Communications and Mobile Computing*, vol. 2, no. 7, pp. 553-666, November 2002.

[85] L. Zheng and D. N. C. Tse, Diversity and Multiplexing: A Fundamental Tradeoff in Multiple-Antenna Channels, *IEEE Transactions on Information Theory*, vol. 49, no. 5, pp. 1073-1096, May 2003.

Systemy wieloantenowe o dużej i małej dynamice zmian transmitancji kanału radiowego

Streszczenie

W ostatnich dziesięciu latach nastąpił niezwykle intensywny rozwój telekomunikacji bezprzewodowej. Spośród systemów radiowych, największe znaczenie osiągnęły sieci komórkowe łączności ruchomej oraz lokalne sieci bezprzewodowe WLAN. Istniejące standardy telekomunikacyjne tych sieci nie są jednak w stanie sprostać rosnącym wymaganiom na jakość transmisji, a przede wszystkim przepustowość w łączu radiowym.

Podstawowymi problemami, występującymi w procesie projektowania łącza radiowego zarówno sieci komórkowych łączności ruchomej, jak i sieci WLAN, są niska wydajność widmowa i propagacja wielodrogowa. Niska wydajność widmowa ogranicza przepustowość systemu radiokomunikacyjnego, wykorzystującego limitowane pasmo częstotliwości. Z kolei propagacja wielodrogowa sygnału radiowego sprawia, że w odbiorniku powstają zaniki sygnału, występuje zjawisko interferencji międzysymbolowej i w konsekwencji wzrasta bitowa stopa błędów.

Techniką radiową, która oferuje nowe możliwości rozwiązania obu wyżej wymienionych trudności są systemy wieloantenowe MIMO. Dodatkowe anteny, występujące zarówno po stronie nadawczej, jak i po stronie odbiorczej łącza radiowego, mogą zostać wykorzystane do zwielokrotnienia szybkości transmisji bez

konieczności zwiększania pasma częstotliwości i mocy sygnałów nadawanych. Systemy wieloantenowe umożliwiają również zastosowanie kodowania przestrzenno-czasowego zwiększającego odporność transmisji na zaniki wielodrogowe i poprawiającego bitową stopę błędów.

Systemy MIMO, których intensywny rozwój trwa od połowy lat dziewięćdziesiątych, uważane są za technikę kluczową dla przyszłych standardów telekomunikacyjnych. Jednak ich integracja ze standardami sieci komórkowych i WLAN przebiega bardzo wolno. Wiele kwestii technicznych nadal jest nierozwiązanych lub wymaga dalszych szczegółowych badań. Wśród problemów otwartych należy wymienić: uproszczenie konstrukcji układów nadawczo-odbiorczych, doskonalenie metod analizy i modelowania kanałów radiowych, projektowanie optymalnych technik kodowania oraz algorytmów estymacji kanału radiowego.

Niniejsza rozprawa doktorska poświęcona jest zagadnieniom związanym z różną dynamiką zmian kanałów radiowych w systemach wieloantenowych. Zaprezentowane badania naukowe dotyczą zarówno wolnozmiennych, jak i szybkozmiennych kanałów radiowych. W ramach rozprawy, postawiono i udowodniono następujące tezy:

1. Przepustowość systemu MIMO w wolnozmiennym kanale radiowym w środowisku wewnątrz budynków może być znacząco zwiększona przez właściwy wybór anten i lokalizacji punktu dostępowego.

2. Implementacja nowego iteracyjnego algorytmu estymacji szybkozmiennego kanału radiowego umożliwia istotną poprawę bitowej stopy błędów bez konieczności stosowania częstych transmisji sekwencji treningowych.

Rozprawa składa się z czterech rozdziałów. W rozdziale pierwszym, zaprezentowano ogólny przegląd tematyki dotyczącej systemów wieloantenowych. Przedstawiono możliwości systemów MIMO w zakresie zwiększania przepustowości i poprawy bitowej stopy błędów w transmisji radiowej. Omówiono problem znajomości charakterystyk kanału radiowego zarówno po stronie odbiorczej, jak i nadawczej systemu. Następnie przedyskutowano techniki kodowania stosowane w systemach MIMO. Opisano również kwestie technik

wielodostępu i transmisji w kanałach z zanikami selektywnymi. Wreszcie, scharakteryzowano działania mające na celu włączenie technik MIMO w standardy telekomunikacyjne.

Rozdział drugi rozprawy poświęcono zagadnieniom dotyczącym analizy i modelowania kanału radiowego. Opisano w nim wpływ propagacji wielodrogowej na działanie systemów wieloantenowych. Następnie, zaprezentowano najważniejsze istniejące modele kanałów radiowych MIMO. Omówiono też kwestie czasowych zmian kanału radiowego i jego estymacji.

W ostatnich dwóch rozdziałach, przedstawiono oryginalne badania autora i główne osiągnięcia naukowe niniejszej pracy. W rozdziale trzecim, powiązanym z pierwszą tezą rozprawy, zaprezentowana została analiza systemu MIMO działającego w środowisku wewnątrz budynków w wolnozmiennym kanale radiowym. Przeprowadzono obliczenia numeryczne oparte na algorytmie *ray tracing*. Na ich podstawie dokonano porównania przepustowości systemu MIMO w różnych konfiguracjach. Wskazano optymalne lokalizacje, rozmieszczenie i charakterystyki anten punktu dostępowego, które pozwalają nawet dwukrotnie zwiększyć przepustowość systemu. Zademonstrowano również nowe możliwości systemów MIMO z antenami adaptacyjnymi.

Rozdział czwarty traktuje o problemach estymacji szybkozmiennego kanału radiowego MIMO. Zaproponowano nowy algorytm ICE, który umożliwia jednoczesną transmisję danych i estymację kanału radiowego. Zaprezentowano również wyniki symulacji komputerowych, które pozwoliły na weryfikację działania algorytmu ICE. Pokazano, że dzięki jego zastosowaniu można zmniejszyć bitową stopę błędów prawie o dwa rzędy wielkości.